MATHEMATICAL MODELLING OF THE CHLOROPHYLL DISTRIBUTION

IN THE FRASER RIVER PLUME, BRITISH COLUMBIA


by


BODO RUDOLF de LANGE BOOM

B.Sc., University of Victoria, 1970


A Thesis Submitted in Partial Fulfilment of

the Requirements for the Degree of

Master of Science

in the Department

of

Physics

and

Institute of Oceanography


We accept this thesis as conforming to the

required standard


THE UNIVERSITY OF BRITISH COLUMBIA

July, 1976

In presenting this thesis in partial fulfilment of the requirements for an advanced degree at the University of British Columbia, I agree that the Library shall make it freely available for reference and study. I further agree that permission for extensive copying of this thesis for scholarly purposes may be granted by the Head of my Department or by his representatives. It is understood that copying or publication of this thesis for financial gain shall not be allowed without my written permission.

Department of _Physics (Oceanography)_

The University of British Columbia
2075 Wesbrook Place
Vancouver, Canada
V6T 1W5

Date _3 August 1976_

ABSTRACT

The horizontal chlorophyll a distribution observed in the
Strait of Georgia near the mouth of the Fraser River appears to
reflect the influence of the river discharge. Mathematical
models are developed to attempt to explain the observed
distribution in terms of such factors as the velocity field, the
available light and the grazing and sinking of the phytoplankton
population.

A steady state, two dimensional model is developed for the
upper layer. The downstream velocity is modelled using a
modified form of the downstream velocity in a jet; the vertical
entrainment is represented by an empirical expression, while the
cross-stream velocity is calculated from the vertically
integrated continuity equation. A vertically integrated
conservation equation is written for the chlorophyll
concentration by balancing advection against the source-sink
term (net production minus grazing and sinking). Temperature
effects are not modelled directly and nutrients are not
considered as limiting.

The first model is simplified by assuming: a constant depth
of the upper layer, vertical entrainment proportional to the
downstream velocity, and a uniform vertical distribution of
chlorophyll. In model II the layer depth varies with distance
from the river mouth, a more complex relation for the vertical
entrainment is used and more realistic vertical profiles are
employed for the horizontal velocity and the chlorophyll
concentration.

Although the observed downstream maximum in the horizontal

chlorophyll distribution is not reproduced, the results indicate that the velocity field, the available light in the water column and the value of the maximum production rate (a function of water temperature) are the most important parameters influencing the distribution. Sinking is of secondary importance while grazing appears to be relatively unimportant.

TABLE OF CONTENTS

## LIST OF TABLES

## LIST OF FIGURES

ACKNOWLEDGEMENTS

This work was made possible by the assistance of a number of people. First and foremost I would like to express my gratitude to my supervisor Dr. Paul H. LeBlond, whose assistance, encouragement and patience enabled this work to be completed.

I am grateful to Dr. T. R. Parsons for suggesting this topic and for his assistance and criticism. Dr. S. Pond deserves thanks for his comments and criticism.

Many of the staff and students of the Institute of Oceanography also contributed to this work, particularly in the data collection. The officers and crew of the C.S.S. Vector deserve thanks for their cooperation. Much invaluable advice in developing the computer programs was provided by the staff of the U.B.C. Computing Centre.

Finally I wish to thank Mary for her encouragement and understanding.

CHAPTER 1.  GENERAL OUTLINE

Background

This work deals with the interaction of physical and biological processes in the ocean on a mathematical basis. As described by Parsons and de Lange Boom (1972), a great number of interactions are possible between the physical and the biological components of a marine ecosystem. In the present discussion, the horizontal distribution of chlorophyll $\underline{a}$ (a measure of the phytoplankton concentration) in the estuary of the Fraser River will be examined. In this situation, the physical effects on the biological parameters (e.g. advection of chlorophyll $\underline{a}$ ) are much more pronounced than the biological effects on the physical parameters (e.g. light absorption by phytoplankton), and the interaction is essentially one-sided, the physical acting on the biological component.

The area of interest is the Strait of Georgia, located between Vancouver Island and the mainland coast of British Columbia (Fig. 1 ). Waldichuk (1957) and Tully & Dodimead (1957) have described the physical oceanography of this body of water. The longitudinal axis of the Strait of Georgia lies in a north-west to south-east direction. Access to the Pacific is through restricted passes having strong tidal streams, both in the south via the Gulf Islands and Juan de Fuca Strait and in the north via the passages leading to Johnson Strait.

The land-locked nature of the Strait of Georgia and the large amount of fresh water inflow from various rivers leads to typical estuarine conditions. The stratification is strongest
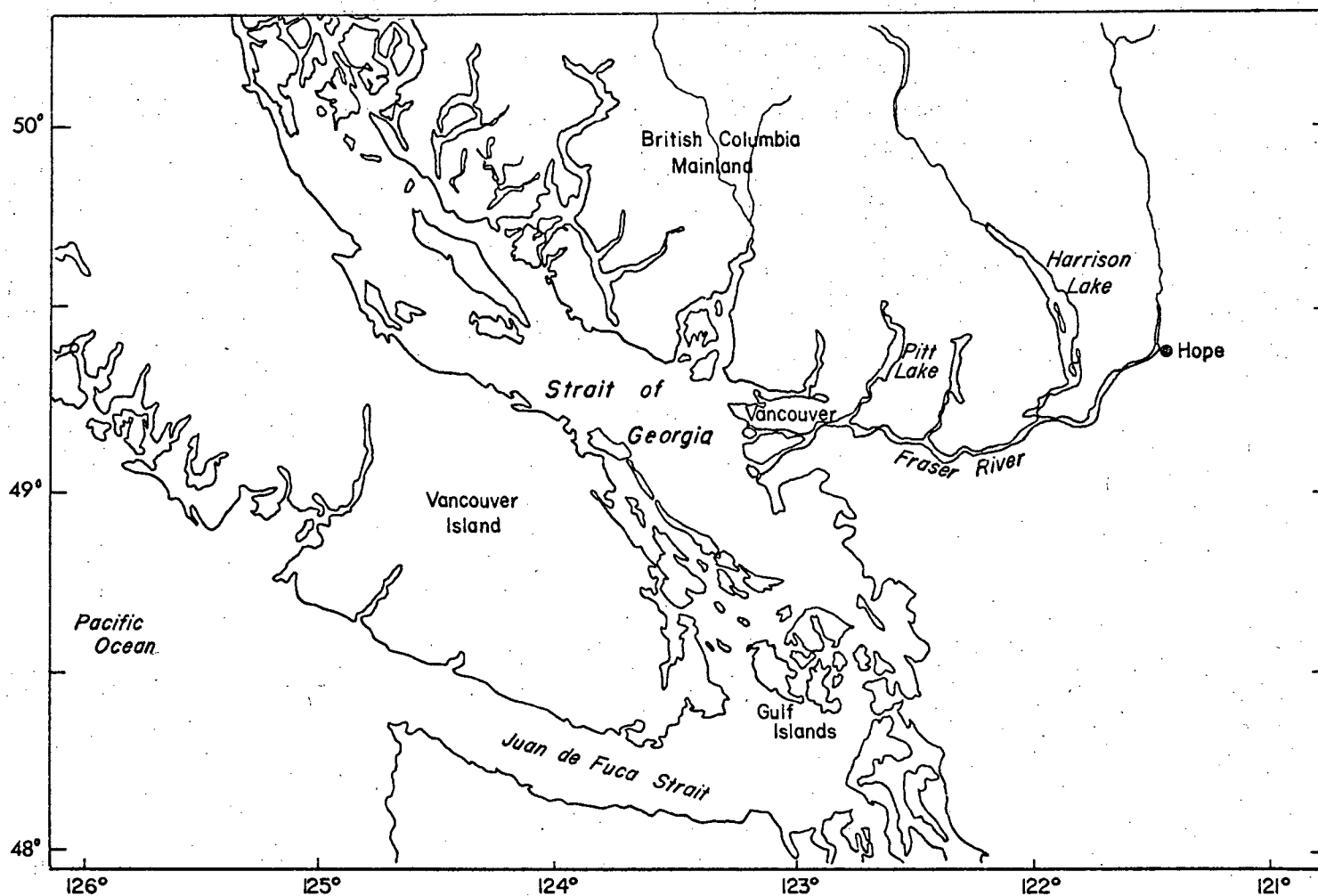
Fig. 1.  Map showing the general study area.

in summer and weakest in winter, coinciding with variations in river discharge.

The largest river emptying into the Strait of Georgia is the Fraser River (Fig. 2 ). Its discharge varies seasonally and yearly (Fig. 3 ), minimum outflow generally occurring in February or March and maximum outflow in June. Both the magnitude of the maxima and minima as well as the date on which they occur varies from year to year. The mean of the yearly maxima is about $8.5 \times 10^3$ m$^3$/s with a mean yearly discharge of $3.2 \times 10^3$ m$^3$/s. It is not uncommon for the discharge to vary by nearly an order of magnitude between extremes. Between 80% and 90% of the total outflow of the river is via the Main (South) Arm (Giovando and Tabata, 1970). At the mouth of the Main Arm (at Sand Heads), the surface velocity does not reflect the large seasonal changes in discharge. Instead the variations in the velocity are mainly tidally induced, although a seasonal component is present. A salt wedge is found in the river (Hodgins, 1974), penetrating as far as New Westminster at times of low river flow.

The large discharge of the Fraser River exerts a considerable influence on the surface waters of the Strait of Georgia, particurlarly in the vicinity of the river delta. Among the more obvious effects are the silt content of the river water (giving the surface waters their typical muddy brown colour near the river), the low salinity values, and the surface velocities due to the momentum of the river water. Nutrient levels are also low relative to the more saline water of the Strait of Georgia.

Fig. 2. Detailed map of the study area.
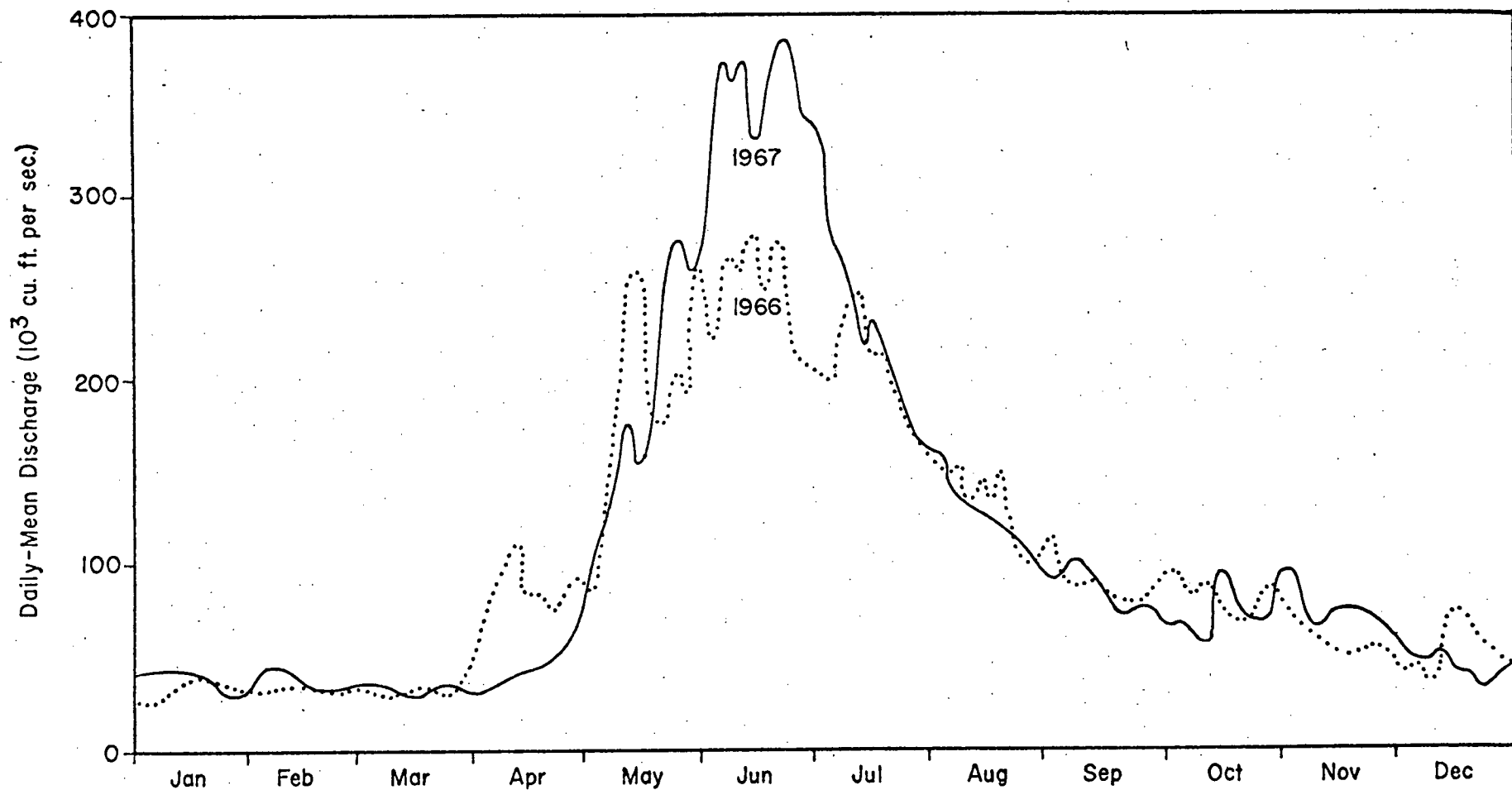
Fig. 3. Seasonal variation of the Fraser River daily mean discharge measured at Hope, B.C.

5

The surface layer of water directly influenced by the river is often called the Fraser River plume. The bottom boundary of the plume is taken to be the bottom of the halocline, the thickness being in the order of 2 to 10 m. Horizontal bounds are harder to fix since there are other rivers discharging into the Strait of Georgia and mixing tends to smooth out the distinguishing characteristics of the Fraser River plume. Aside from river discharge, the position, characteristics and extent of the plume are also determined by wind and tide as well as such modifying factors as the Coriolis effect, centrifugal force and topography. The silt content of the water is not always an indication of the dynamical extent of the plume (S. Pond, pers. com.). In summer the plume can extend right across to the Gulf Islands (Fig. 4 ), as far north as Howe Sound and south of Active Pass, while in winter the extent is much smaller. Mixing due to winds acts to further decrease the extent of the plume.

Problem: The Horizontal Chlorophyll Distribution

Chlorophyll concentration is a measure of the abundance of phytoplankton, the first step of the aquatic food web. Measurements taken in 1967 and reported by Parsons, Stephens and LeBrasseur (1969) and Parsons, LeBrasseur, Fulton and Kennedy (1969) indicate maxima of chlorophyll $\underline{a}$ and zooplankton concentrations associated with the Fraser River plume (Fig. 5 ). The chlorophyll $\underline{a}$ maximum appears to form an arc centered on the mouth of the Main Arm of the Fraser River. The highest concentrations of zooplankton are further from the river mouth and there is not the definite arc found in the chlorophyll $\underline{a}$
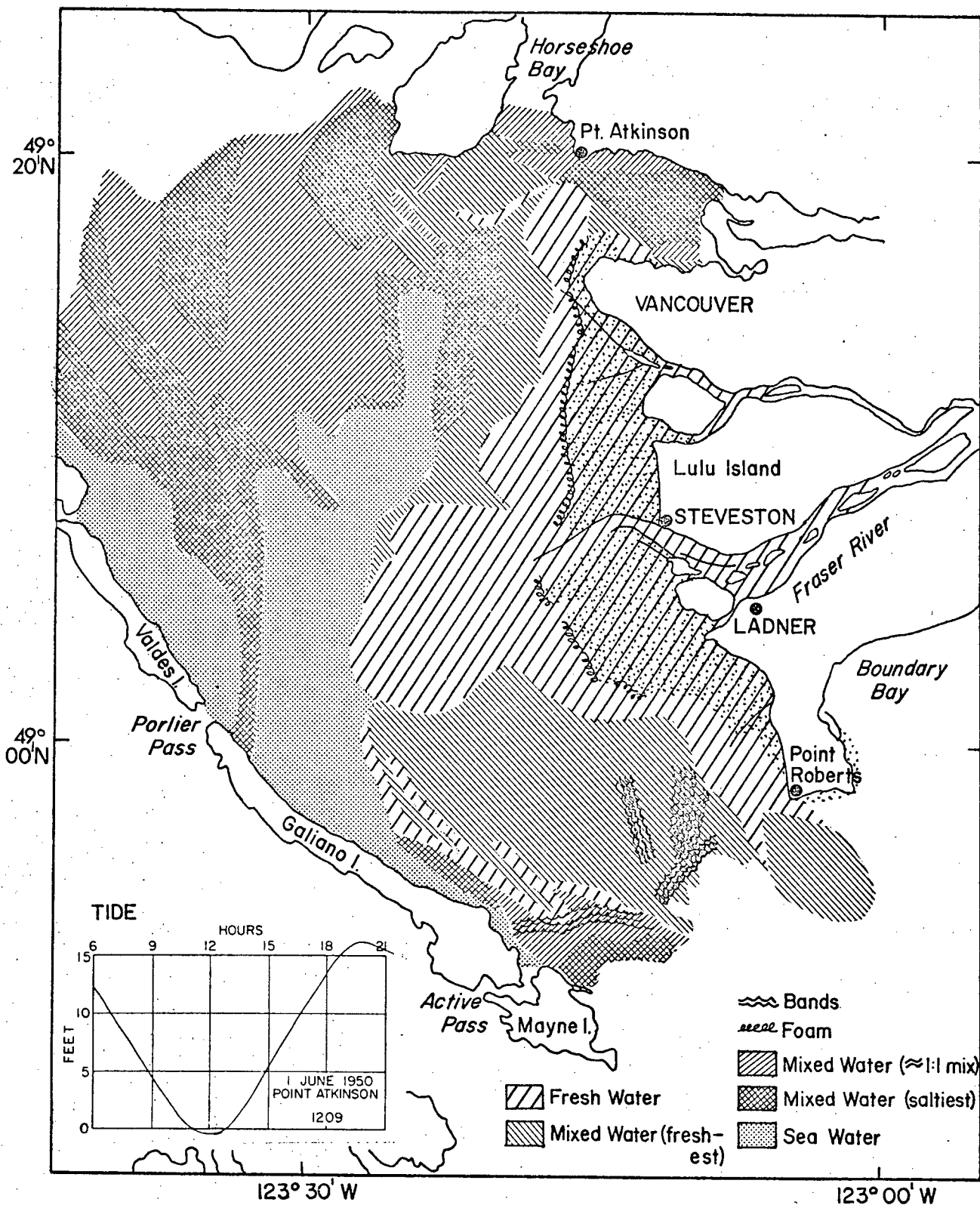
Fig. 4. The Fraser River plume position as derived from aerial photographs, after Tabata, 1972.
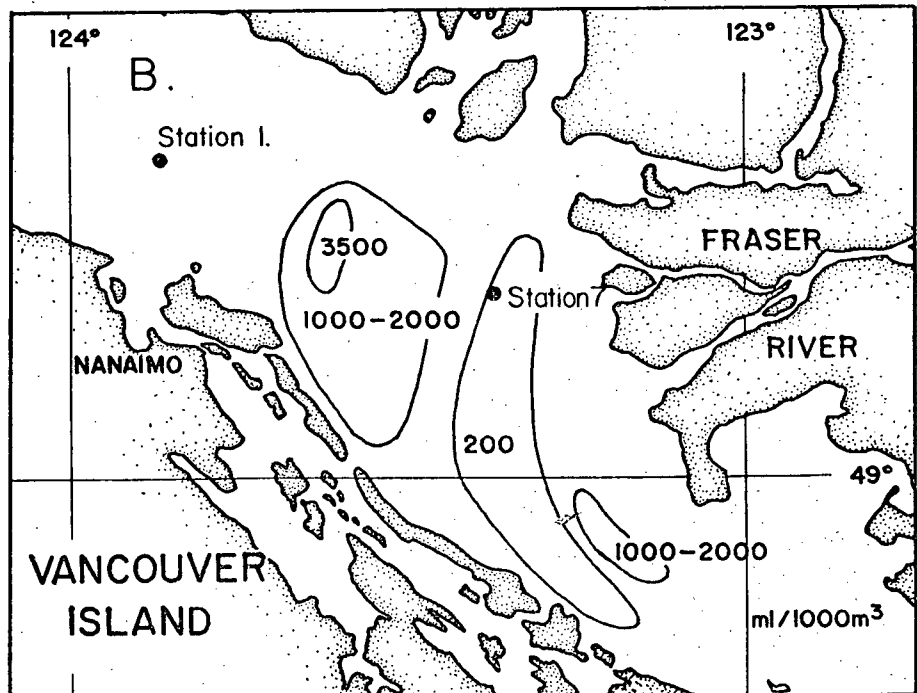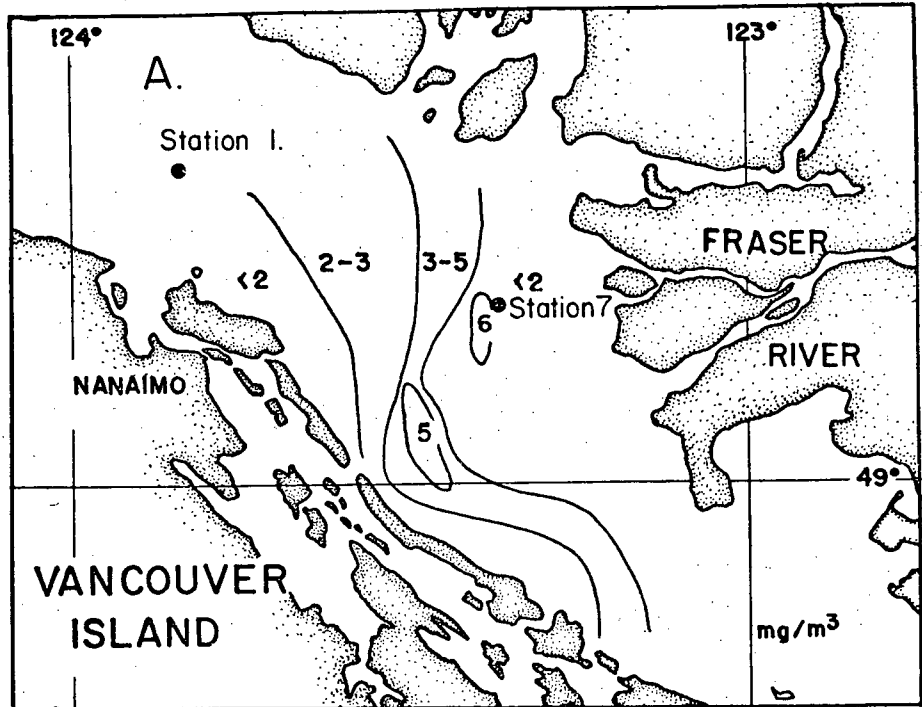
Fig. 5. Horizontal distribution of chlorophyll a, (A) and zooplankton, (B) in the Strait of Georgia; after Parsons, Stephens and LeBrasseur, 1969.

distribution. Further measurements taken in 1972 also show a maximum in the chlorophyll distribution with distance from the river mouth (Fig. 6 ) (unpublished data; Parsons, pers. com.).

The distribution of chlorophyll a  is in actual fact not so simple since phytoplankton distributions are in themselves 'patchy' (Fig. 7 ) i.e. variations in concentration occur over length scales between 10 and $10^3$ m (Platt, 1972). These variations are probably due to both physical and biological processes although no satisfactory explanation as yet exists.

The question arose as to whether it was possible to account for the observed chlorophyll distribution in terms of the Fraser River outflow as well as such factors as the available light, grazing and sinking. Biological factors must be considered since chlorophyll is not a conservative property in the same way as salinity. The understanding of the relationship between the Fraser River plume and the chlorophyll distribution is important if the impact of man-made changes (such as damming the Fraser River or discharging more effluent into the river) is to be assessed.

At this point it may be worth mentioning a few of the features of phytoplankton. Ecologically, the role of phytoplankton in the aquatic environment is equivalent to that of green plants in the terrestrial environment. By photosynthesis, phytoplankton organisms transform nutrients into cellular material using the sun's energy. Herbivorous zooplankton in turn grazes on the phytoplankton.

Phytoplankton populations are made up of single cell organisms, although some species have complex external
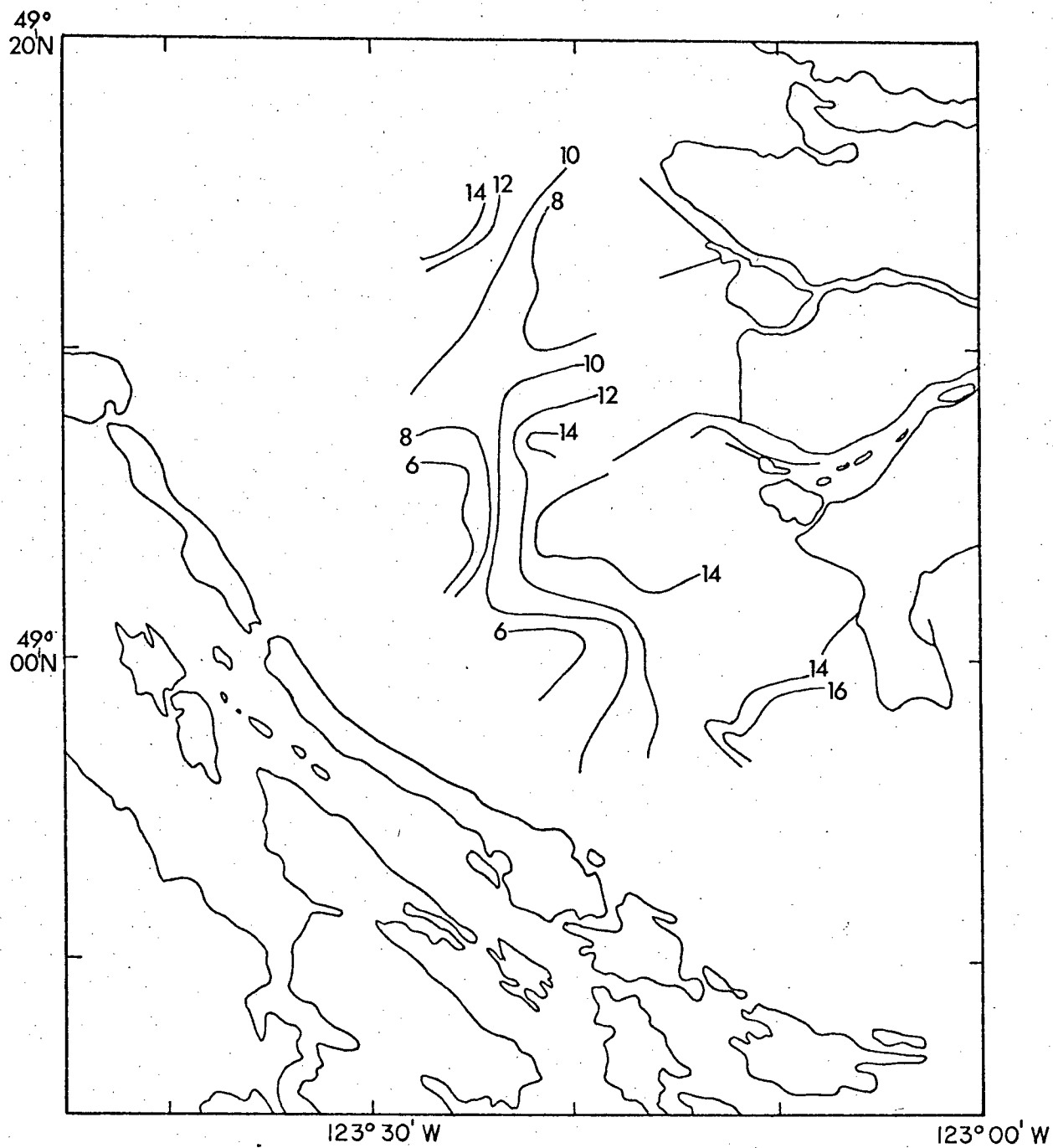
Fig. 6. Horizontal distribution of chlorophyll _a_ in terms of relative fluorescence; March, 1973.
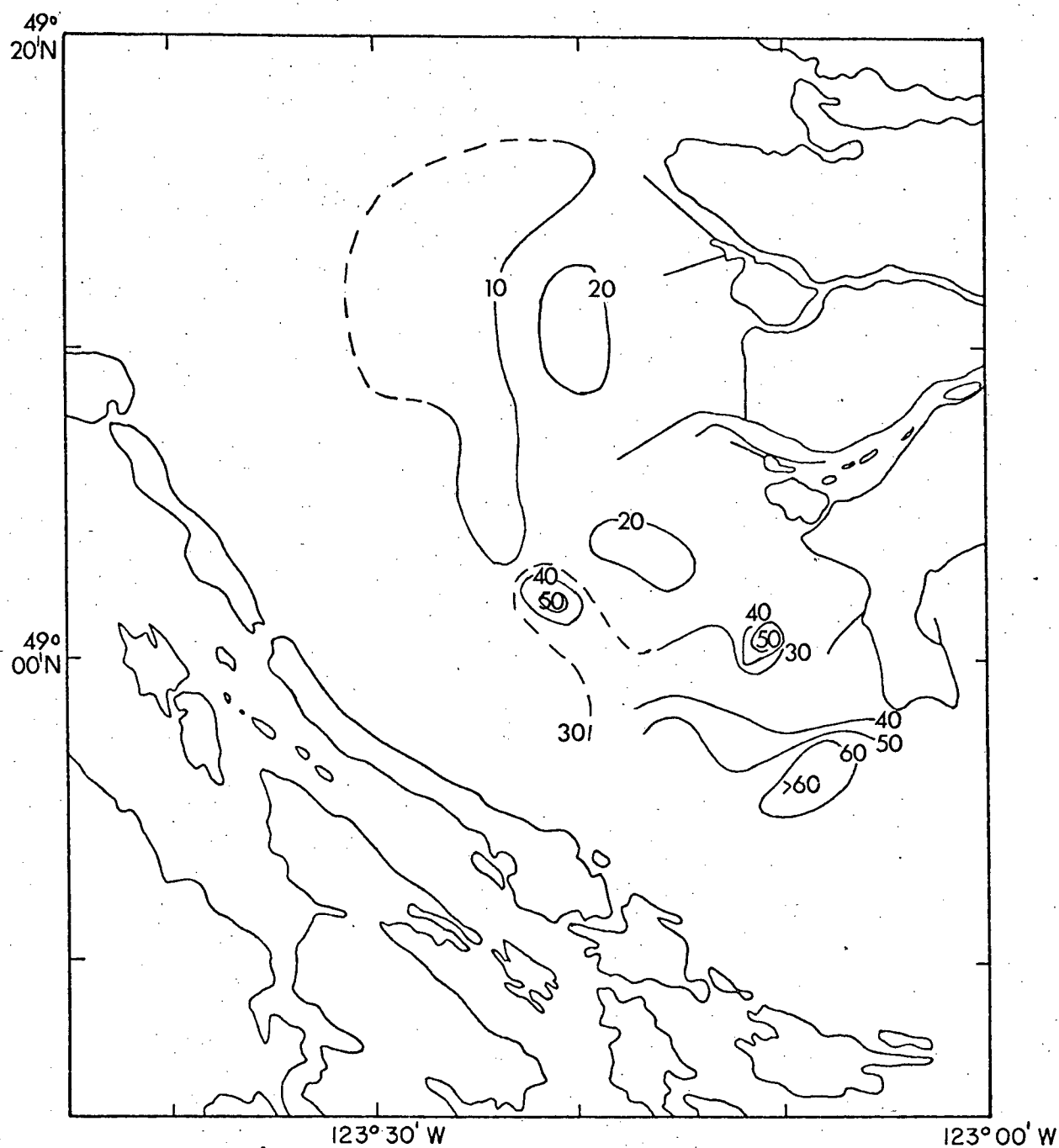
Fig. 7. Horizontal distribution of chlorophyll _a_ showing patchiness; July, 1973.

structures (e.g. dinoflagellates) or form long chains. Generally speaking they are almost neutrally bouyant and immobile. Any motion relative to the water is by sinking. An exception to this rule are the flagellates which can move through the water using their flagella and attain speeds comparable to phytoplankton sinking rates (Parsons and Takahashi, 1973). Sinking rates vary according to species as well as environmental conditions such as nutrient levels. Thus the motion of phytoplankton is determined mainly by the movement of the surrounding water.

As one might expect, light plays an important part in determining the growth of a phytoplankton population. The light intensity at any point depends on surface light intensity, the transparency of the water and the depth.

Another important factor is the nutrient concentration, with low concentrations decreasing the photosynthetic rate. The most important nutrients are nitrates, phosphates and silicates although trace elements and organic compounds in small quantities are also important. In the Fraser River estuary nitrogen is the limiting nutrient in most cases (Takahashi et al., 1973).

Temperature is another variable affecting the rate of photosynthesis. Provided other factors are not limiting, increasing temperature increases the photosynthetic rate up to an optimum temperature (which varies with species), above which the rate decreases with temperature.

Factors tending to decrease phytoplankton biomass are respiration, sinking and grazing. Respiration is the use by the

organism of stored energy to maintain the life processes. The respiration rate is not constant but varies with environmental conditions (Parsons and Takahashi, 1973). Similarly, sinking rates vary with environmental conditions.

Grazing is due to zooplankton feeding and is dependent on both the concentration of the food source and the concentration of the grazers. As the food supply increases the grazing rate (fraction of zooplankton body weight ingested by an organism per unit time) increases, asymptotically approaching a maximum rate.

The Approach To The Problem

In order to make the problem tractable it was necessary to quantify the factors discussed above. A model was put together, consisting of mathematical expressions for the relationships which tied the physical and biological components together.

A conservation equation was written for chlorophyll which included advection as well as sources and sinks of chlorophyll. The source term was the net photosynthesis which included the effect of respiration. Nutrients were not considered to be limiting during the time period that was modelled (mid-winter to pre-freshet spring) (Parsons et al., 1970; Takahashi et al., 1973). Similarly the temperature was not included directly. Temperature was included indirectly by using different values for the maximum photosynthetic rate at different times of the year. When one considers the amount of scatter in the temperature relation (Takahashi et al., 1973) plus the fact that (at any given time) the temperature within the plume does not vary more than a few degrees (Fig. 8 ), then
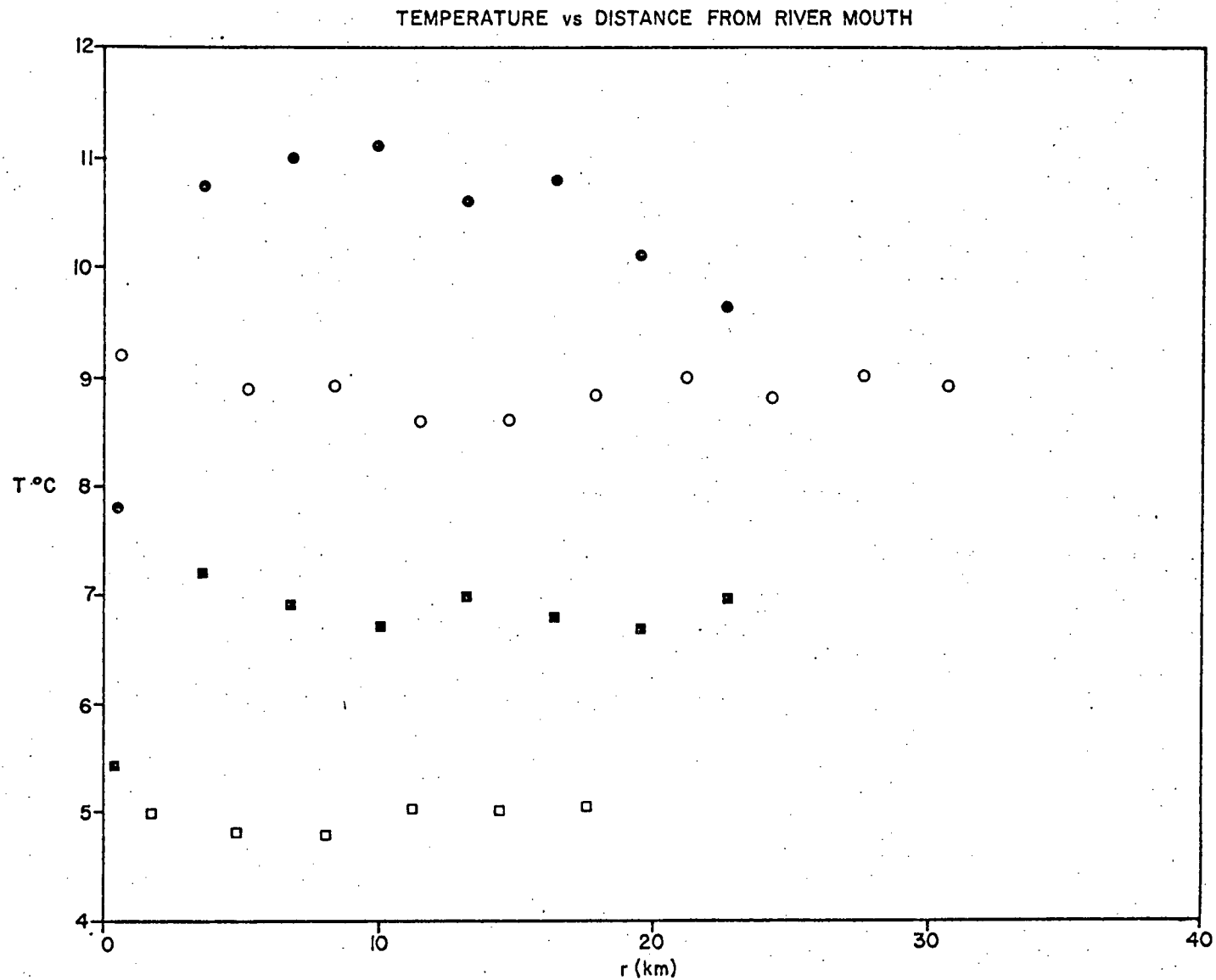
Fig. 8. Temperature at 1 m as a function of distance from the river mouth ( o November, 1971; □ February, 1972; ▣ March, 1972; ● May, 1972).

this approach is not unreasonable.

The sink terms used were grazing and sinking. Other possible losses (such as natural mortality) were assumed not to be important. Since the zooplankton population (the grazers) was not itself modelled, certain assumptions, based on observational data, had to be made about the zooplankton distribution. An arc-like horizontal distribution was assumed with the maximum value occurring at some distance from the river mouth (determined from available data ). For the sinking speed of phytoplankton a constant value was used. The natural situation is too complex to justify greater precision since size and shape of the organism as well as environmental conditions affect the sinking speed (Parsons and Takahashi, 1973).

The approach in modelling was to use a slight modification of the downstream velocity in a jet as discussed by Wiegel, (1970). Continuity was then used along with an experimental expression for the vertical velocity to calculate the cross-stream component of the horizontal velocity. The effect of the barrier of the Gulf Islands was not included, i.e. a semi-infinite sea is assumed in the horizontal plane.

CHAPTER 2. THE PHYSICAL COMPONENT: THE FLOW FIELD

As the aim of this study is to examine and compare the relative influences of physical and biological factors in determining the distributions of a scalar quantity (chlorophyll a ) we shall have to make a number of assumptions which will allow us to see through the complexities of the various interactions. The most sweeping assumptions concern the nature of the flow pattern issuing from the mouth of the Fraser. There is no existing adequate description of the tidally pulsed outflow of a fresh water stream into a broad saline body of water. Even the steady-state case is not well understood; although a number of studies of thermal plumes have been carried out, they cannot be directly applied to the flow out of a river coming out at a nearly critical internal velocity over a salt wedge.

Nevertheless, in order to obtain some representation of the flow, we shall first assume steady-state conditions, i.e., that 1) the net fresh water outflow is independent of time, and that 2) the influence of tidal variations may somehow be considered as averaging out over the time scale involved in setting up a distribution pattern corresponding to the prevailing steady conditions. The first steady-state assumption may not be too tragic, since short-period fluctuations in river discharge are of relatively small amplitude. Neglecting the rapid and important tidal variations finds justification only in our ignorance of how to account for them and in the rather limited aim of this type of study, which is not to work out a good description of the varying plume pattern but to study the

response of phytoplankton to the presence of a (mean) current of a reasonable form.

In the absence of a correct two-dimensional description of river flow into a saline basin, we chose what we thought was the most appropriate jet flow pattern available in the literature. Wiegel (1970) has reviewed the studies of jets and river plumes and we have used a Gaussian jet flow from his work.

To specify this flow pattern, let us first introduce a Cartesian coordinate system $(x,y,z)$ as shown in Fig. 9 , with x increasing downstream from the river mouth, y positive southwards and z positive upwards. The components of the velocity vector $\underline{u}$ are denoted by $(u,v,w)$ in the three coordinate directions. The river plume will be assumed to extend from the surface $z = 0$ to some depth $z = -h(x,y)$. The average horizontal velocity component over that layer will then be

$$U(x,y) = \frac{1}{h}\int_{-h}^{0} u \, dz \; ; \qquad V(x,y) = \frac{1}{h}\int_{-h}^{0} v \, dz \qquad (2.1)$$

Wiegel (1970) gives an empirical formula for the axial velocity of an axisymmetric jet issuing from an orifice of diameter $D_0$ into an unbounded body of fluid:

$$\frac{u}{u_0} = \frac{1}{2\,C_2}\,\frac{D_0}{x}\,\exp\left(-\frac{1}{2\,C_2^2}\,\frac{r^2}{x^2}\right) \qquad (2.2)$$

$C_2$ is an experimental constant, x is the distance from the orifice in the downstream direction, and r is the radial distance from the jet axis. Results due to Abraham (1960) indicate that a similar expression may be used for the discharge
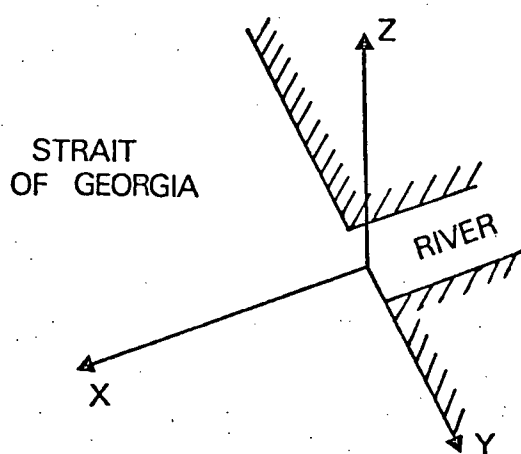
Fig. 9. The co-ordinate system employed in the model.

of a river on the surface of a body of receiving water, provided
y is substituted for r. The form which we shall adopt, and
which allows for plume spreading as well as its slowing down
with distance from the river mouth, will be

$$U h = \frac{k_1}{x + x_0} \exp \left( -k_2 \, y^2 / (x + x_0)^2 \right) \qquad (2.3)$$

The upper layer downstream transport thus decays away from the
mouth and spreads to give a Gaussian transverse profile. The
parameter $x_0$ is introduced to insure that the transport remains
finite at x = 0; its value was chosen to make the width of the
jet, as measured between the points where the Gaussian falls to
0.38 of its peak value, equal to one kilometer at the river
mouth (x = 0). For $k_2$, the value employed by Wiegel (1970) was
also used here. Thus

$$x_0 = 5 \times 10^3 \text{ m} \; ; \quad k_2 = 96[\, 1.0 + 0.19(\rho_w/\rho_0 - 1) \,]^{-2} \simeq 96$$

where $\rho_0$ is the density of the discharged water and $\rho_w$ that of
the salt water underneath the plume. Since $(\rho_w/\rho_0 - 1)$ is
small, $k_2$ is well approximated by $k_2 \simeq 96$. The value of $k_1$ is
adjusted to the value of velocity $U_0$ and depth $h_0$ at the centre
of the river mouth (x = y = 0):

$$k_1 = U_0 \, h_0 \, x_0$$

The magnitude of $U_0$ can then be varied to model various flow
conditions. The non-dimensionalized downstream velocity
distribution $U h / U_0 h_0$ is illustrated in Fig. 10 for h = constant.
Plots of the streamline pattern cannot be constructed before
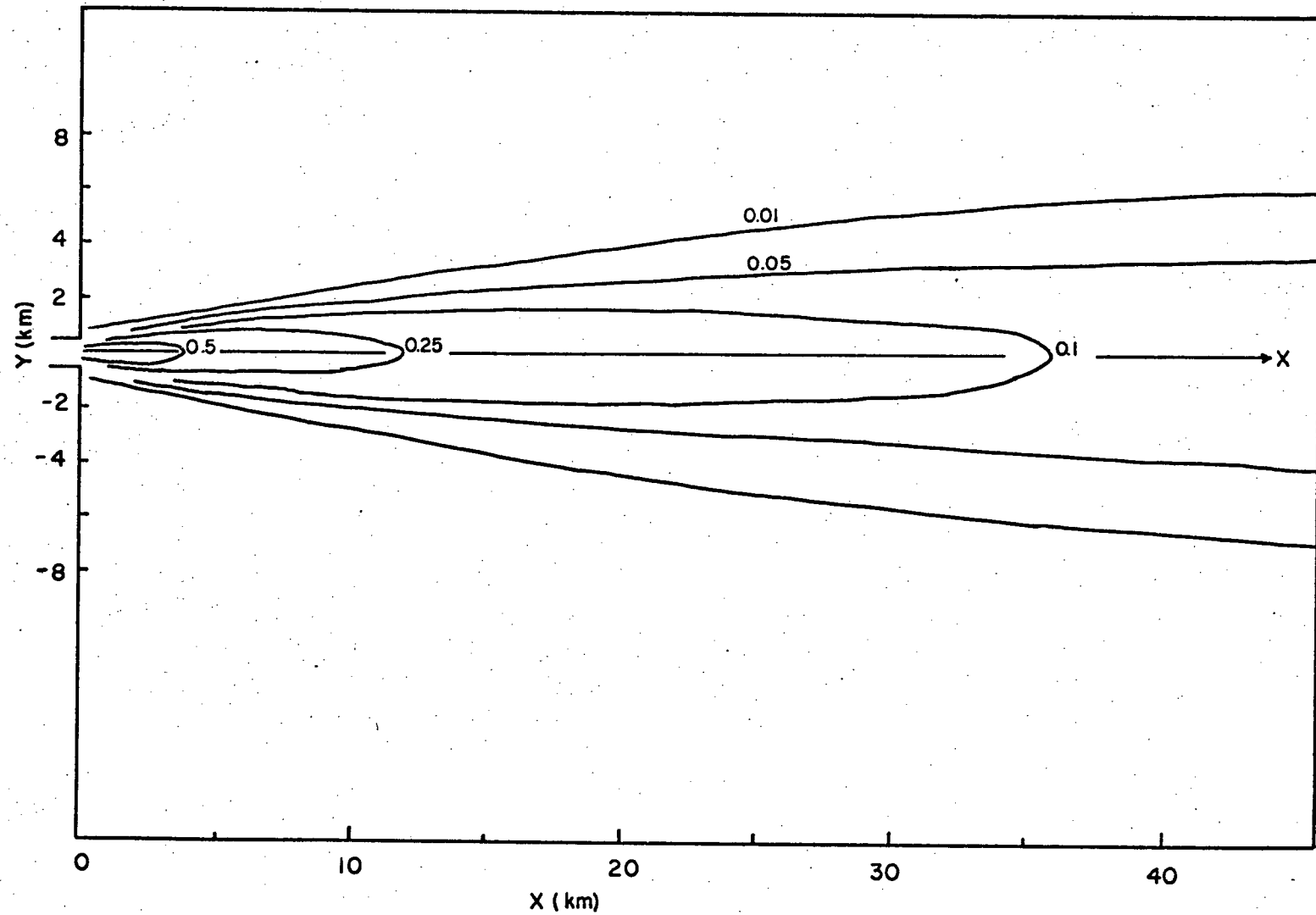further assumptions have allowed us to specify the cross-stream
velocity component, V.

Fig. 10. The non-dimensionalized downstream velocity distribution ($Uh/U_o h_o$) for h = constant.

The influence of the Coriolis force is neglected entirely. This assumption may be tenable near the river mouth, where the inertial terms dominate the flow, but cannot really be expected to hold far downstream, after the plume has slowed down. The effect of the sloping bottom on the plume is also ignored, as the bottom slopes quite steeply off Sand Heads, and the presence of the salt water beneath effectively isolates the upper layer from the bottom. Finally, lateral friction and entrainment are not considered: the plume is so thin compared to its width and the area of its underside so large compared to that of its lateral edges that it is reasonable to assume that everywhere in the plume, except very near the edges, entrainment and friction will occur only at the bottom of the plume. Only the downstream velocity distribution is given by (2.3); to construct a two dimensional flow field, some assumptions have to be made concerning the vertical entrainment velocity found at $z = -h$. Letting

$$w(x, y, -h) = w(-h)$$

for brevity, we use a relationship obtained by Keulegan (1966) for the vertical velocity across the interface of a model salt wedge estuary:

$$w(-h) = m\left(\sqrt{U^2 + V^2} - U_c\right) \qquad (2.4)$$

where $m$ is a constant; $U_c$, the critical velocity, is given by

$$U_c = c'\left(\nu_2\, g\, \frac{\Delta\rho}{\rho}\right)^{1/3} \qquad (2.5)$$

with $c'$ = constant, $\nu_2$ = the viscosity of the lower layer, $\Delta\rho$

the density difference between the lower and the upper layer and $\rho$ the density of the upper layer. Equation (2.4) is only valid for super-critical flow.

- It is then possible to complete the description of the flow field by using the continuity equation. It will be convenient to write the horizontal velocity components as

$$u = \gamma(x,y,z)\, U(x,y)$$
$$v = \gamma(x,y,z)\, V(x,y) \tag{2.6}$$

where we assume the same vertical velocity profile $\gamma(x,y,z)$ for both components. Because of the definitions (2.1), the profile function must of course satisfy

$$\int_{-h}^{o} \gamma\, dz = h \tag{2.7}$$

In an incompressible fluid,

$$\nabla \cdot \underline{u} = 0 \tag{2.8}$$

so that, integrating (2.8) over the upper layer depth, substituting from (2.6) and letting

$$\underline{U} = \left( U(x,y),\, V(x,y) \right)$$

we have

$$\int_{-h}^{o} \nabla \cdot \left( \underline{U}\gamma \right) dz + w(x,y,o) - w(x,y,-h) = 0 \tag{2.9}$$

The surface vertical velocity $w(x,y,0)$ vanishes and (2.9) may be

integrated into the form

$$\nabla \cdot (\underline{U} h) = w(-h) + \gamma(-h) \underline{U} \cdot \nabla h \qquad (2.10)$$

The right hand side of this relation is recognized as the velocity component normal to the sloping interface $h(x,y)$ and into the upper layer. Expanding (2.10) and writing it as a differential equation for $V$, the transverse horizontal velocity, we have

$$\frac{\partial V}{\partial y} + f(x,y) V = g(x,y) \qquad (2.11)$$

where

$$f(x,y) = \frac{1 - \gamma(-h)}{h} \frac{\partial h}{\partial y} \qquad (2.12)$$

and

$$g(x,y) = \frac{w(-h)}{h} - U \frac{(1 - \gamma(-h))}{h} \frac{\partial h}{\partial x} - \frac{\partial U}{\partial x} \qquad (2.13)$$

Given $U(x,y)$ from (2.3) and $w(-h)$ from (2.4), and an explicit form for $\gamma(x,y,z)$, (2.11) becomes a differential equation for $V(x,y)$. Since $w(-h)$ contains $V^2$, it is not strictly possible to integrate (2.11) directly. However, in areas where $V^2 < U^2$, such as near the axis of the plume, an iteration technique can readily be used to obtain successively better estimates for $V$, starting from $V^2 \ll U^2$, so that $w(-h) = m(U-U_c)$. The first approximation for small $V$ is then found by integrating (2.11):

Two models will be considered below: a simple one, followed by a more complex one. For each we shall specify explicit dependences for $\gamma(x,y,z)$ and values of the constants m and c'. More precise estimates of the transverse flow velocity will then be found for each one of the models.

# CHAPTER 3.  THE CHLOROPHYLL CONSERVATION EQUATION

Phytoplankton, and hence the chlorophyll concentration used to quantify its density, is safely assumed to be a passive scalar variable, advected by the flow but not modifying it in any fashion. The biological-physical interaction is in that case unidirectional: all from the physics to the biology.

Let us write the chlorophyll concentration $n(x,y,z)$ as

$$n(x,y,z) = \nu(x,y,z) \, M(x,y) \qquad (3.1)$$

where

$$M(x,y) = \frac{1}{h} \int_{-h}^{0} n \, dz \qquad (3.2)$$

is then the average concentration over the upper layer. It follows that the profile function $\nu(x,y,z)$ must satisfy

$$\int_{-h}^{0} \nu \, dz = h \qquad (3.3)$$

A steady-state conservation equation for chlorophyll may be written as

$$\nabla \cdot (\underline{u} n) = Q \qquad (3.4)$$

where $Q$ is a source strength function, which may depend on $\underline{u}$ and $n$ as well as space-coordinates. The function $Q$ will include the growth rate, the sinking rate, zooplankton grazing and any other process affecting the chlorophyll density in a non-conservative manner.

As we are interested in what happens in the upper layer
$-h \leq z \leq 0$, we integrate (3.4) over that layer:

$$\int_{-h}^{0} \nabla \cdot (\underline{u}n)\, dz + w(0)n(0) - w(-h)n(-h) = \int_{-h}^{0} Q\, dz \qquad (3.5)$$

Using (2.1) and (3.1), Leibnitz's rule, and the condition
$w(0) = 0$, (3.5) becomes:

$$\nabla \cdot \left( M\underline{U}\,\Omega \right) = M\nu(-h) \left\{ \gamma(-h)\left( U\frac{\partial h}{\partial x} + V\frac{\partial h}{\partial y}\right) + w(-h) \right\}$$

$$+ \int_{-h}^{0} Q\, dz \qquad (3.6)$$

with $\nu(-h) = \nu(x,y,-h)$ and

$$\Omega\,(x,y) = \int_{-h}^{0} \gamma\nu\, dz \qquad (3.7)$$

Combining (2.10) and (3.6) so as to eliminate the $\nabla \cdot \underline{U}$ terms we
find

$$\underline{U}\cdot\nabla M = \frac{1}{\Omega} \int_{-h}^{0} Q\, dz + \frac{M}{\Omega}\left\{ \frac{\Omega}{h}\underline{U}\cdot\nabla h - \underline{U}\cdot\nabla\Omega \right.$$

$$+ \frac{\left(h\nu(-h) - \Omega\right)}{h}\left(w(-h) + \gamma(-h)\underline{U}\cdot\nabla h\right) \Big\} \qquad (3.8)$$

which is further abbreviated as

$$\underline{U}\cdot\nabla M = H\left(M,U,V,x,y\right) \qquad (3.9)$$

where H(M,U,V,x,y) is the right hand side of (3.8).

As $\Omega$ always turns out to be proportional to h in the example chosen, it is clear that the first two terms in the bracket prefixed by $M/\Omega$ cancel out and that

$$H(M,\underline{U},\underline{x}) = \frac{1}{\Omega} \int_{-h}^{0} Q \, dz - \frac{M}{h} \left\{ \left( 1 - \frac{h\nu(-h)}{\Omega} \right) \cdot \right.$$

$$\left. \left( w(-h) + \gamma(-h) \underline{U} \cdot \nabla h \right) \right\} \qquad (3.10)$$

Any net increase or decrease in the concentration of chlorophyll is then due to 1) internal sources (the Q term) and 2) advection through the bottom of the upper layer (the second term).

CHAPTER 4.  GENERAL METHOD OF SOLUTION

Let  t  be  the  time  elapsed in travelling from the river
mouth to some point (x,y) along a  streamline  (streamlines  and
pathlines  are  identical  in this steady state situation).  The
rate of change of position along a streamline is then given by

$$\frac{Dx}{Dt} = U(x,y) \qquad\qquad (4.1)$$

$$\frac{Dy}{Dt} = V(x,y) \qquad\qquad (4.2)$$

Since D/Dt = $U\partial/\partial x$ + $V\partial/\partial y$, (3.9) may be written as

$$\frac{DM}{Dt} = H(M,U,V,x,y) \qquad\qquad (4.3)$$

Given functional forms , and initial values for U, V and  M,  it
is  possible to integrate the above equations step by step along
streamlines to obtain a map of the  horizontal  distribution  of
velocity  and  chlorophyll.   This method of solution is broadly
applicable in the above form to any kind of scalar field  M(x,y)
for  which  a  source-sink function Q(x,y,z) can be defined.  It
could for example be readily applied to provide  a  quantitative
account  of  sediment load in the plume, or of concentrations of
chemical species, such as observed for trace elements by  Thomas
(1975).   Alternately,  the  inverse  problem of determining the
velocity field which leads to an  observed  distribution  M(x,y)
might  be  attempted using (4.1) to (4.3), although it might not
be possible, depending on the form of Q(x,y,z), to find a unique

solution to that problem.

CHAPTER 5. SOURCES AND SINKS OF CHLOROPHYLL

A number of influences are covered by the source strength function $Q(x,y,z)$, and they will now be discussed and given appropriate parameterizations in terms of environmental factors. Three sources and sinks of chlorophyll in the upper layer are considered: primary production, zooplankton grazing and sinking.

The production of particulate organic matter by phytoplankton occurs at a rate P usually called the photosynthetic rate and expressible in terms of grams of chlorophyll produced per unit time per gram of existing chlorophyll. The usual units in which P is given are in terms of grams of carbon fixed per unit time per gram of chlorophyll: we can transform from one set of units to the other using a conversion factor (g chlorophyll/g carbon). Productivity is light sensitive and an expression originally suggested by Steele (1962) and used by Takahashi et al. (1973) is employed here:

$$P = \alpha b P_m I \exp(1 - bI) \tag{5.1}$$

P is the chlorophyll production rate, in units of $(time)^{-1}$, $\alpha$ converts from carbon units, in which $P_m$ is expressed, to chlorophyll units; b is a constant with the dimensions of minutes/langley while I is the light intensity in langleys/minute.

It is clear from (5.1) that P has a maximum value $(\alpha P_m)$ at an optimal light intensity

$$I_{op} = 1/b \tag{5.2}$$

Takahashi et al. (1973) found from a best fit of available experimental data, a value of $I_{op}$ = 0.18 ly/min, so that from (5.2), b = 5.56 min/ly. This directly calculated value for b gives a better fit to the experimental curves than that computed by Takahashi et al. (1973) (b = 5.37 min/ly) by an improper numerical technique which does not satisfy (5.2).

The maximum rate of carbon fixation $P_m$ varies with nutrient availability and temperature. As mentioned earlier the temperature in the Fraser River plume does not vary by more than a few degrees at any one time but does vary with the season (Fig. 8). Given the scatter observed by Takahashi et al. (1973) in the $P_m$(T) observations it is quite justifiable to take $P_m$ = constant everywhere in the plume for any one simulation. Observations by Parsons et al. (1970) show that nutrient levels in the Strait of Georgia are high enough not to be limiting factors in production, so that we will completely neglect the dependence of $P_m$ on nutrient concentrations. Possible values of $P_m$ will range from $4.4 \times 10^{-4}$ to $12.4 \times 10^{-4}$ g carbon/g chlorophyll/sec, depending on the mean temperature of the plume (and thus on the time of the year).

To take into account the effect of respiration (i.e. that there exists a minimum energy requirement to maintain life without growth) the concept of a compensation light intensity $I_c$ (Parsons and Takahashi, 1973, p. 64) is introduced into (5.1), which now becomes

$$P = \alpha b P_m (I - I_c) \exp(1 - b(I - I_c)) \qquad (5.3)$$

This equation is valid only for $I \geq I_c$. For $I < I_c$, P will be taken as equal to zero (Fig. 11 ). Values of $I_c$ measured by Parsons, Stephens and LeBrasseur (1969) over four months vary from 0.006 to 0.01 ly/min. A constant value consistent with those data will be taken for any one simulation.

As indicated by Caperon (1967), the concept of constant respiration implied by (5.3) is not likely to be valid for all light intensities. However, in the abscence of a better expression, equation (5.3) accounts for the effect of respiration.

The carbon to chlorophyll ratio varies from 25 for vigorously growing phytoplankton in the presence of excess nitrate to 60 for unhealthy organisms in nitrate depleted water (Antia et al., 1963). A fairly conservative value of 40 has been used here, thus giving a conversion factor $\alpha = .025 = 1/40$.

An expression for zooplankton grazing of phytoplankton has been given by Ivlev (1961). The rate of chlorophyll removal by grazing ($\mathcal{G}$ = mg of chlorophyll/m³/time) is

$$\mathcal{G} = Z G \left( 1 - \exp(-d_1 n) \right) \tag{5.4}$$

where Z is the zooplankton (wet weight) density in mg/m³, G the maximum grazing rate in units of milligrams of chlorophyll per milligram of zooplankton per unit time, $d_1$ is a constant with units of m³/mg of chlorophyll and $n(x,y,z)$ is the chlorophyll concentration as before. A nearly equivalent expression has been used here,
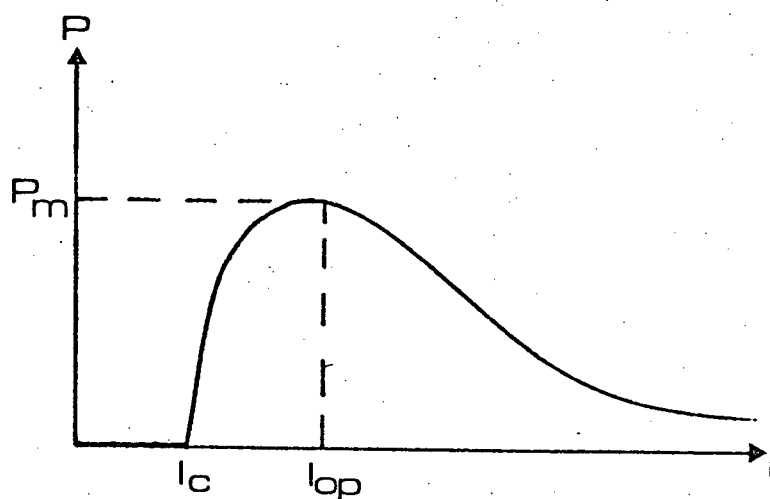
Fig. 11.  Chlorophyll production rate, P, as a function of light intensity, I; equation (5.3).

$$\mathcal{Y} = Z G \frac{n}{d_2 + n} \tag{5.5}$$

where $d_2$ is another constant with the dimensions of milligrams of chlorophyll per unit volume. The choice of (5.5) instead of (5.4) is primarily motivated by the fact that the second expression is easier to integrate over the upper layer for the vertical dependences of n chosen below. The expression (5.5) shows a similar behaviour to Ivlev's relation (Fig. 12 ), but increases more slowly. Over a limited range of n, the two expressions may be made to agree closely by appropriately selecting the constant $d_2$; this is indeed the case over the region of interest, with n generally varying less than an order of magnitude (Parsons, Stephens and LeBrasseur, 1969; Parsons et al., 1970).

On the basis of figures given by Parsons and Takahashi (1973) a value of $d_2$ = 5 mg/m³ was used. This results in an ingestion rate of half the maximum rate for chlorophyll concentrations of 5 mg/m³ and about 0.83 of the maximum rate at 25 mg/m³.

The voracity of zooplankton organisms varies with the species considered and with the life stage of any one species. Figures quoted by Parsons and Takahashi (1973) led us to use an ingestion rate equal to 70% of the wet weight per day. Combining this with an average dry to wet weight ratio of about 0.2 and a carbon to dry weight ratio of 0.5, as drawn from the data given by the same authors, and with the carbon to chlorophyll conversion factor ( $\alpha$ = 1/40) used above, we
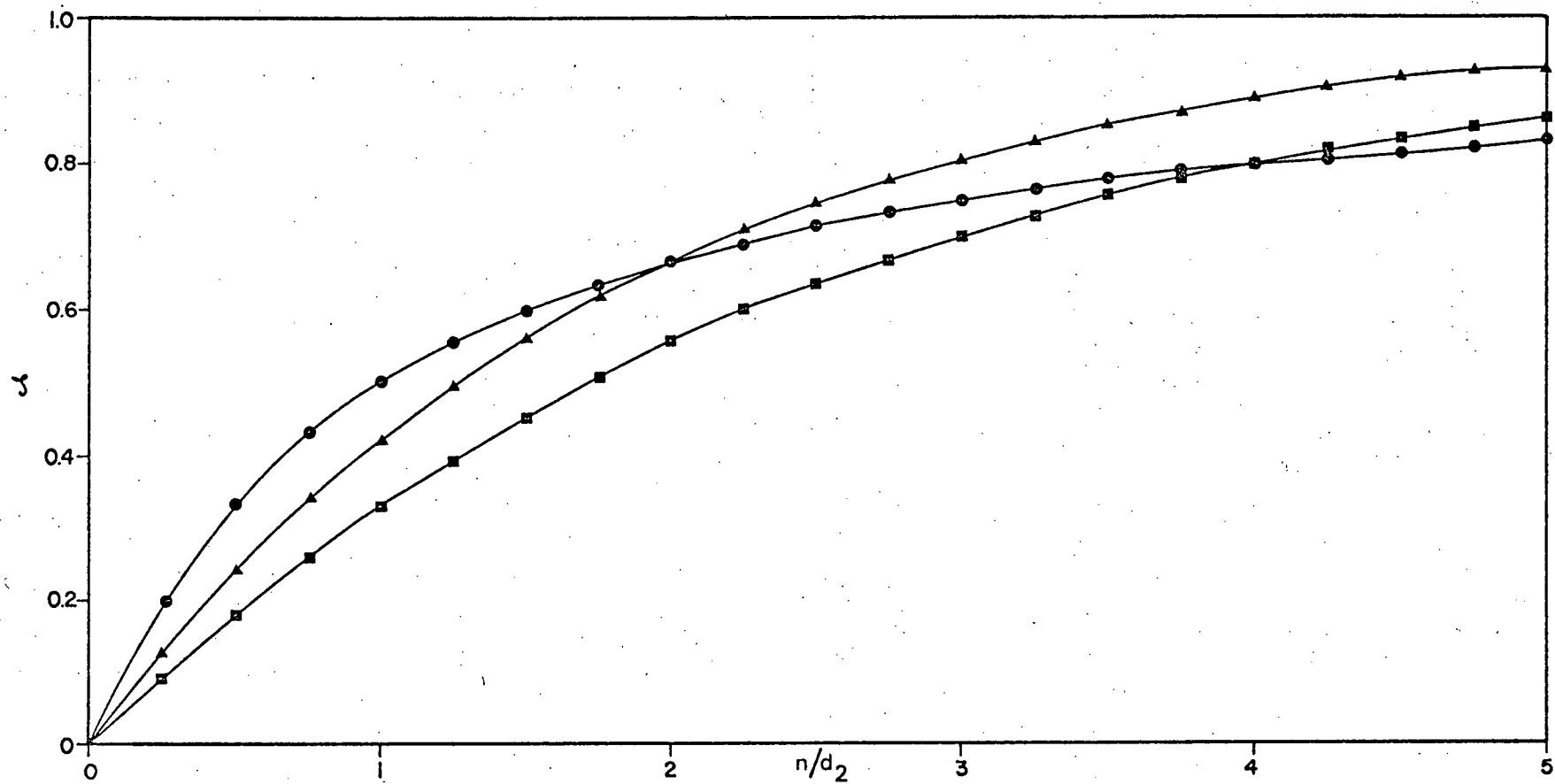
Fig. 12.   Comparison of the curves from equations (5.4) and (5.5); ● eqn. (5.4); ▲ eqn. (5.5), $d_2 = \ln 3/2 d_1$ ; ▦ eqn. (5.5), $d_2 = \ln 5/4 d_1$ .

calculate G as

$$G = \frac{0.7}{24 \times 3600} \times 0.2 \times 0.5 \times \frac{1}{40} \simeq 2 \times 10^{-8} \frac{mg\ chlorophyll}{mg\ zooplankton-sec}$$

A somewhat lower value ($G = 1 \times 10^{-8}$) is found if the results of Stephens et al. (1969) are used for the wet to dry weight conversion. As all these factors are likely to be quite variable (especially the ingestion rate), we will stick to the $G = 2 \times 10^{-8}$ mg chlorophyll/mg zooplankton-sec value.

The sinking rate is usually written as

$$S = w_s \frac{\partial n}{\partial z} \qquad (5.6)$$

following Riley et al. (1949), with $w_s$ a sinking speed. Smayda (1970) gives values of $w_s$ between 0 and 30 m/day for sinking rates of living phytoplankton, based on observations on about 25 species. Values used in the present calculations range from $1.2 \times 10^{-5}$ m/sec to $5.8 \times 10^{-5}$ m/sec (1 to 5 m/day).

The local source strength Q is then the sum of the above three effects:

$$Q = nP + \mathcal{S} + S \qquad (5.7)$$

What is needed is the integral of Q over the upper layer.

As the upper layer is continuously agitated by wind waves and by internal waves (Gargett, 1976), the turbulence level in the upper few meters is quite high, and the near-surface phytoplankton crop will be carried back and forth vertically over a depth range of a few meters by mechanical mixing. Besides, phytoplankton from near the surface will also gradually

sink down with a small velocity $w_s$. A typical phytoplankton organism will thus experience, over a period of a few hours, light conditions which are averaged over a certain depth. We shall assume conditions in the upper layer to be turbulent enough to use the averaged light intensity $\bar{I}$, given by

$$\bar{I} = \frac{1}{h} \int_{-h}^{0} I_o \exp(\mu z) \, dz \qquad (5.8)$$

with $\mu$ the extinction coefficient (in $m^{-1}$) and $I_o$ the light intensity at the surface, as representative of conditions experienced by the whole upper layer phytoplankton population. The photosynthetic available radiation (PAR) lies in the wave length range 400-700 nm. Following Takahashi et al. (1973), we use Strickland's (1958) assumption that the PAR at the sea surface is one half the total solar radiation at the surface. The radiation intensity varies with cloud cover and sea roughness but the best we can do here is to use monthly mean insolation values for $I_o$, as computed by Parsons, Stephens and LeBrasseur (1969). $I_o$ will then denote only the PAR; its values range from 0.03 to 0.10 ly/min. The average value $\bar{I}$ is readily estimated from (5.8) as

$$\bar{I} = \frac{I_o}{\mu h} \left( 1 - \exp(-\mu h) \right) \qquad (5.9)$$

Values of $\mu$ have been calculated from unpublished data provided by T.R. Parsons for the Fraser River plume itself and range from 0.3 to 0.8 $m^{-1}$ for the period of interest. These values agree closely with other measurements in this region (Parsons, 1965).

The integrated value of  nP  will then be

$$\int_{-h}^{0} \nu M \overline{P} \, dz = M \overline{P} \int_{-h}^{0} \nu \, dz$$

where $\overline{P}$ is the photosynthetic rate corresponding to the  average light intensity $\overline{I}$.  Using (3.3),

$$M \overline{P} \int_{-h}^{0} \nu \, dz = M \overline{P} h \qquad\qquad (5.10)$$

The integral of zooplankton  grazing  will  depend  on  the vertical  dependence  used for n, i.e. on the function $\nu(x,y,z)$. The integrated sinking rate is simply

$$\int_{-h}^{0} S \, dz = w_s(0) \, n(0) - w_s(-h) \, n(-h)$$

Since the flux through the upper surface, at z = 0, must be zero (we  can  integrate to z = 0 + $\epsilon$, where n(0 + $\epsilon$) = 0, since that is in the air, above the water surface, and let $\epsilon \to 0$  to  show that the first term must vanish), the net rate of sinking out of the upper layer is

$$\int_{-h}^{0} S \, dz = - w_s(-h) \, \nu(-h) \, M \qquad\qquad (5.11)$$

The integrated source strength is then

$$\int_{-h}^{0} Q \, dz = M \left\{ \overline{P} h - G \int_{-h}^{0} Z \left( \frac{\nu}{d_2 + \nu M} \right) dz - w_s(-h) \nu(-h) \right\} \qquad (5.12)$$

In  a completely horizontally non-divergent upper layer and

with horizontally independent $\nu$, the right hand side of (5.12) would be the only contribution to changes in chlorophyll. The local relative importance of photosynthetic growth rate, zooplankton grazing and sinking would then completely determine the distribution of chlorophyll a in the upper layer. One could then write (5.12) as

$$\int_{-h}^{0} Q \, dz = M \, \phi(x,y)$$

and if $\phi$ (x,y) were a constant, integrate (3.9), or rather its time dependent formulation (4.3) to find

$$M = M_o \exp \phi t \qquad (5.13)$$

The simple exponential growth represented by (5.13) is readily understood as arising from the balance of the various source terms which make up $\phi$ (x,y). In a non-uniform flow field, (5.13) may still be regarded as determining instantaneous local chlorophyll variations. This purely local behaviour may of course be completely masked by the other terms present in H(M,U,V,x,y) (equation 4.3), arising from the non-homogeneity of the flow field. The simplest example of this masking effect is obtained by comparing the sinking term $-Mw_s$ (-h) $\nu$(-h) with the vertical advection term Mw(-h) $\nu$(-h) which occurs in (3.8); it is obvious that the two vertical transport terms are opposite in their action and that sinking or ascent takes place according to the sign of ($w_s$ (-h) - w(-h)). More detailed comparisons of the relative influence of local sources to flow divergence on phytoplankton distribution will be given later. The obvious

lesson that we may expect to learn from solving (4.1) to (4.3) along pathlines is that the kinematics of the flow field may play a very significant role in establishing the observed pattern of phytoplankton distribution. It is a comforting thought however, that since the advective processes merely redistribute phytoplankton and neither create nor destroy it, a chlorophyll balance performed over the whole volume of interest will be independent of the flow pattern and will reflect the net effect of the source term Q, integrated over that volume. Our assumption of time-independence thus implies that the total quantity of chlorophyll in the volume of water considered is constant and that, over the whole volume, a balance has been reached between production, grazing and sinking:

$$\iiint Q(x,y,z) \, dx \, dy \, dz = 0$$

Although this is not true over a period in the order of months, over a few days this is certainly valid.

# CHAPTER 6. DATA

In order to obtain realistic values for the parameters in the model it was necessary to make simultaneous measurements of the most important parameters. Although quite a large amount of data had been collected in Georgia Strait, the nature of our problem required that the biological parameters be measured in the Fraser River plume. Since the major variations occured in a downstream direction it was decided to take measurements along the axis of the plume. This presented some problems since the plume is influenced by both wind and tide and the area to be covered was quite large.

The C.S.S. Vector was the vessel used for the measurements. The data were collected in conjunction with work being done by T.R. Parsons of the Institute of Oceanography, U.B.C. in the Fraser River plume. Temperature and salinity profiles were measured as well as the photosynthetic radiation. As part of the biological program chlorophyll and zooplankton samples were also collected. At a later date an attempt was made to measure the horizontal distribution of chlorophyll $\underline{a}$ using a fluorimeter. We had no success since the scatter in the calibration curve was of the same magnitude as the observed fluctuations in the fluorimeter output.

For the first cruise in the series (Gulf 1, November, 1971) the plume position was determined visually from a small aeroplane. The boundaries and general extent of the plume were relayed to the ship. A series of ten stations (Fig. 13 ) were then occupied as rapidly as possible up to 32 km from the mouth of the Main Arm of the Fraser River. For the second cruise
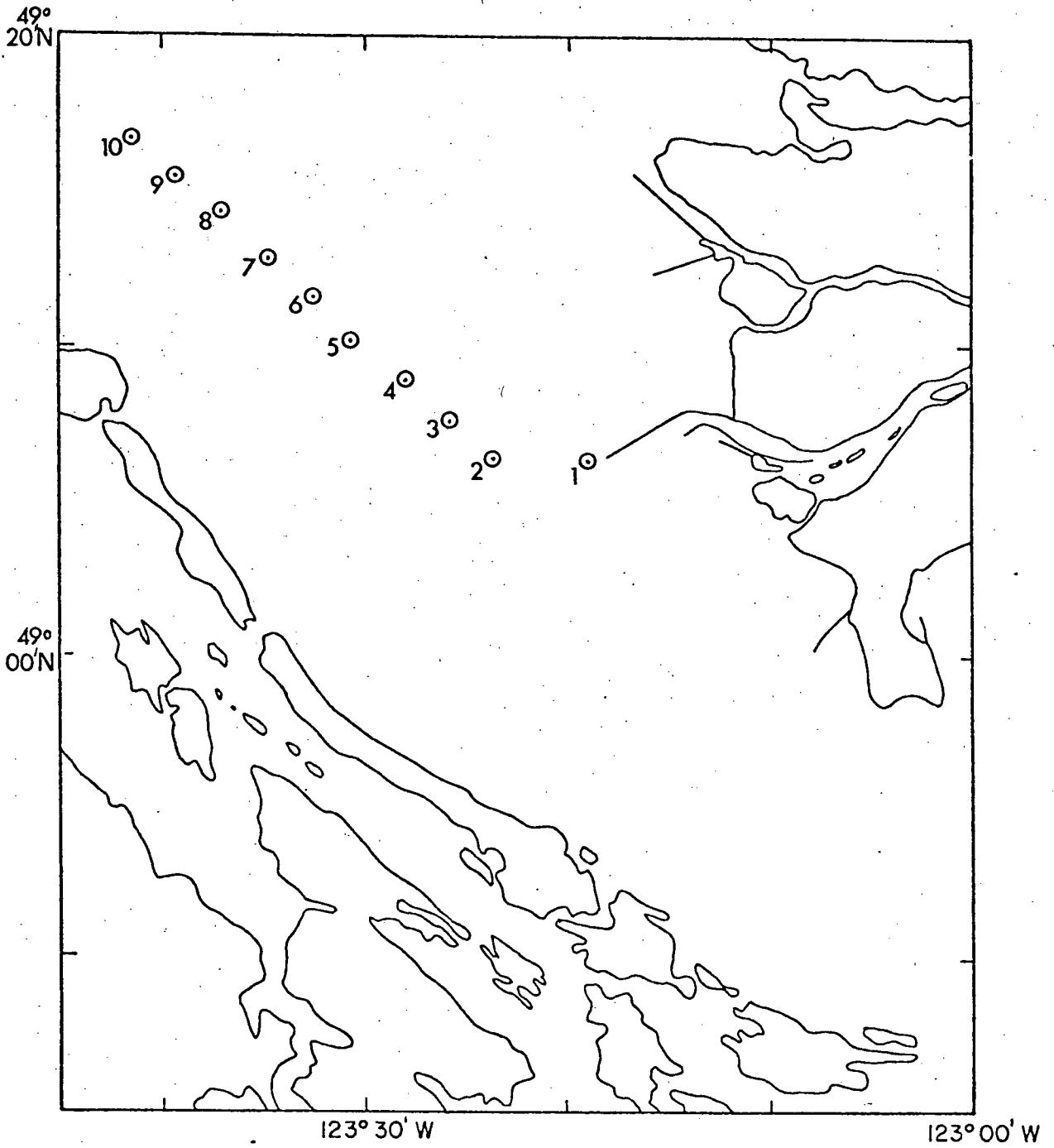
Fig. 13.   Location of stations, cruise Gulf 1; November, 1971.

(February, 1972), a different method of determining the plume position was attempted since it was not possible to obtain the use of an aircraft. The method was to take salinity and temperature profiles in the upper 20 meters in a coarse grid of stations and then deduce the plume position (Fig. 14 ). The drawback of this approach was that one does not obtain an instantaneous picture and that, by the time the ship is in position to start the main series of stations, the plume may have changed significantly. This time, a series of stations was occupied along lines radiating out from the mouth of the river. No success was achieved in following the axis of the plume. Visual observation from the ship was also unsuccessful in determining the plume position due to the small angle between the line of sight and the water surface. For simplicity, later cruises occupied stations whose positions were unchanged for the remainder of the program. These stations (Fig. 15 ) were chosen to extend from the river mouth to the north west. Although these stations were not always in the same location relative to the plume, the positions were consistant from cruise to cruise and time was not spent attempting to locate the plume each time.

Salinity and temperature profiles were measured with an Industrial Instruments RS 5. The accuracy for these measurements is taken to be $\pm$ 0.1‰ and $\pm$ 0.1 C$^o$. Fig. 16 shows the salinity profiles from cruise Gulf 1, while all the salinity and temperature data are presented in the Appendix. The vertical extinction coefficients were determined using a $2\pi$ light meter fitted with a selenium cell. With this instrument the light intensity at depth is compared with the intensity at
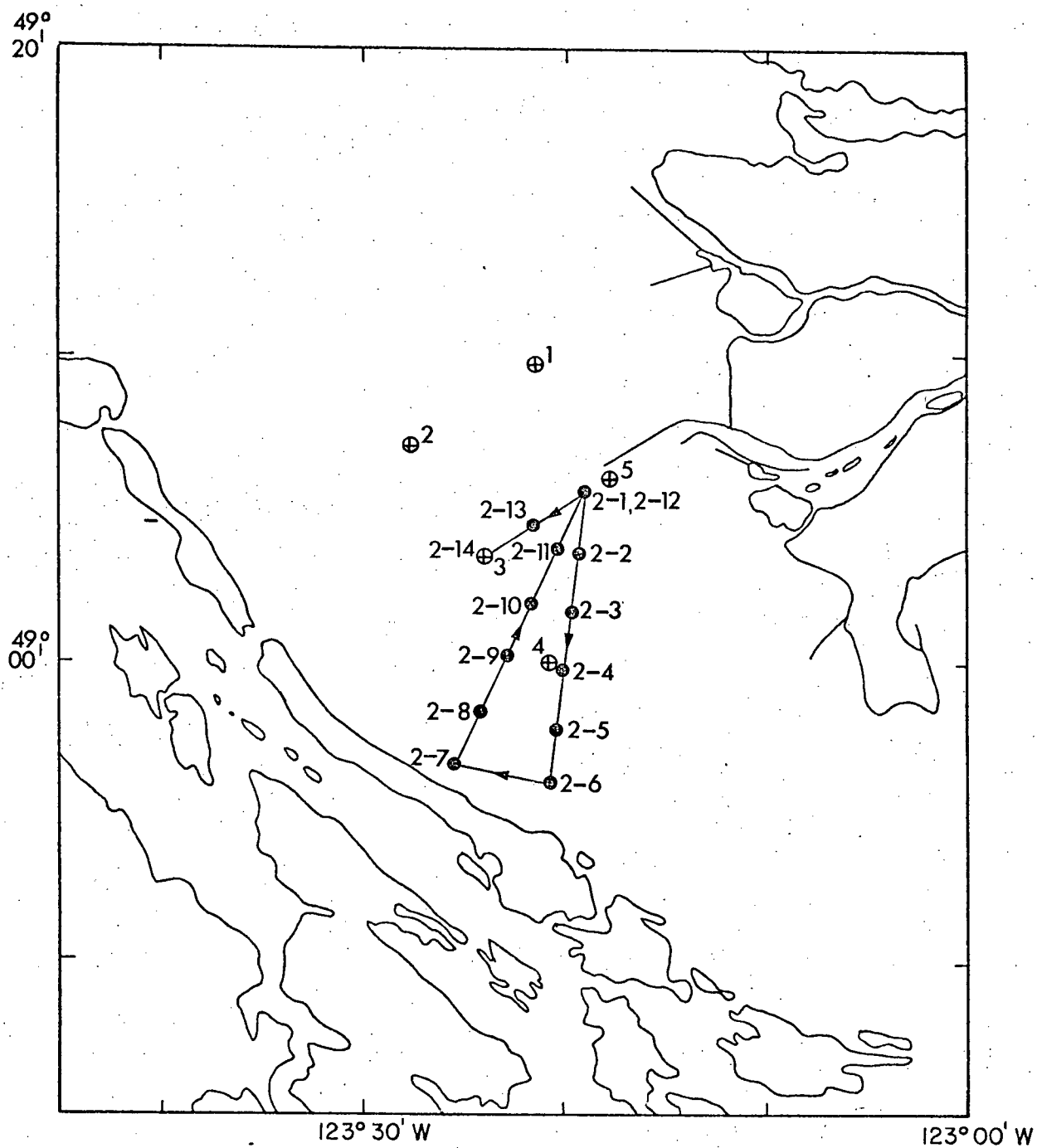
Fig. 14. Location of stations, cruise Gulf 2; February, 1972.
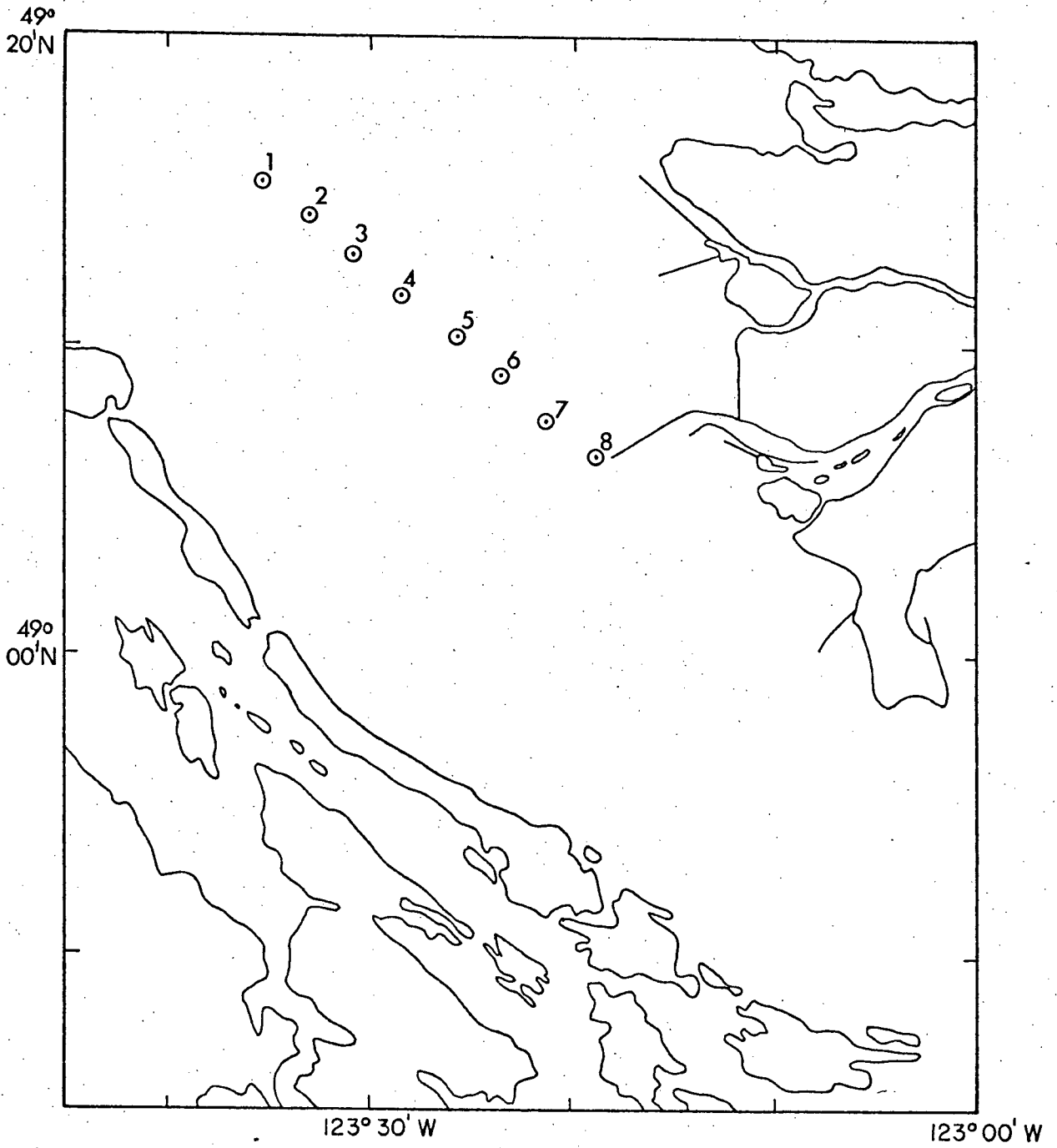
Fig. 15.   Station positions, cruise Gulf 3 and subsequent cruises.
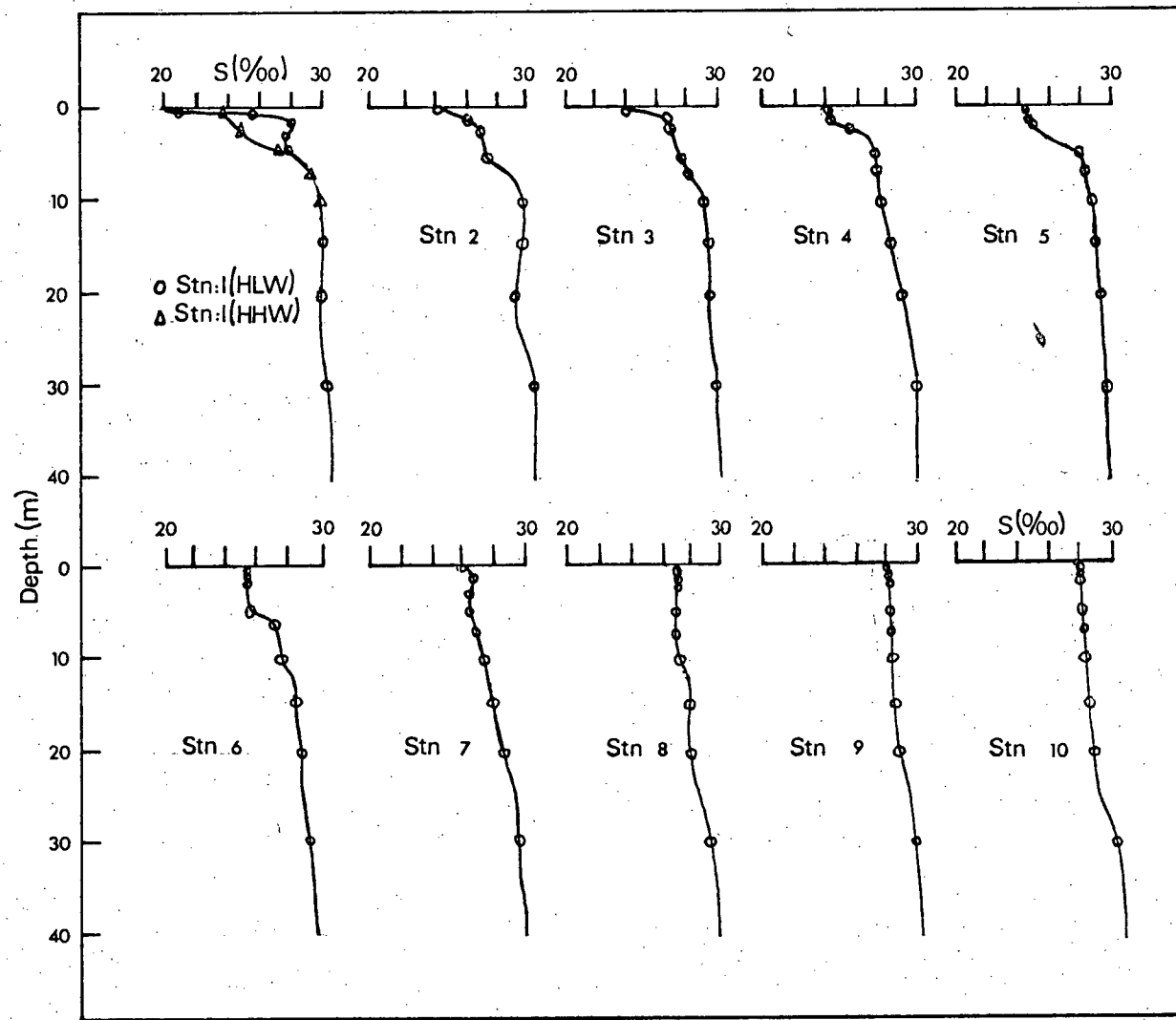
Fig. 16. Salinity profiles from cruise Gulf 1.

the surface, hence extinction coefficients may be calculated. The expected accuracy of the extinction coefficients is $\pm$ 0.05 m$^{-1}$. Fig. 17 gives some sample profiles of the light intensity while Fig. 18 shows the variation of the extinction coefficient with position in the plume. Aside from the extinction coefficient, other parameters were derived from the data. The salinity and temperature profiles were used to determine the depth, h, and the density, $\rho$ , of the plume as a function of distance from the river mouth. The expressions (described later) were fitted using the data from the Gulf 1 cruise since this was the only cruise where the stations were known to be reasonably close to the axis of the plume. While data from one cruise can not be representative of a whole year, certainly during the winter and spring pre-freshet period one would expect the basic characteristics to remain unchanged. Hence the same functions were used for the whole period modelled but the magnitude of the parameters was varied as appropriate.
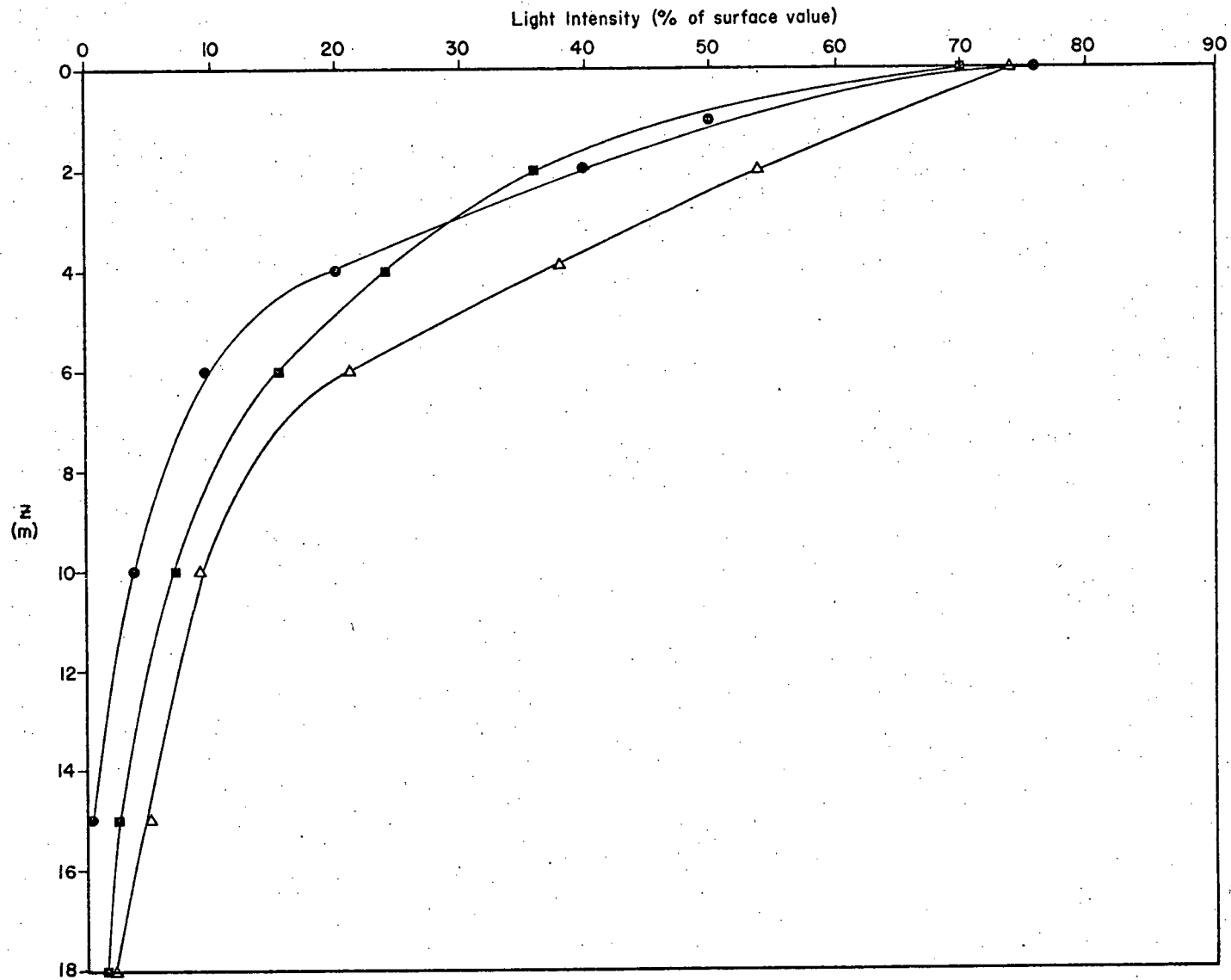
Fig. 17. Light intensity (% of surface value) as a function of depth.
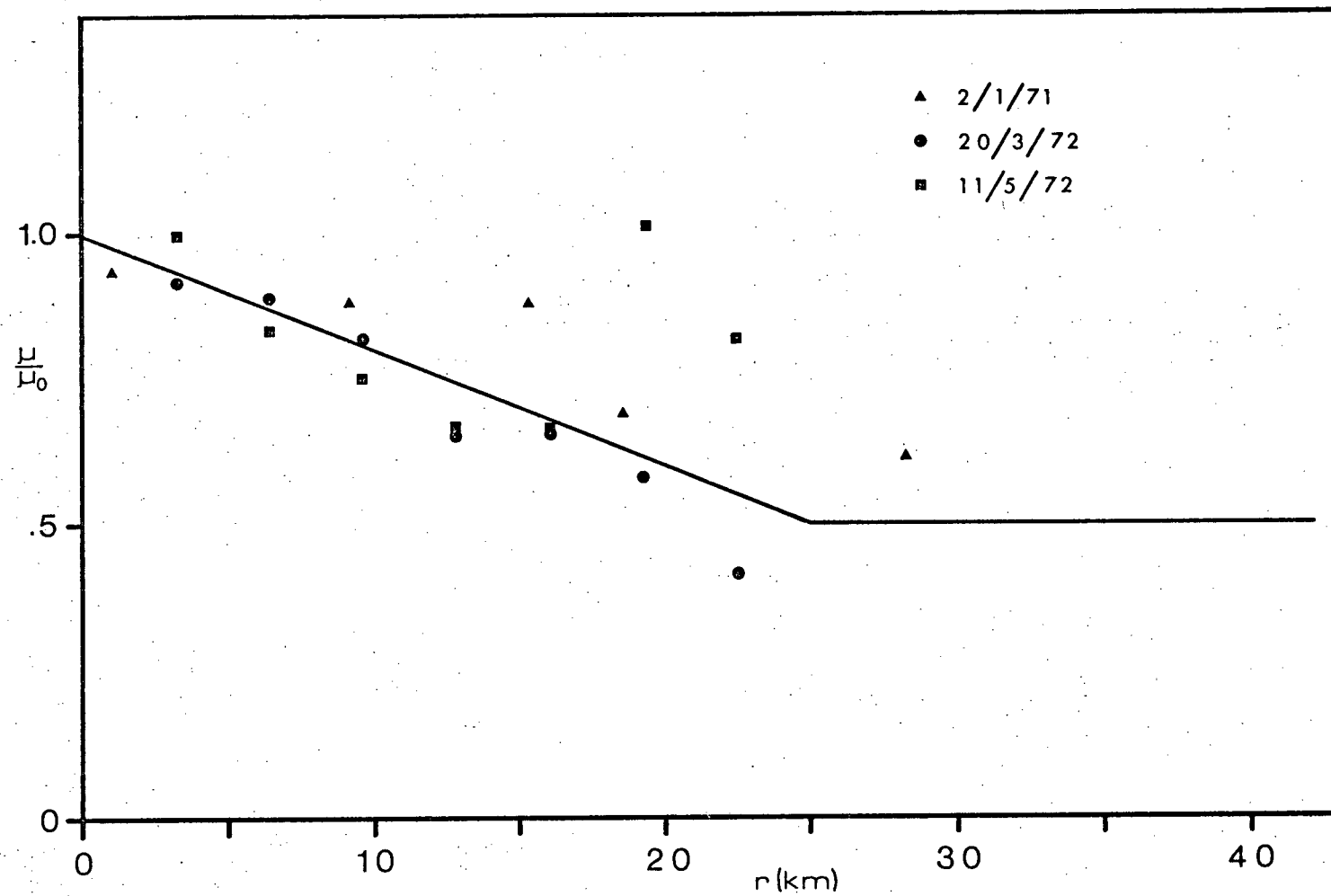
Fig. 18. Non-dimensionalized extinction coefficient, $\mu/\mu_0$, as a function of distance from the river mouth.

# CHAPTER 7. MODEL I: FORMULATION

The pair of models for which results are now presented may be considered as the first two stages in a sequence which will hopefully converge in a small number of steps to a realistic representation of biological-physical interactions in the area of interest. The first model is overly simplistic: the flow field plays a purely advective role in a greatly idealized set of conditions, carrying phytoplankton through areas of different values of the integrated source term. This model is idealized on purpose, to present us with a clearly comprehensible situation, where the influence of the various parameters is easily interpreted. This first attempt may be considered as an introduction to the second, more complex model. The basic premises on which model I is based are listed in this section, together with a discussion of their consequences. Numerical values for the parameters are also introduced and their choice justified. The actual results and their interpretation appear in the next chapter.

The parameterizations associated with the geometry and the current pattern are discussed first (i-iv), followed by the biological components (v-vii).

i) The depth of the upper layer is everywhere the same:

$$h = constant \qquad (7.1)$$

The observed depth of the upper layer actually varies down the plume, but this complication will be included in the second model. In model I, uniform values of h between 2 m and 30 m will be used.

ii) From (7.1) and (2.7), it follows that the profile function $\gamma(x,y,z)$ must also be independent of horizontal position. Experiments performed by Stefan and Schiebe (1970) on the discharge of hot water into a tank suggest a simple parameterization of the profile in the upper layer in terms of the readily integrable function

$$\gamma = \exp(\beta z) \tag{7.2}$$

In view of equation (2.7), $\beta h$ must satisfy

$$\beta h + \exp(-\beta h) = 1 \tag{7.3}$$

iii) The entrainment velocity is simply written

$$w(-h) = m\, U \tag{7.4}$$

which implies that the downstream velocity U is much larger than the cross-stream component V, and also much larger than the critical velocity $U_c$. Both assumptions are probably justifiable near the river mouth, before there is any appreciable spreading of the plume. Once more, the complexities of the full entrainment formula (2.4) are reserved for the more realistic second model.

A numerical value of m was estimated from the salt balance of the plume. Assuming that the increase in salinity observed along the axis of the plume is due uniquely to vertical entrainment from the lower layer, and not from lateral mixing, an estimate of the entrainment velocity w(-h) may be found as follows. Consider a longitudinal segment of the upper layer, as

shown in Fig. 19 . The mass balance is satisfied by

$$U_1 h_1 = U_o h_o + w(-h)L \qquad (7.5)$$

and the salt balance by

$$U_1 h_1 S_1 = U_o h_o S_o + w(-h)LS_b \qquad (7.6)$$

Eliminating $U_1 h_1$, we find

$$\frac{w(-h)}{U_o} = \frac{h_o}{L} \frac{S_1 - S_o}{S_b - S_o} \qquad (7.7)$$

Estimates of the quantities entering the right hand side of (7.7) were made from data gathered by the author on the Gulf 1 cruise already discussed in Chapter 6. Values of the salinity differences between pairs of stations and of the appropriate depth $h_o$ and separation L are shown in Table I . The ratio $w(-h)/U_o$ varies over a wide range of values (from $10^{-5}$ to $4 \times 10^{-3}$). Due to the very low stratification at downstream distances greater than about 25 km, it is probable that the thickening of the upper layer observed beyond Station 8 may be due in part to wind mixing and not to upward entrainment. Accordingly, only the first seven values of Table I were used to form an estimate of m, finding a value of

$$m = 2.4 \times 10^{-4} \qquad (7.8)$$

This estimate is very close to that of Keulegan (1966), who obtained a value of $m = 2.12 \times 10^{-4}$ from experiments in a small scale model.

Under the assumptions (7.1), (7.2) and (7.4), the average horizontal velocity components in the upper layer now obey a simplified form of (2.10):

$$\frac{\partial U}{\partial x} + \frac{\partial V}{\partial y} = \frac{mU}{h} \qquad (7.9)$$
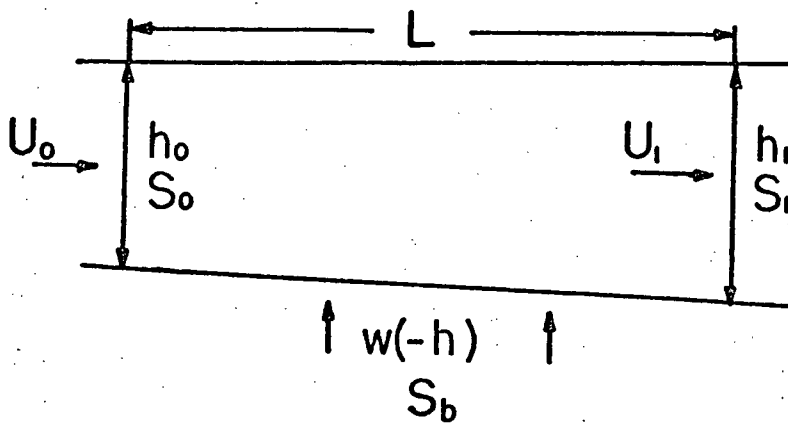
Fig. 19. A segment of the upper layer, showing the quantities used to derive Table I.

TABLE I. Evaluation of entrainment from cruise Gulf 1 data.

| Stn. pair | Separation L (m) | Depth $h_o$ (m) | $(S_1 - S_o)$ ‰ | $(S_b - S_o)$ ‰ | $\dfrac{w(-h)}{U_o}$ |
|---|---|---|---|---|---|
| 1 - 2 | $4.8 \times 10^3$ | 2 | 0.4 | 1.1 | $1.5 \times 10^{-4}$ |
| 2 - 3 | $3.2 \times 10^3$ | 1 | 0.8 | 0.7 | $3.6 \times 10^{-4}$ |
| 3 - 4 | $3.2 \times 10^3$ | 5 | $\sim 0.01$ | 1.2 | $\sim 10^{-5}$ |
| 4 - 5 | $3.2 \times 10^3$ | 5 | 0.2 | 1.3 | $2.4 \times 10^{-4}$ |
| 5 - 6 | $3.2 \times 10^3$ | 5 | $\sim 0.01$ | 1.4 | $\sim 10^{-5}$ |
| 6 - 7 | $3.2 \times 10^3$ | 7 | 1.3 | 0.8 | $3.6 \times 10^{-4}$ |
| 7 - 8 | $3.2 \times 10^3$ | 7 | 0.2 | 0.8 | $5.5 \times 10^{-4}$ |
| 8 - 9 | $3.2 \times 10^3$ | 15 | 0.7 | 0.8 | $4.1 \times 10^{-3}$ |
| 9 - 10 | $3.2 \times 10^3$ | 30 | 0.2 | 1.4 | $1.3 \times 10^{-3}$ |

Since U > 0, the upper layer flow is everywhere divergent, pathline separation increases downstream and, in the absence of source terms, the density of any passive scalar carried by the flow will decrease downstream. This decrease is a direct consequence of dilution with entrained water. Only in the case where the lower layer is as rich as the upper one in that passive scalar will there be no dilution and hence no downstream decrease in concentration.

Choosing w(-h) independent of V allows direct integration of (2.11). Using (7.1) and (7.4), the coefficients f(x,y) and g(x,y), given by (2.12) and (2.13) take explicit forms

$$f(x,y) = 0 \; ; \qquad g(x,y) = \frac{mU}{h} - \frac{\partial U}{\partial x} \qquad (7.10)$$

Hence,

$$V(x,y) = \int \left( \frac{mU}{h} - \frac{\partial U}{\partial x} \right) dy + const. \qquad (7.11)$$

In the abscence of the Coriolis force, V will be antisymmetric about the downstream axis, so that we may assume V(x,0) = 0, which fixes the constant of integration. Recalling U(x,y) as written in (2.3), (7.11) becomes

$$V(x,y) = \left( \frac{m}{h} + \frac{1}{x+x_0} \right) \int_0^Y U \, dy$$

$$- \frac{2k_2}{(x+x_0)^3} \int_0^Y y^2 U \, dy \qquad (7.12)$$

Numerical values for $\dot{V}(x,y)$ are calculated from the resulting analytic expression. The three dimensional structure of the river plume is now completely specified by equations (2.3), (7.4) and (7.12). Typical flow fields and streamline patterns are depicted in the next section (Figs. 23,24,31,32).

iv) The plankton profile function $\nu(x,y,z)$ is also taken horizontally uniform. In addition, the vertical structure is ignored and we use

$$\nu = 1 \qquad -h < z \leq 0 \qquad (7.13)$$

The only justification behind this choice is its extreme simplicity. More complex profiles, based on data, will be used in model II.

The integral $\Omega$ of the product of the profile functions, as defined in (3.7), reduces to

$$\Omega = h \qquad (7.14)$$

The upper-layer chlorophyll density equation (3.8) then takes the particularly simple form

$$U\frac{\partial M}{\partial x} + V\frac{\partial M}{\partial y} = \frac{1}{h}\int_{-h}^{0} Q\, dz - \frac{mUM}{h}(1-\nu(-h)) \qquad (7.15)$$

with $\nu = 1$, as per (7.13), and $\nu$ continuous across $z = -h$, the last term on the right hand side of (7.15) vanishes. There is then no dilution of chlorophyll concentration due to entrainment and the only contribution to changes in $M$ is from the local source terms. The role of the flow field is then simply to carry parcels of water through areas of varying strength of the

source term. Such an advective role may of course be extremely important in determining the overall shape of the chlorophyll distribution, since the amount of time spent in regions of positive or negative source strength, and hence the ultimate concentrations reached due to the effect of such sources, will depend directly on the local strength of the flow. At the opposite extreme, we might consider a vertical chlorophyll profile with $\mathcal{V} = 1$ for $-h < z \leq 0$, $\mathcal{V} = 0$ for $z \leq -h$. In that case, there would be a velocity dependent dilution effect in (7.15), decreasing with U away from the mouth of the river and away from the axis of the plume. An examination of both extreme cases will provide us with an estimate of the role of dilution by entrainment.

We now pass to a discussion of the biological parameters.

v) A considerable amount of silt is usually found in suspension at the mouth of the Fraser River. The extinction coefficient $\mu$ is increased by the presence of suspended particulate matter and this dependence affects the mean light intensity $\overline{I}$ and in turn the average photosynthetic rate $\overline{P}$. The silt load is pictured as decreasing away from the river mouth according to an elliptical distribution illustrated in Fig. 20 . Thus if s(x,y) is the silt load, it takes constant values on the ellipses

$$x^2 + 4y^2 = r^2 \qquad (7.16)$$

with s(r) a decreasing function of r. This distribution is not meant to reflect any observed conditions but merely gives a plausible pattern in the area of the river mouth.

Direct measurements of the extinction coefficient were
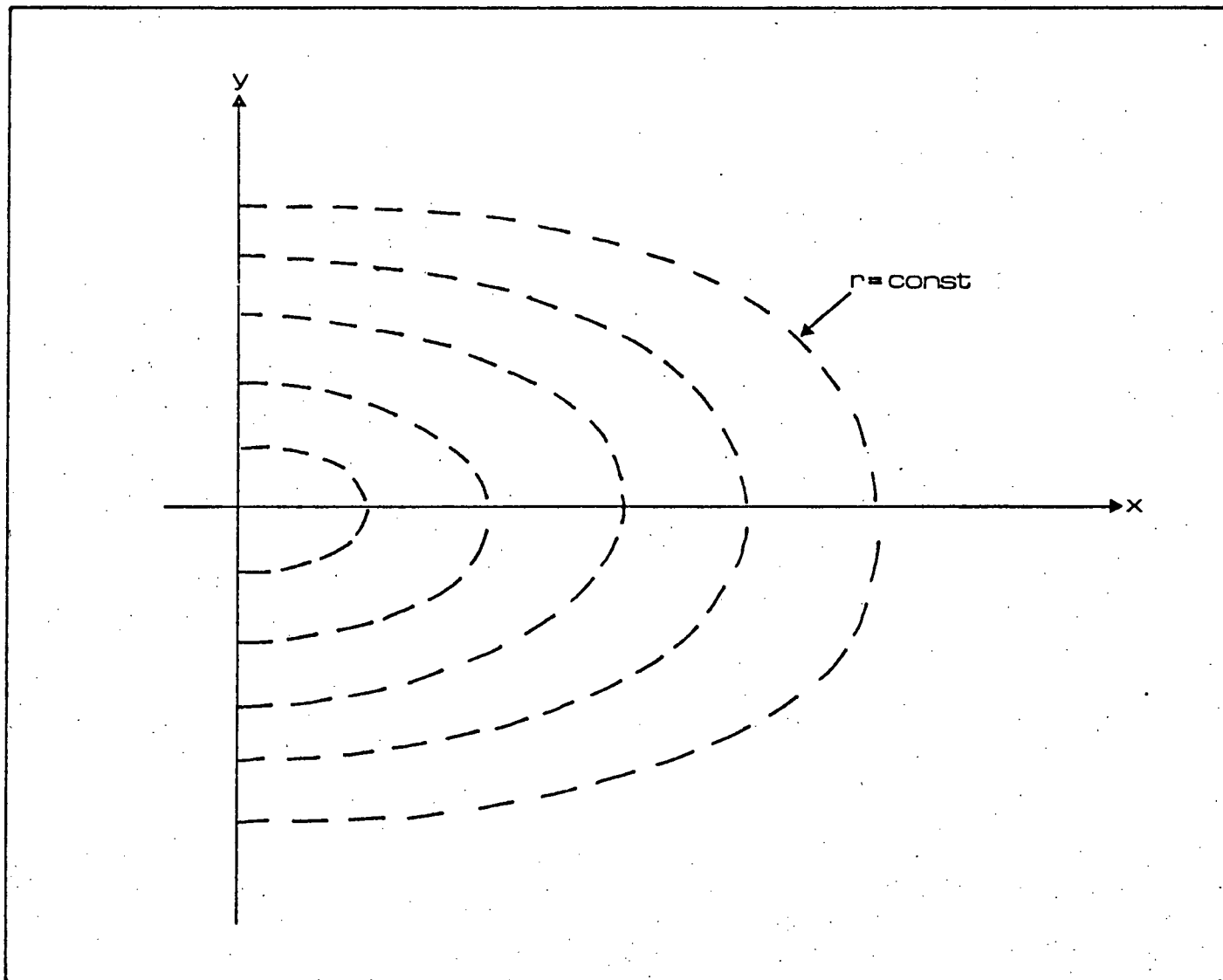
Fig. 20. Elliptical distribution of contours of r = constant (from equation (7.16)).

taken in the Fraser River plume (Chapter 6 ) and suggest a distribution of $\mu$ according to

$$\mu = \mu_0 \left(1 - \frac{r}{2r_0}\right) \qquad o \le r \le r_0$$

$$\mu = \frac{\mu_0}{2} \qquad\qquad r_0 \le r \tag{7.17}$$

as shown in Fig. 18, with $r_0 = 2.5 \times 10^4$ m. Values of $\mu_0$ have been taken in the range $0.3\ m^{-1} \le \mu_0 \le 0.8\ m^{-1}$ based on the measurements.

vi) It has already been seen in Fig. 5 that there is a semi-annular maximum in the zooplankton distribution off the mouth of the Fraser River. Data collected during the cruises show similar maxima (Fig. 21 ). This kind of distribution has been represented by the Gaussian form

$$Z = Z_1 + Z_m \exp\left\{-c_2(r-r_1)^2\right\} \tag{7.18}$$

centered about $r_1 \simeq 8 \times 10^3$ m, with $c_2 = 5.0 \times 10^{-8}\ m^{-2}$ and with r as given in (7.16). The zooplankton concentrations $Z_1$ and $Z_m$ vary seasonally from minimum values of 15 and 35 mg/m³ in mid-winter to 450 and 1050 mg/m³ in May and June.

vii) The integrated zooplankton feeding term in (5.12) reduces, for $\nu = 1$, to

$$\int_{-h}^{o} \mathcal{S}\, dz = -\frac{MGZh}{d_2 + M} \tag{7.19}$$

For the purpose of this first model, this has been simplified further by approximating the M dependence by a pair of straight lines (see Fig. 22 ), so that the zooplankton feeding term over
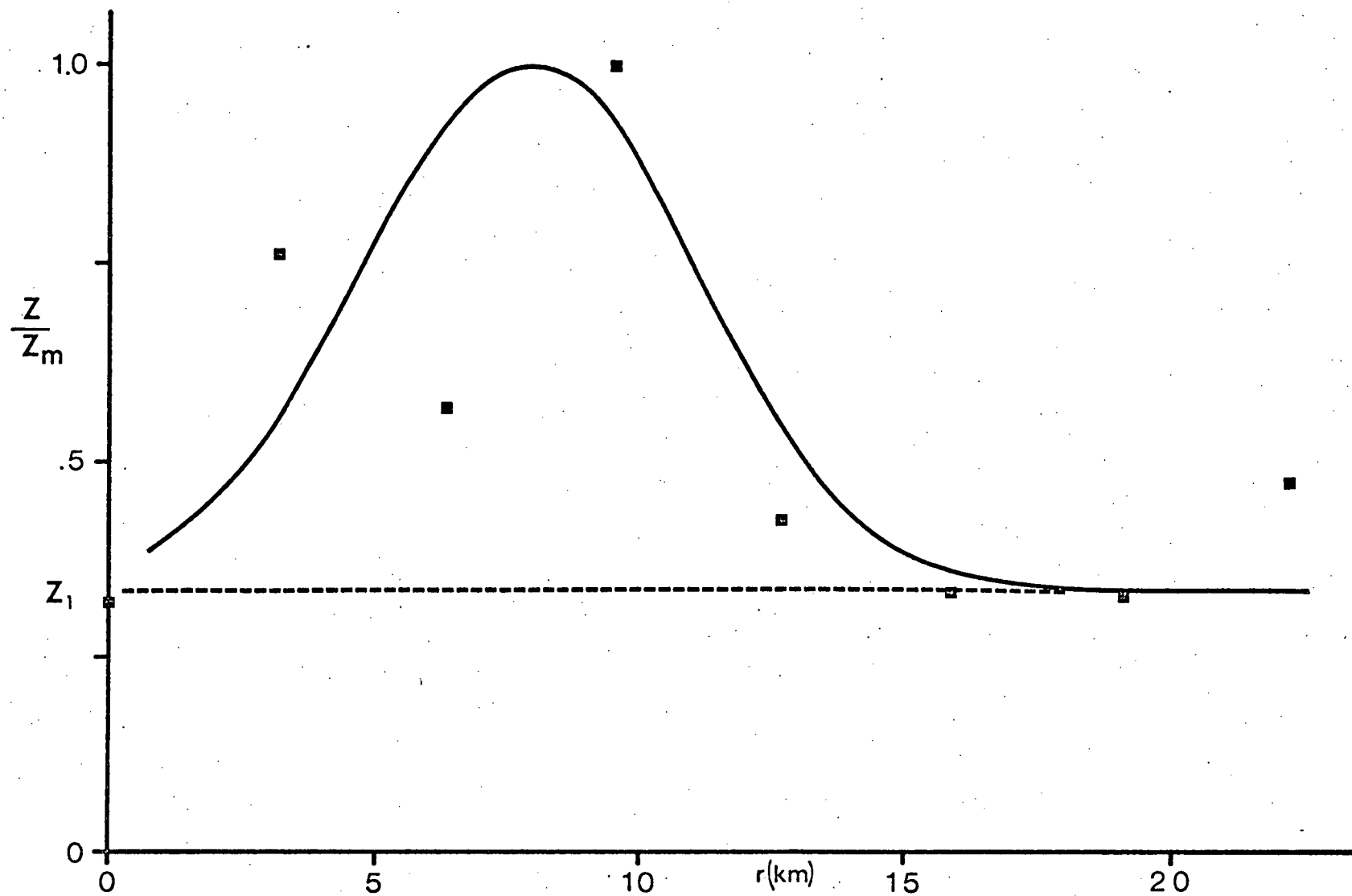
Fig. 21. Average zooplankton distribution as a function of distance from the river mouth; solid line represents eqn. (7.18).
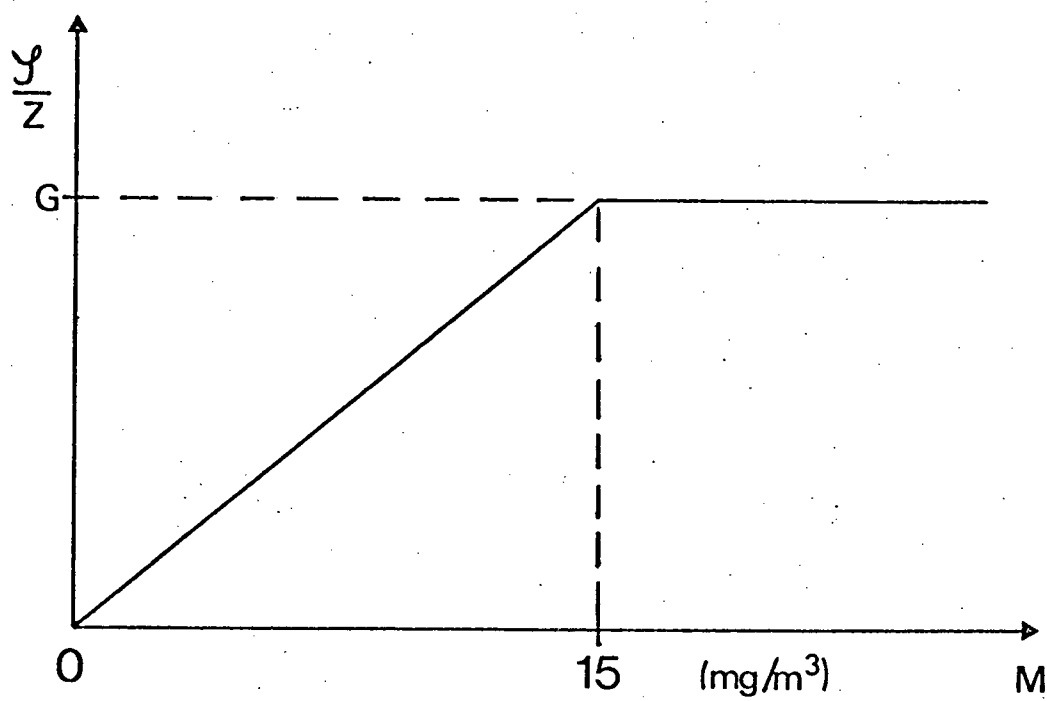
Fig. 22.   The grazing relation of model I, based on eqn. (7.20).

the upper layer is written as

$$\int_{-h}^{0} \mathscr{S}\, dz = - M a' Z h \qquad 0 \leq M \leq 15 \ \mathrm{mg}/\mathrm{m}^3$$
$$= - 15 a' Z h \qquad M \geq 15 \ \mathrm{mg}/\mathrm{m}^3 \qquad (7.20)$$

The constant a' = 1.35 x 10⁻⁹; 15a' = G = 2 x 10⁻⁸ mg of chlorophyll per mg of zooplankton per sec, the value introduced for the maximum feeding rate in Chapter 5.

The average source strength $1/h \int_{-h}^{0} Q\, dz$ then has the form

$$M\left\{ (\overline{P} - a' Z) - w_s(-h)/h \right\} \qquad 0 \leq M \leq 15 \ \mathrm{mg}/\mathrm{m}^3$$
$$M\left(\overline{P} - w_s(-h)/h\right) - 15 a' Z \qquad M \geq 15 \ \mathrm{mg}/\mathrm{m}^3 \qquad (7.21)$$

$\overline{P}$ is defined as in (5.3), with the average light intensity obtained from (5.9) and the extinction coefficient $\mu$ given by (7.17).

For the lower range of M, the whole right hand side of (7.15) is proportional to M. In its time dependent form (i.e. along a pathline), that equation then reads

$$\frac{DM}{Dt} = M F_1(t) \qquad (7.22)$$

where

$$F_1(t) = \left\{ \overline{P} - a' Z - \frac{w_s(-h)}{h} - \frac{m\, U}{h}\left(1 - \nu(-h)\right) \right\} \qquad (7.23)$$

is a function of time only along a pathline through the dependence of the coordinates x and y on the time elapsed while moving along a pathline. Thus $F_1(t)$ is the local exponential

growth rate and M will decay or increase locally according to whether $F_1(t)$ is negative or positive. The influence of each one of the factors at work is clearly identifiable in $F_1(t)$ and can be estimated at every point of the field.

For higher concentrations, $M \geq 15$ mg/m³, (7.15) may be written

$$\frac{DM}{Dt} = MF_2(t) - 15\,a'\,Z \qquad (7.24)$$

with

$$F_2(t) = \left\{ \overline{P} - \frac{w_s(-h)}{h} - \frac{mU}{h}(1 - \nu(-h)) \right\} \qquad (7.25)$$

The chlorophyll concentration is then subject to an exponential growth rate $F_2(t)$ and a linear decay at a rate 15a'Z.

CHAPTER 8. MODEL I: RESULTS

Streamline patterns resulting from the assumed downstream velocity (2.3) and the simplified entrainment law (7.4) are shown in Fig. 23 and Fig. 24 for two depths of the upper layer, h = 2 m and 5 m respectively. It is obvious that the rate of spreading of this type of plume is strongly dependent on the value of h. The origin of this dependence is readily found. On the axis of the plume (y = 0) we have, from (2.3) and (7.9)

$$\left.\frac{\partial V}{\partial y}\right|_{y=0} = U\left(\frac{1}{x+x_o} + \frac{m}{h}\right) \qquad (8.1)$$

The second term, due to entrainment, is a constant and its effect on the spreading of streamlines away from the axis does not decrease downstream. With $x_o = 5 \times 10^3$ m and $m = 2.4 \times 10^{-4}$, the divergence term due to entrainment exceeds the first term for x > 3.3 km when h = 2 m, but only for x > 15 km when h = 5 m. The premature appearance of an appreciable transverse velocity for h = 2 m pushes water particles off the top of the Gaussian downstream velocity profile, U rapidly decreases and the streamlines begin to diverge very early (Fig. 23). For larger values of h, this divergence is retarded.

The variation of M along a streamline is determined by the sign of the right-hand-side of (7.22) (or (7.24) for $M \geq 15$ mg/m³). Looking at the growth rate as written in (7.23) we note that $w_s$ (-h), h and $\nu$ (-h) do not change along a streamline. The other parameters: U, Z and $\overline{P}$ vary along streamlines according to functional forms given above. The
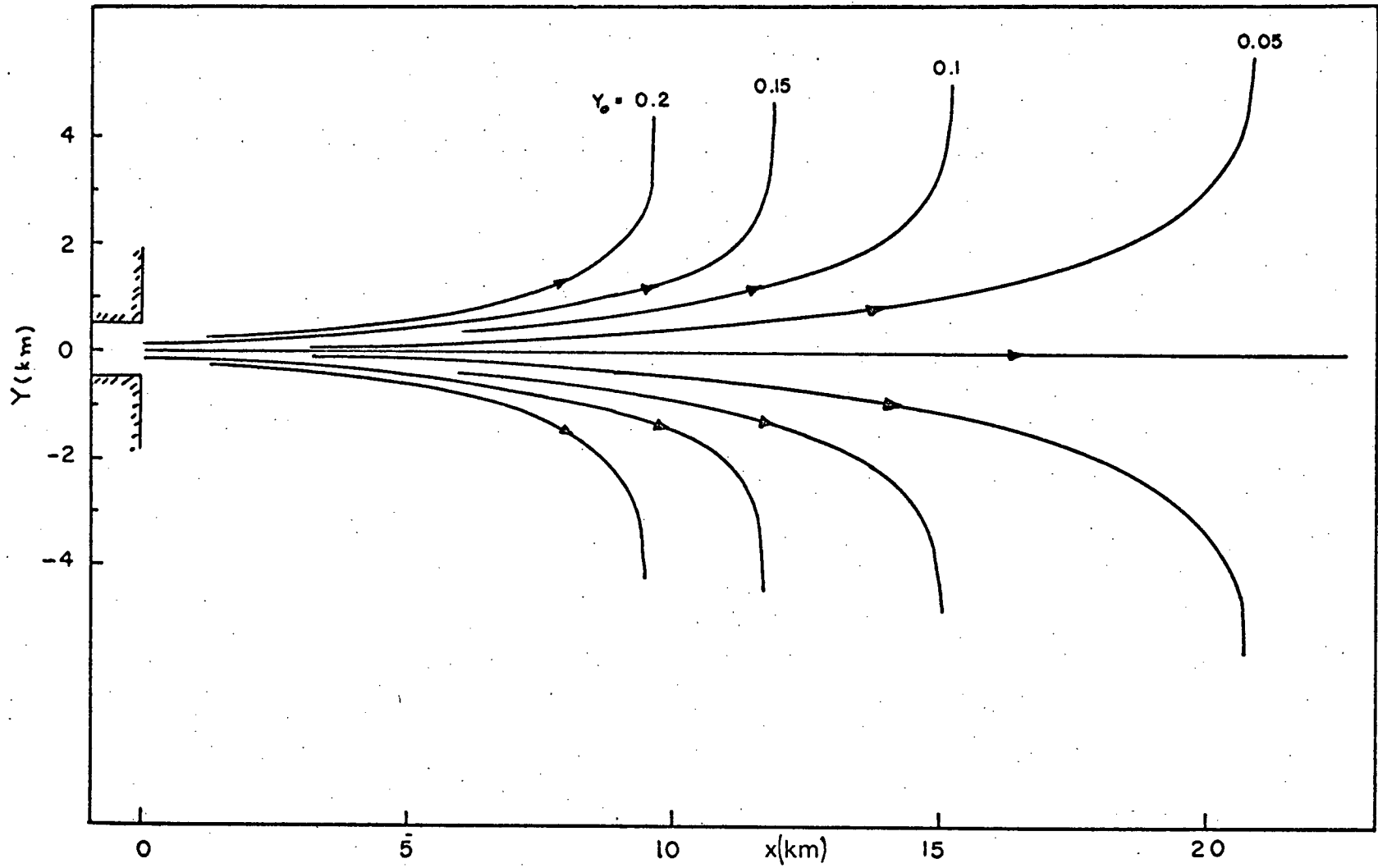
Fig. 23.   Streamline pattern of the horizontal velocity; model I with h = 2 m.
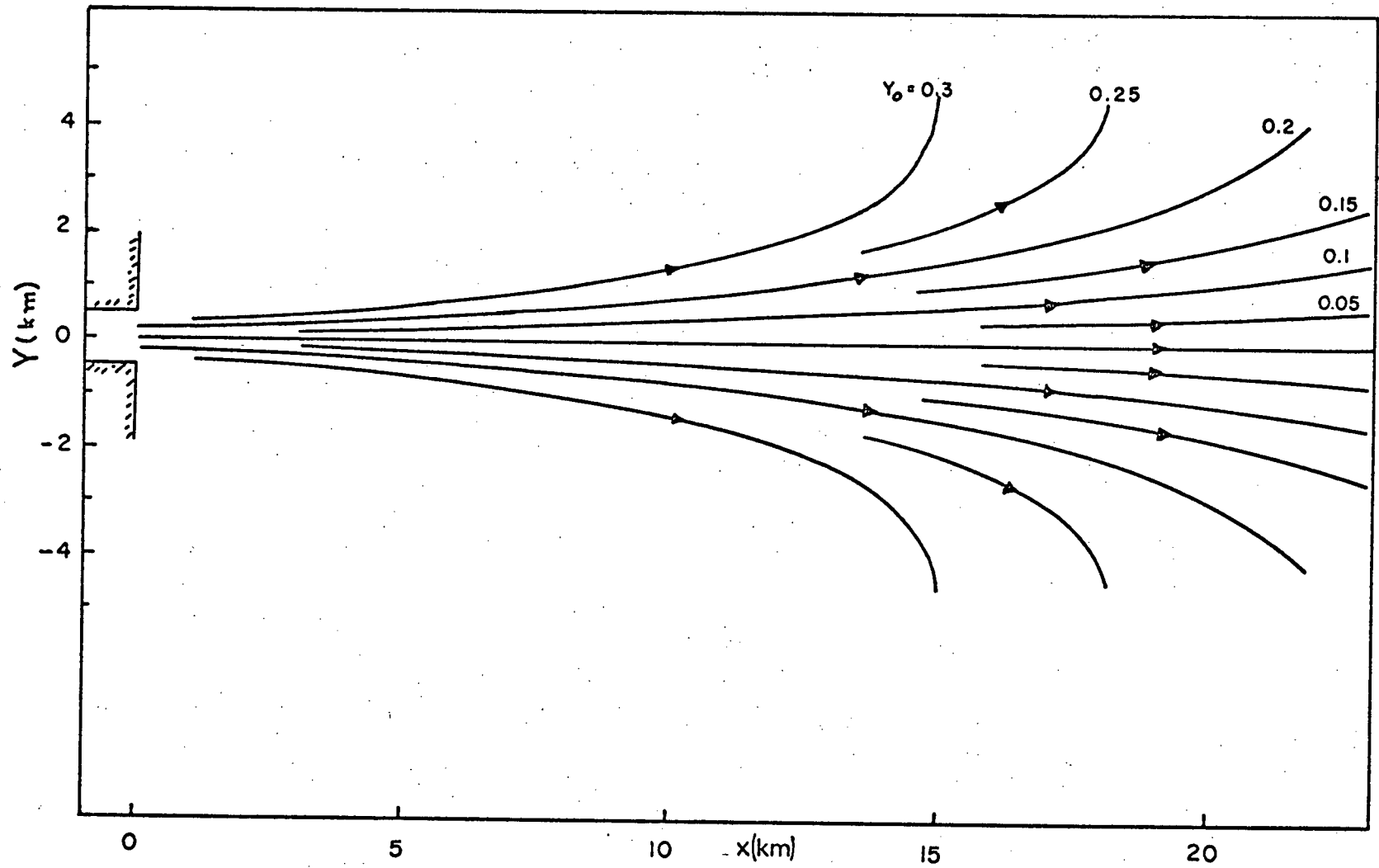
Fig. 24.  Streamline pattern of the horizontal velocity; model I with h = 5 m.

field of M has been computed following the scheme outlined in Chapter 4, for a range of values of all these parameters. These ranges correspond to various conditions, such as to be expected in different months of the year and under maximum and minimum growth rates, sinking ($w_s$ (-h)) or dilution ($\nu$(-h)) rates and zooplankton grazing. The influences of the parameters on the phytoplankton distribution have been isolated and will be presented below. In Table II , we list the values of those parameters which are not varied in the examples discussed below; while the varied parameters will be given for each example.

a) Variation in upper layer depth.

The influence of the upper layer depth on the flow field has already been noted above. Changes in h also affect the photosynthetic rate $\overline{P}$ through their influence on the average light intensity $\overline{I}$, as given by (5.9); they also influence the sinking and dilution terms (the last two terms) in (7.23). Fig. 25 shows the variation of M along the axial (y = 0) streamline in summer conditions ( $P_m$ = 2.2 x $10^{-5}$ ) and with a low sinking rate for $h_o$ = 2 m and $h_o$ = 5 m, in the absence of any chlorophyll dilution due to entrainment ($\nu$(-h) = 1). DM/Dt > 0 everywhere, but is larger, due to increased average light intensity, for the thinner layer.

b) Chlorophyll dilution by the entrained flow.

The parameter $\nu$(-h) can take values from 0 to 1, depending on the chlorophyll concentration just below the upper layer. When $\nu$(-h) = 1, there is no dilution of the upper layer

TABLE II.   Model I parameters held constant.

| Parameter | Value |
|-----------|-------|
| $k_2$ | 96 |
| m | $2.4 \times 10^{-4}$ |
| $c_2$ $(m^{-2})$ | $5.0 \times 10^{-8}$ |
| $r_o$ (m) | $2.5 \times 10^4$ |
| $x_o$ (m) | $5.0 \times 10^3$ |
| b (min/ly) | 5.56 |
| a' | $1.35 \times 10^{-9}$ |
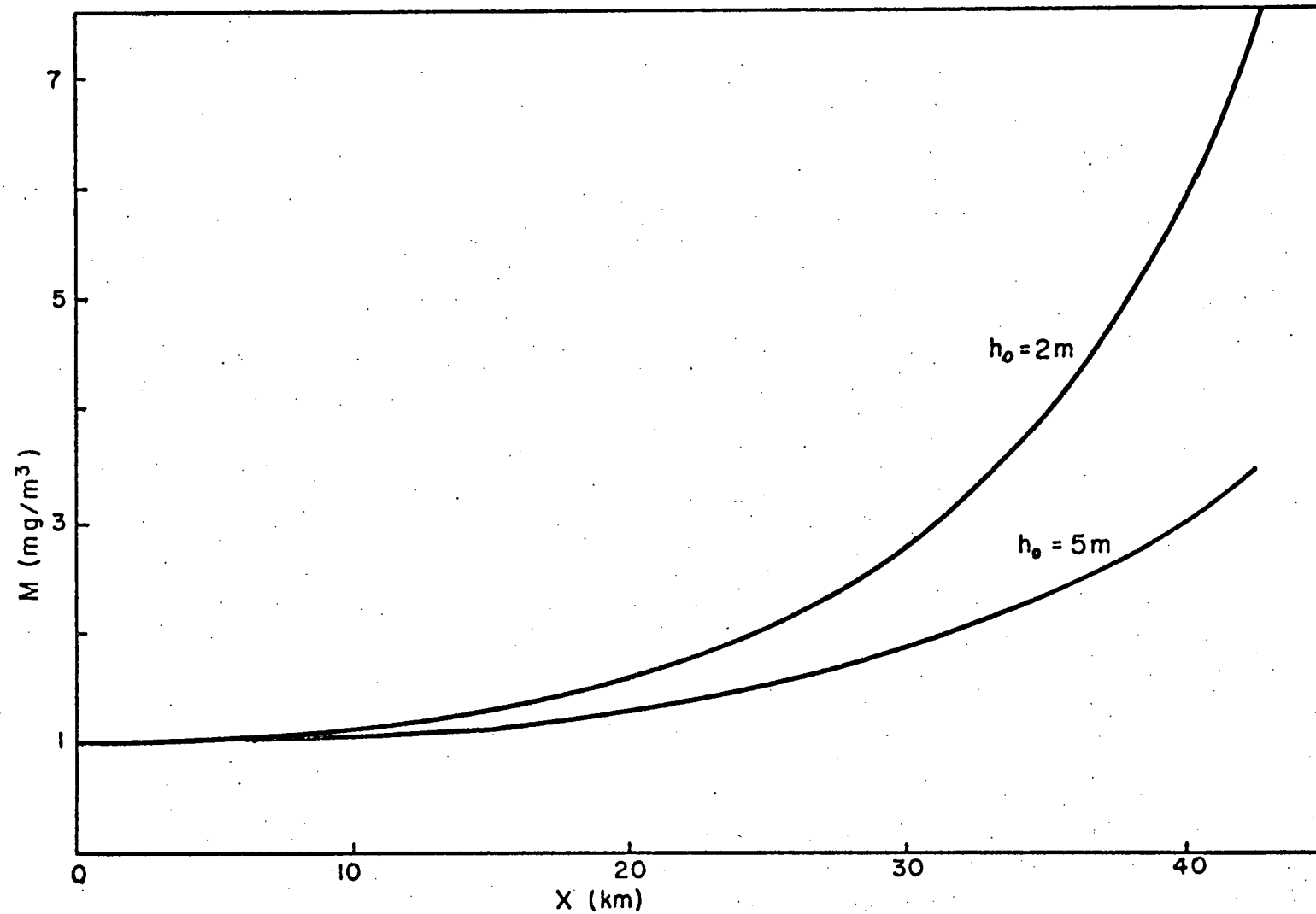
Fig. 25. Variation of M along the axial streamline; model I, May conditions with h = 2 m and h = 5 m.

chlorophyll content M; at the extreme end of the range, $\mathcal{V}(-h) = 0$, one finds a maximum degree of dilution. That such dilution is sufficient to reverse the growth trend of M is seen from Fig. 26 where M is plotted on the downstream axis for May conditions for $\mathcal{V}(-h) = 0$ and $\mathcal{V}(-h) = 1$.

c) Sinking rates.

The obvious effect of an increased sinking rate, given otherwise identical conditions is shown in Fig. 27 along the axial streamline. Under May conditions, no dilution by entrainment and a 5 m upper layer depth, a five-fold increase in sinking rate is sufficient to transform a net growth to a net decay of chlorophyll concentration.

d) Seasonal variation.

The variation of phytoplankton concentration M along the axial streamline is shown in Fig. 28 under three sets of conditions, typical of the months of January, March and May respectively. The values of the parameters which change from curve to curve are shown in Table III .

The main factors which differentiate the three situations are seen from Table III to be: 1) The mean upper layer depth, which is greater in late spring, due to increased runoff (Fig. 3). An increased depth would tend to decrease the rate of growth of M, as seen in Fig. 25; the influence of the upper layer depth variation is obviously more than overcompensated by other factors! 2) The zooplankton biomass increases from January to May, corresponding to an increasing chlorophyll
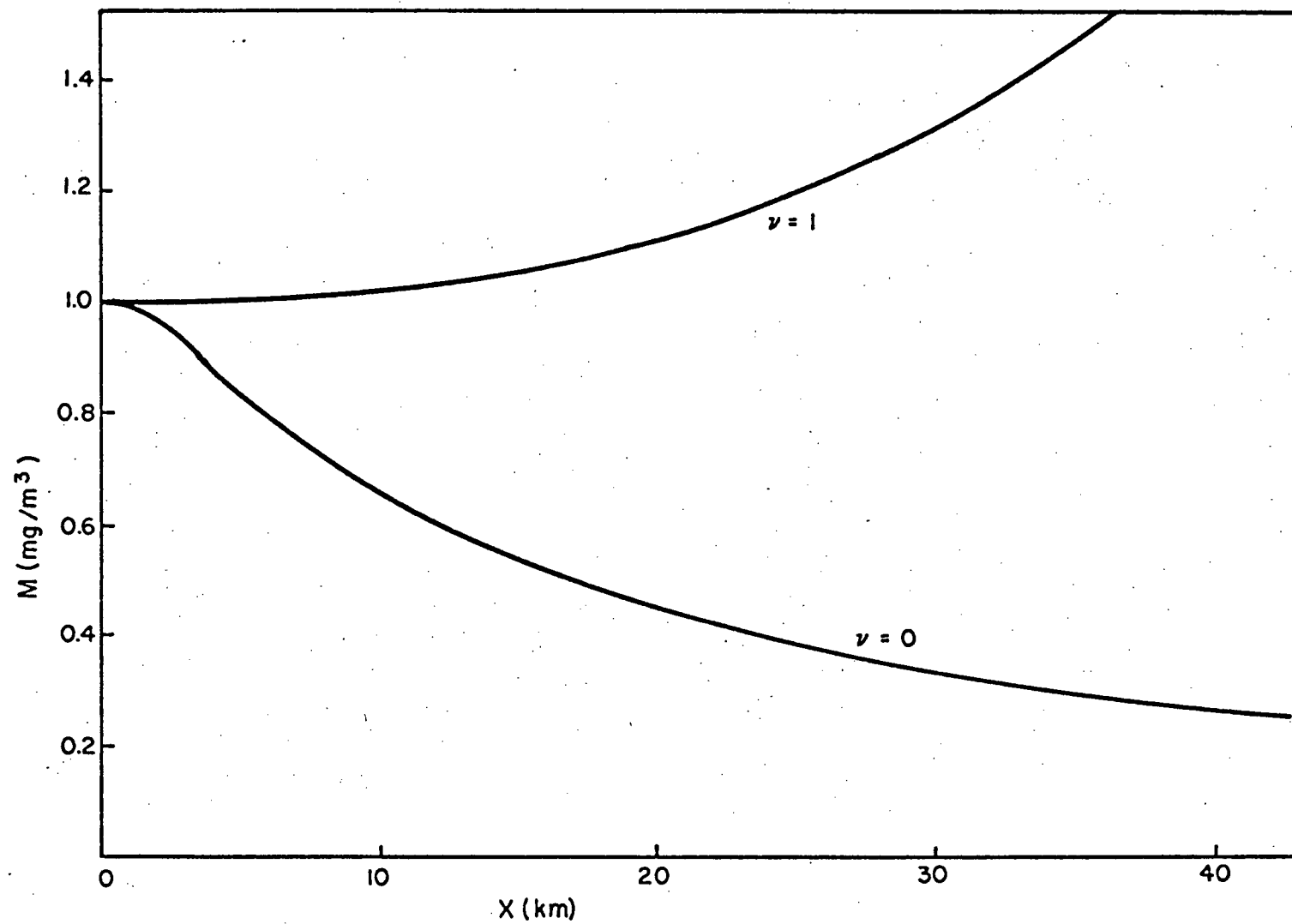
Fig. 26. Variation of M along y = 0; model I, May conditions with full and no dilution.
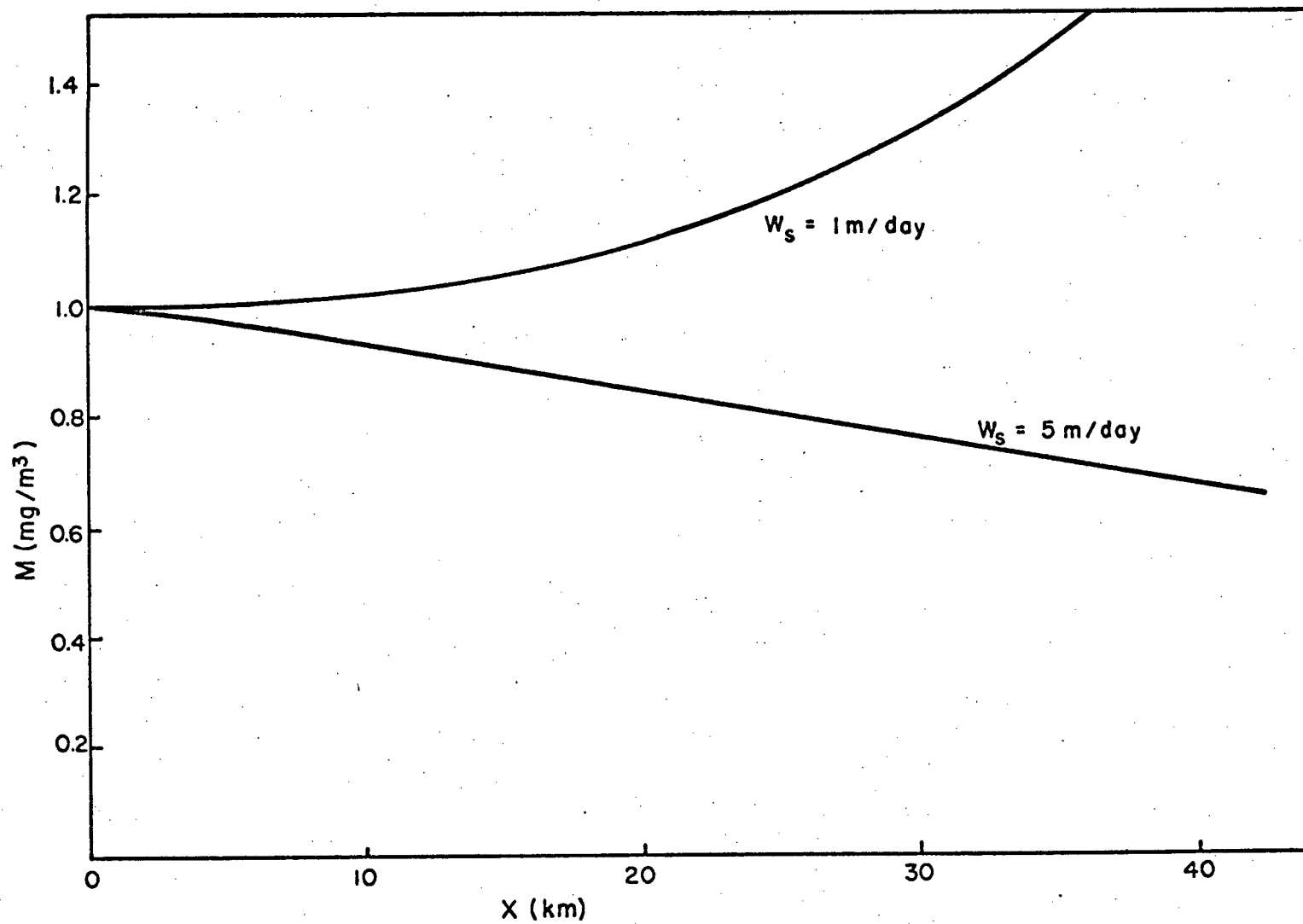
Fig. 27. Variation of M along y = 0; model I, May conditions showing the effect of an increased sinking rate.
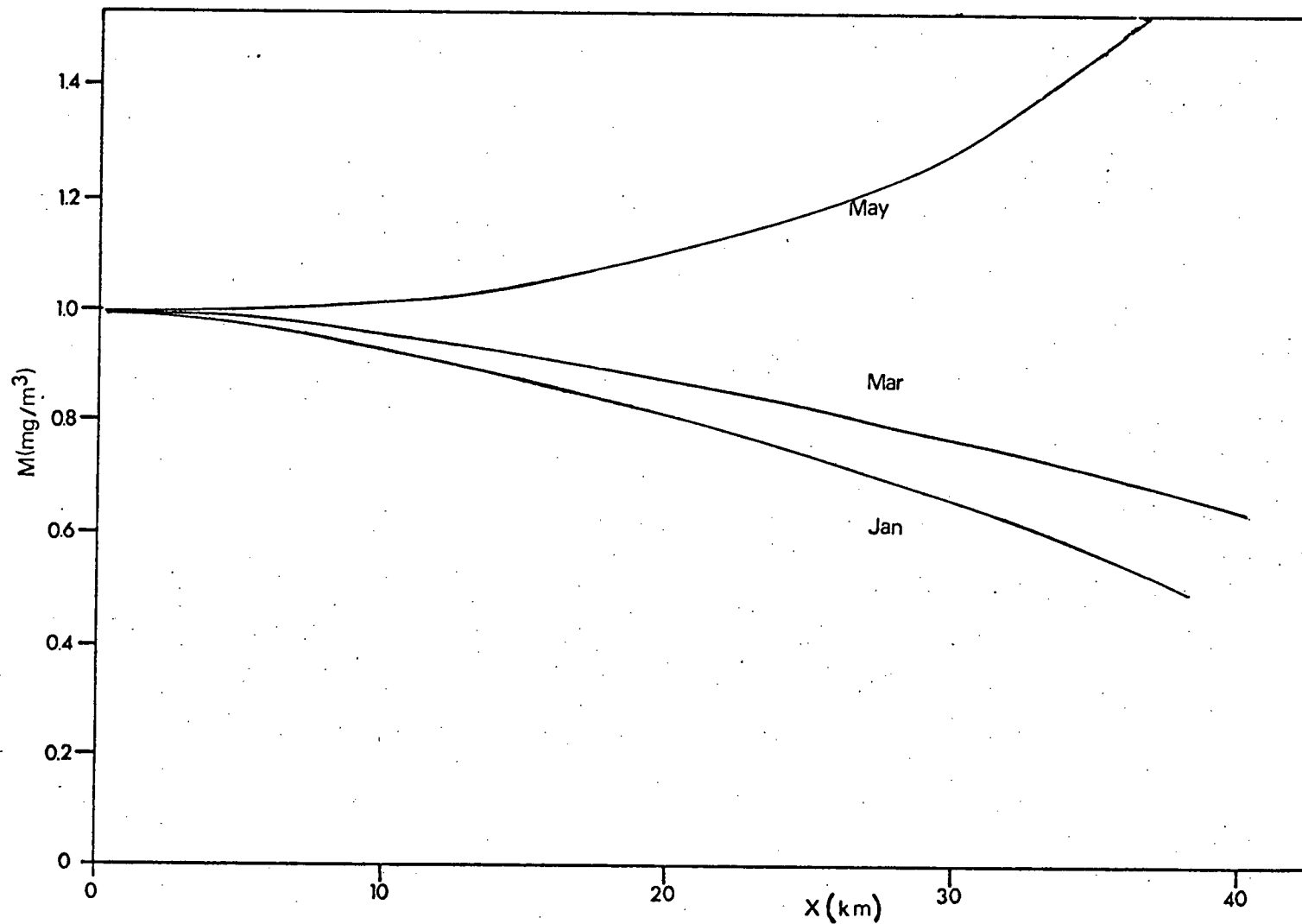
Fig. 28. Variation of M along y = 0; model I showing seasonal variation.

TABLE III.    Seasonal variation of model I parameters.

| Parameter | January | March | May |
|-----------|---------|-------|-----|
| $U_o$ (m/sec) | 1.0 | 1.0 | 2.0 |
| $h_o$ (m) | 2.0 | 2.0 | 5.0 |
| $r_l$ (m) | $8.0 \times 10^3$ | $8.0 \times 10^3$ | $1.5 \times 10^4$ |
| $Z_l$ (mg/m$^3$) | 15 | 150 | 450 |
| $Z_m$ (mg/m$^3$) | 35 | 350 | 1050 |
| $P_m$ (sec$^{-1}$) | $1.1 \times 10^{-5}$ | $1.3 \times 10^{-5}$ | $2.2 \times 10^{-5}$ |
| $I_c$ (ly/min) | $0.6 \times 10^{-2}$ | $0.7 \times 10^{-2}$ | $1.0 \times 10^{-2}$ |
| $I_o$ (ly/min) | $3.0 \times 10^{-2}$ | $4.0 \times 10^{-2}$ | $1.0 \times 10^{-1}$ |
| $\mu_o$ (m$^{-1}$) | 0.3 | 0.4 | 0.8 |

withdrawal term. Again, this factor cannot be of fundamental importance to the relative shape of the three curves, since the trend from winter to late spring is in a direction opposite to that which would result from the variations of zooplankton alone. 3) The net productivity increases markedly from January to May, through increases in $P_m$, associated with the heating of the surface waters, and in $I_o$, the input of solar radiation. It is this increase in productivity which determines the seasonal change in character of the curves of Fig. 28.

e) Zooplankton grazing.

As observed above, increases in the zooplankton sink term in (7.23) or (7.25) are overcompensated on a seasonal basis by increases in productivity. In order to estimate the influence of zooplankton grazing by itself, the May curve of Fig. 28 is compared to the axial distribution of M under the same conditions but in the absence of any zooplankton ($Z_l = Z_m = 0$) (Fig. 29 ). This figure has been plotted on the same scale as many of the other figures to show the rather negligible influence that zooplankton grazing has in this model on chlorophyll concentration during high productivity conditions.

f) Strength of the mean flow.

In order to isolate the influence of the magnitude of the flow velocity, the axial chlorophyll concentration was calculated for two different river outflow velocities ($U_o$ = 1 m/sec and 2 m/sec) for May conditions, as shown in Fig. 30 . At any given distance from the mouth, the value of M
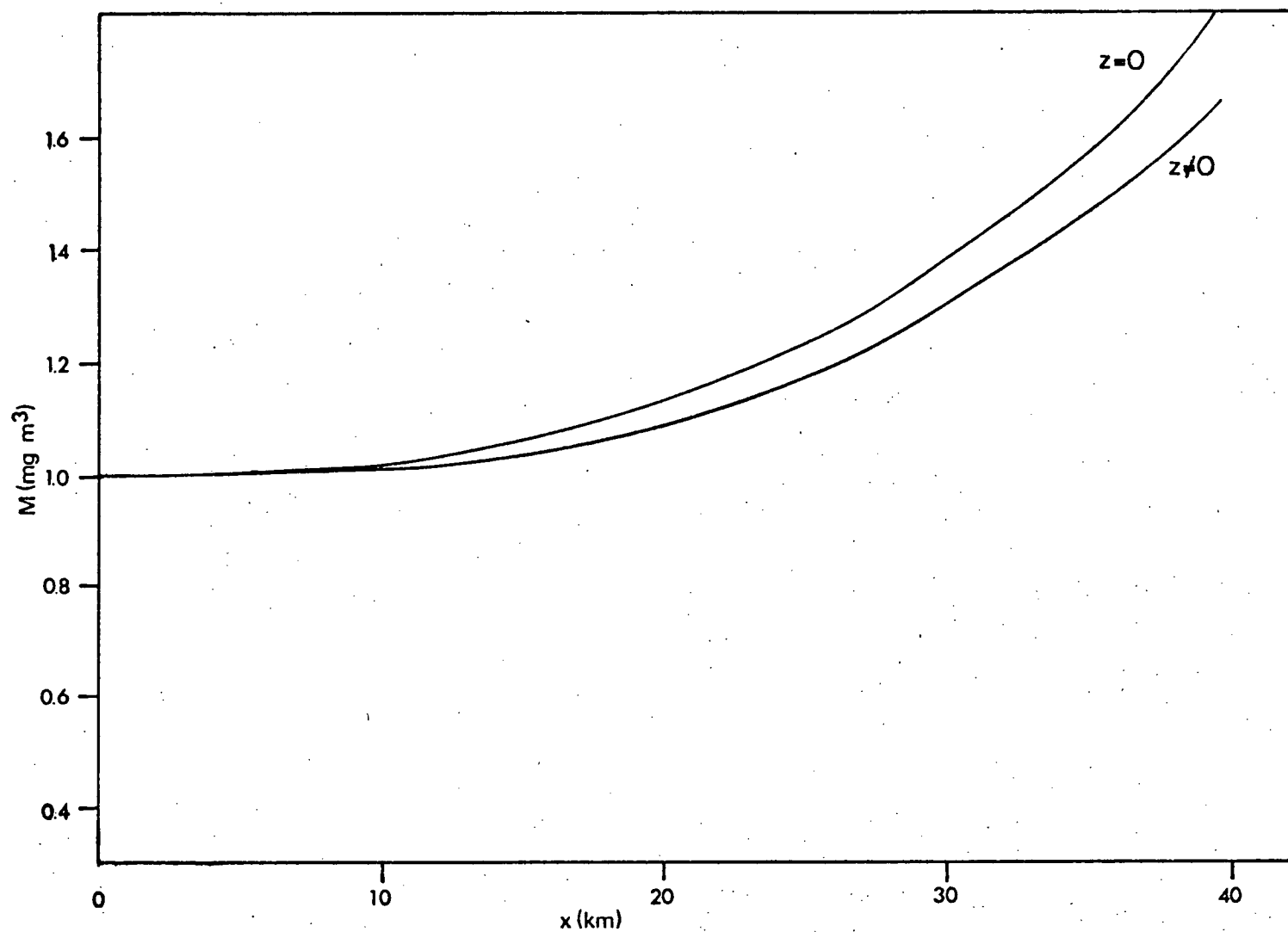
Fig. 29. Variation of M along y = 0; model I (May) showing the effect of no grazing (Z = 0).
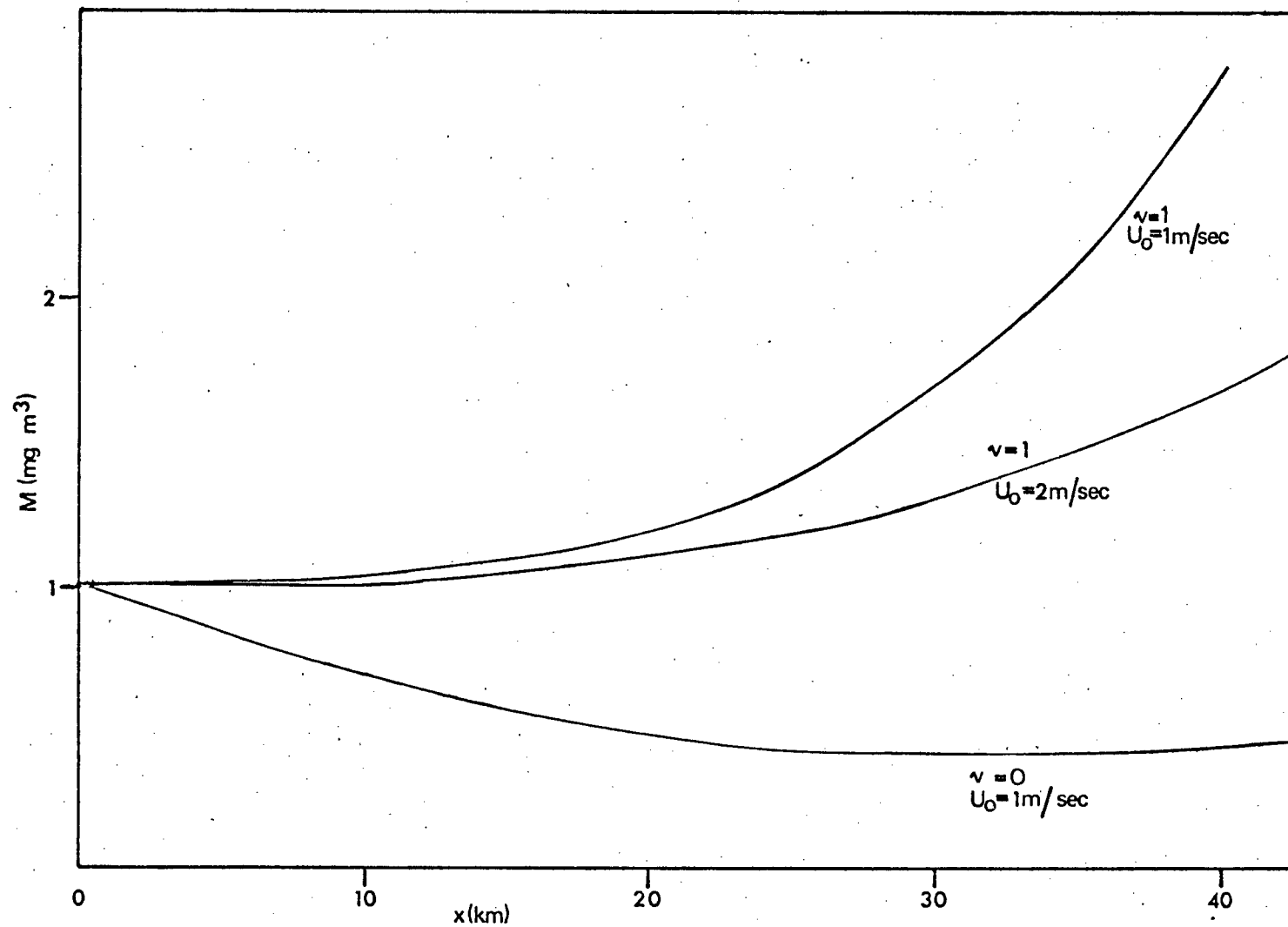
Fig. 30.  Variation of M along y = 0; model I, May conditions with the effect of increased velocity and maximum dilution.

is increased for a decreased flow field. Looking back at the effect of the velocity in (7.23), it is clear that in the absence of dilution ($\mathcal{V}$ = 1), the flow field plays a purely advective role and that if the net source-sink term is positive the rate of growth at any point is unchanged by decreasing the flow velocity. The value of M should then increase since it takes longer to reach any given point when $U_o$ is reduced. In the case of maximum dilution, ($\mathcal{V}$ = 0), a decrease in $U_o$ also decreases the sink term with the effect shown in Fig. 30 (compare with Fig. 26). The chlorophyll concentration decreases initially because of the higher dilution rate, but recovers after falling to a minimum value.

g) Lateral distribution of chlorophyll.

Looking back once more at the source terms (7.23) or (7.24), one notices that the variables U, Z and $\overline{P}$ which vary along any one streamline because of their spatial dependence will also change in passing from a streamline to another. The variation of M along the axial streamline may thus not be representative of what happens over the rest of the (x,y) plane. Although M was calculated along a number of streamlines in each case above for which only its variation along the axis y = 0 has been displayed, only two types of lateral distribution emerged from the integrations.

In all cases but one, the monotonicity exhibited by the M variation along the axis was mimicked on the other streamlines. The M contours shown on Fig. 31 correspond to the high productivity May conditions holding for the $h_o$ = 2 m curve of
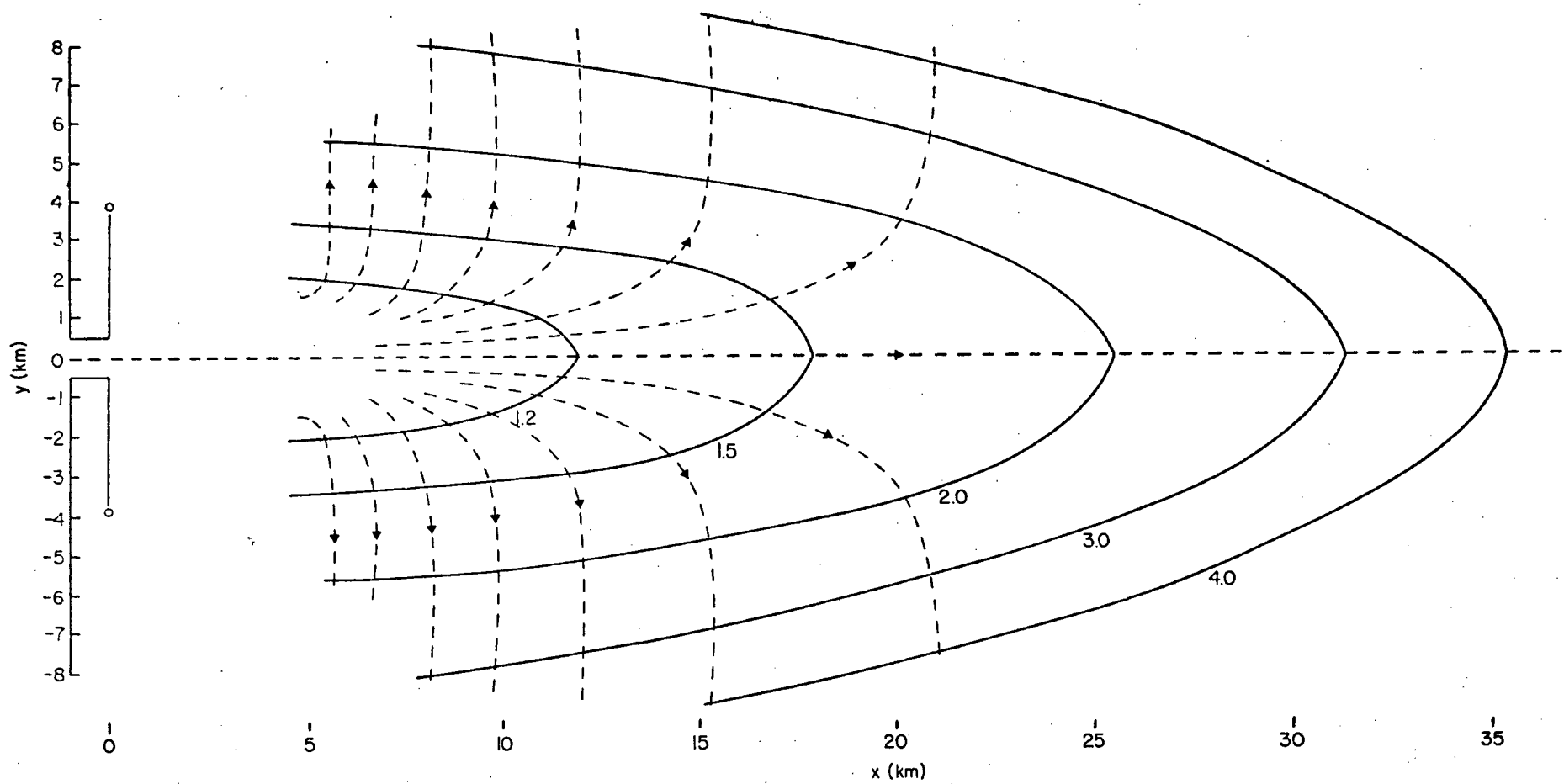
Fig. 31.  Horizontal distribution of M for model I, May conditions.

Fig. 25 and to the streamline pattern of Fig. 23. In these circumstances, the chlorophyll concentration increases uniformly along each streamline and, in the (x,y) plane, thus increases in all directions away from the mouth of the river. The chlorophyll distribution has the form of an elongated rising trough oriented along the axis of the flow.

The corresponding distribution for those cases where a uniform decrease in M is found (the $\mathcal{V} = 0$ curve of Fig. 26; the larger sinking rate curve of Fig. 27; the March and January curves of Fig. 28) is not illustrated. The spatial distribution is very similar to that shown for uniformly increasing M, except that there is now a descending ridge.

The only case where a non-monotonic behavior was found along any streamlines was for the full dilution ($\mathcal{V} = 0$) May conditions curve shown in Fig. 26 and Fig. 30. For the high flow rate ($U_o$ = 2 m/sec) a uniform decrease in M is found there only along the axis; on the other streamlines (Fig. 32 ) an initial diminution of chlorophyll concentration is always followed by an eventual recovery and an increase in M. In order to see whether the mimimum in M on the non-axial streamlines is associated with zooplankton grazing, the ellipse on which the zooplankton density is a maximum, according to (7.18), has been traced as a thin dotted line on Fig. 32. If the zooplankton were responsible for the chlorophyll depletion, one would expect the minima of M, as indicated by crosses on the various streamlines, to fall on or near the ellipse. This is clearly not the case. It seems most likely that the diminution of M along the streamline segments lying near the axis is associated
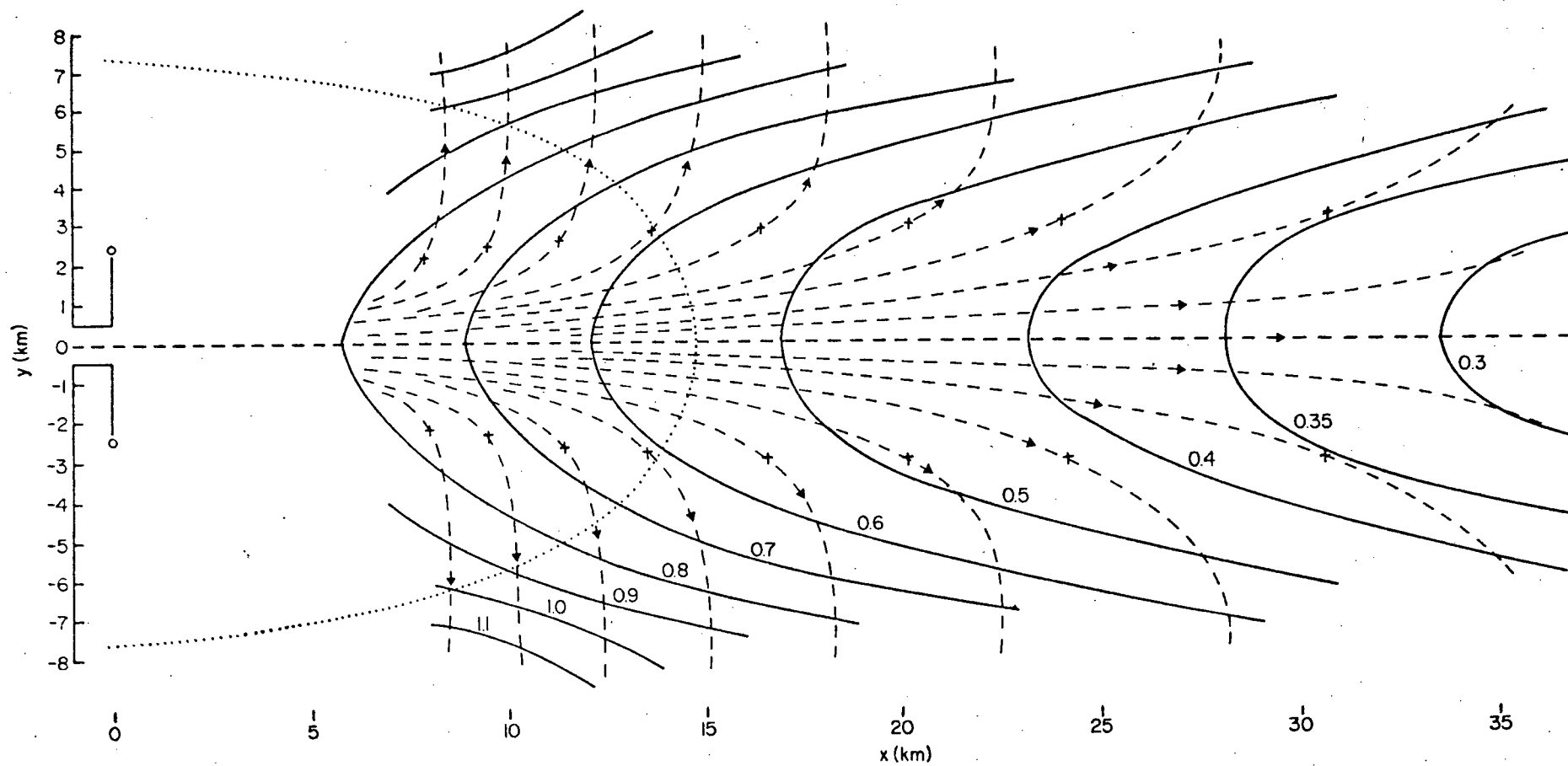
Fig. 32.  Horizontal distribution of M for model I, May conditions with $U_o$ = 2 m/sec and $\nu$ = 0.

with the diluting effect of the entrainment of chlorophyll-free water from below. The dilution is most pronounced near the axis since it is proportional to U, and falls rapidly off the axis according to the Gaussian form chosen for U in (2.3). The position of the minima of M along curves which nearly parallel the axis strongly supports this interpretation.

## Discussion

The simple model just explored has shown the relative effects of many of the parameters affecting chlorophyll concentration. It appears in particular that the seasonal variation is primarily determined by changes in productivity through increased insolation and warming of the upper layers. This fact is of course well known and it is certainly not worth constructing a numerical model to confirm it. More surprising is the very weak influence of zooplankton grazing on the chlorophyll density; the M curves are almost uniquely determined by productivity factors and dynamic factors such as dilution entrainment. Furthermore, in none of the above results is there any indication of the formation of a downstream maximum in M, as appears in Fig. 5, a feature which we set forth to explain in constructing the model. In view of this the model has been refined, as presented below, mainly to yield better estimates of dynamic effects.

# CHAPTER 9. MODEL II: REFINEMENTS

In order to bring the premises of the model into closer agreement with the observations taken in the Gulf 1 to Gulf 3 cruises, a number of approximations and simplifications used above have been abandoned. What were deemed more appropriate forms for the entrainment function, the depth of the upper layer, and the vertical profiles of velocity and chlorophyll density, have been used and are presented below.

i) Instead of the simplified form (7.4), the entrainment velocity w(-h) was expressed in terms of the complete expression (2.4), with $U_c$ as given in (2.5). Repeating these expressions for convenience,

$$w(-h) = m\left(\sqrt{U^2 + V^2} - U_c\right) \qquad (9.1)$$

$$U_c = c'\left(\nu_2 \, g \, \frac{\Delta\rho}{\rho}\right)^{1/3} \qquad (9.2)$$

where $m = 2.4 \times 10^{-4}$ as before; $g = 9.8$ m/sec$^2$ and $\nu_2 = 10^{-6}$ m$^2$/sec. Keulegan (1966) gives two values for c': one (c' = 7.3) for arrested salt wedges, the other (c' = 5.6) for stagnant salt pools. The latter value was chosen here as more appropriate to the plume.

The density contrast $\Delta\rho$ between the lower and the upper layer diminishes downstream, and this variation has been taken into account. The variation of $\sigma_t$ ($\sigma_t = (\rho - 1) \times 10^3$) at the surface as a function of distance from the river mouth is plotted in Fig. 33 from data taken in Gulf 1. The fitted curve

$$\sigma_t = 21.75 - 6.25 \exp(-kx) \qquad (9.3)$$
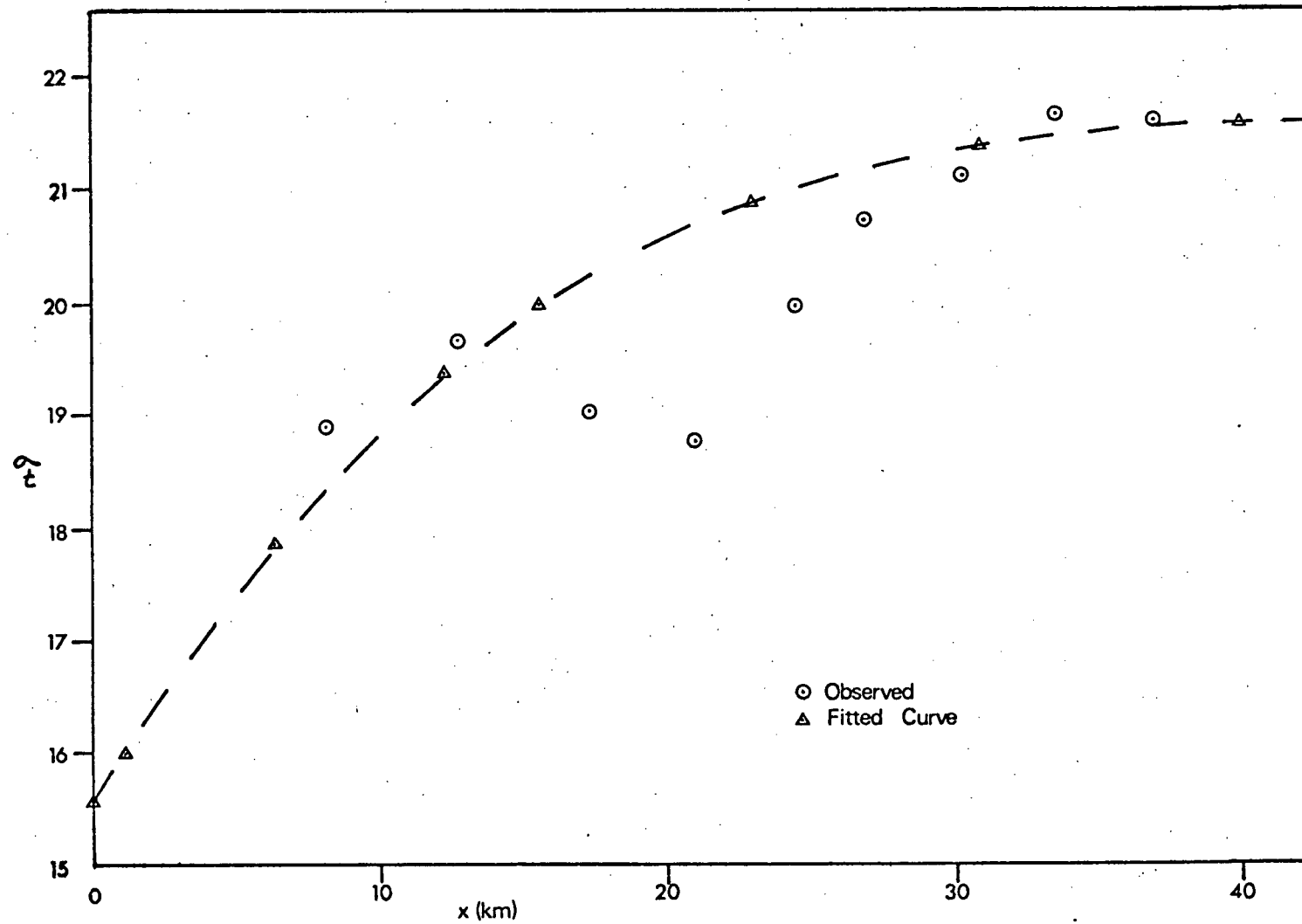
Fig. 33.   The variation of the surface $\sigma_t$ as a function of distance from the river mouth.

with $k = 0.935 \times 10^{-4}$ is also shown in Fig. 33. This curve was chosen for its simplicity; the overall fit of (9.3) to the data points is tolerable, although (9.3) is well above the observational values for $12 < x < 25$ km. In the lower layer a constant density of $\rho_l = 1.0235$ was used.

Now that $w(-h)$ includes $V$, (2.10) becomes non-linear in $V$ and is no longer simply integrated to yield (7.12) for $V$ in terms of $U$. The velocity field was now computed using the following procedure. Given $U(x,y)$ in (2.3) and $U_c$ in (9.2), the continuity equation (2.10) was integrated to find $V$, with the help of (9.1), through the following iterative process.

1- for a given value of x and starting on $y = 0$ (where $V = 0$), $w(x,0,-h)$ was evaluated from (9.1).

2- at a point off the axis, $y = \delta$, it was assumed that $w(x,\delta,-h) = w(x,0,-h)$ which allows the calculation of $V(x,\delta)$ from (2.10).

3- using the computed $V$, an updated value of $w(x,\delta,-h)$ was calculated from (9.1).

4- at $y = 2\delta$, $w(x,2\delta,-h)$ was found by extrapolation from the values of vertical velocities at $y = 0$ and $y = \delta$. $V(x,2\delta)$ is then calculated from (2.10).

5- an updated $w(x,2\delta,-h)$ is estimated from (9.1) using $V(x,2\delta)$.

6- at $y = 3\delta$, $w(x,3\delta,-h)$ is obtained by extrapolation and the process continues.

The velocity field was mapped in this fashion for various values of $\delta$. A value of $\delta = 10$ m was found, by comparison with finer grid computations, to give sufficient accuracy.

In routine integration of the biological-physical model, an even simpler method of integration was used. At any point $(x,y)$, $w(x,y,-h)$ was estimated from (9.1) with $U = U(x,y)$ and $V = 0$. $V(x,y)$ was then calculated from (2.10) for that value of $w(-h)$. The results of this simpler method agreed with the iteration process outlined above within 1% for $|V| < U$. In the biological calculations (3.8), $w(-h)$ was updated with the value of $V$ substituted back into (9.1).

ii) The depth of the upper layer, identified with the depth of the bottom of the halocline, frequently increases rapidly around $x = 25$ km. From the salinity profiles for Gulf 1 shown in Fig. 16, the thickness of the upper layer (normalized with respect to $h_o = 15$ m) have been plotted in Fig. 34 . The rapid deepening of the upper layer has been modelled with the curve

$$h = h_o \left\{ f_1 + \tanh \left[ B \left( \frac{r}{r_o} - 1 \right) \right] \right\} \qquad (9.4)$$

with $r$ as given by (7.17). The origin of the hyperbolic tangent was always chosen at $r_o = 25$ km and the steepness factor $B = 3.5$. For $r \gg r_o$,

$$h_+ \simeq h_o (f_1 + 1) \qquad (9.5)$$

while for $r \ll r_o$,

$$h_- \simeq h_o (f_1 - 1) \qquad (9.6)$$

From which

$$h_o = (h_+ - h_-)/2 \qquad (9.7)$$

$$f_1 = (h_+ + h_-)/(h_+ - h_-) \qquad (9.8)$$

In most runs, $h_-$ was kept constant at 2 m and only $h_+$ was
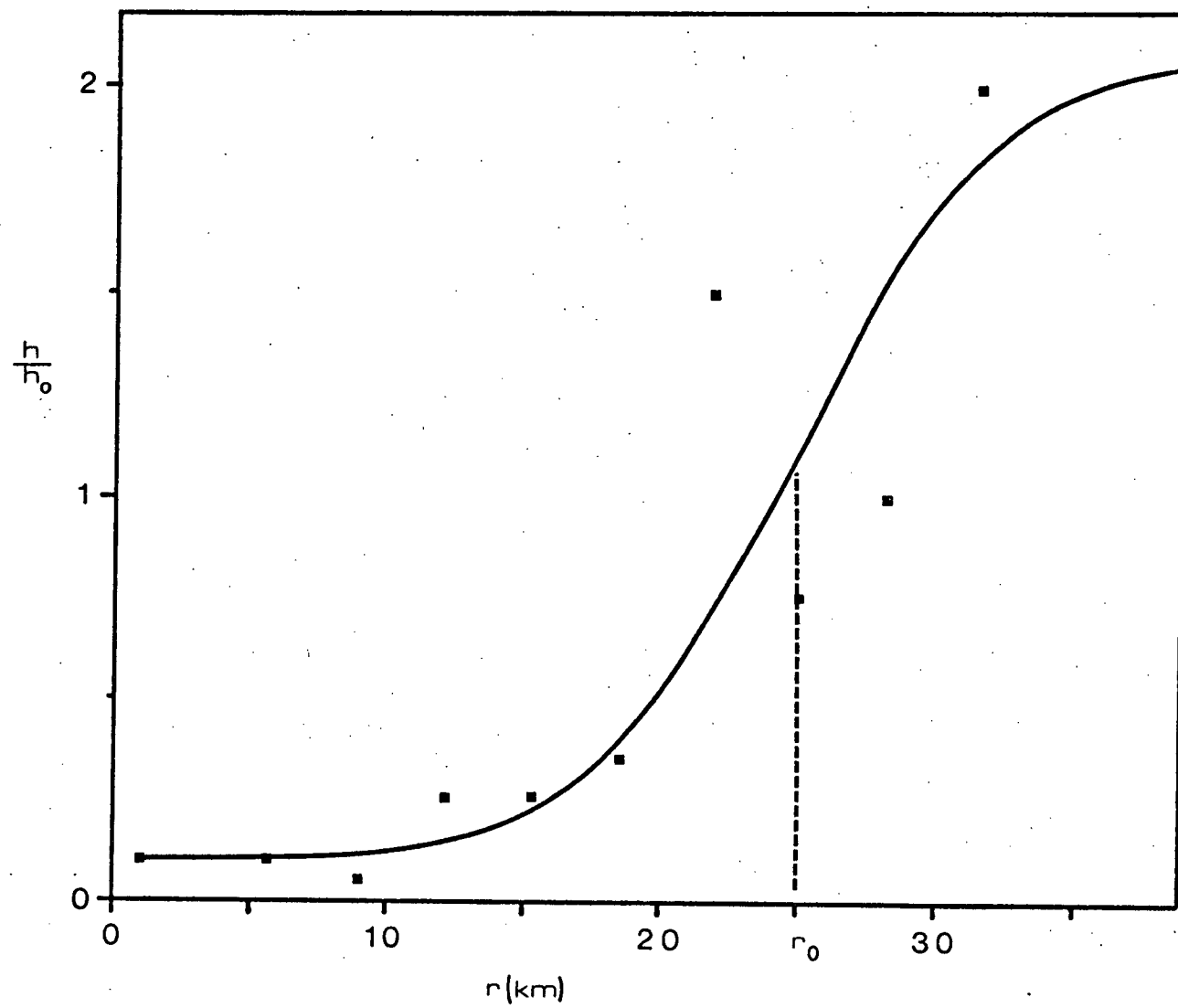
Fig. 34.   The normalized upper layer depth as a function of distance from the river mouth.

varied.

The rapid change of depth embodied in (9.4) should be expected to have some important consequences on the flow field and on the chlorophyll concentration. If h increases rapidly in (2.3), U will decrease accordingly, thereby decreasing the rate of entrainment and dilution. An increased mixed layer depth also leads, from (5.9), to a decreased mean light intensity and thus to decreased productivity.

iii) In an attempt to include more realistic vertical profiles of u and v, current meter data from Tabata et al. (1970) were examined. These are shown in Fig. 35 together with a fitted curve of the form

$$\gamma(x,y,z) = \frac{1}{X}\left\{ 1 + \tanh\left(A\left(\frac{z}{h} + 1\right)\right)\right\} \tag{9.9}$$

The value of A was adjusted to provide the best visual fit to the current profiles. Curves of $\gamma$ for various values of A are shown in Fig. 36 . A = 1 gave the best fit and is the curve shown in Fig. 35.

The requirement (2.7) that the integral of $\gamma(z)$ equal the depth of the upper layer imposes the relation

$$X = 1 + \frac{\ln(\cosh A)}{A} \tag{9.10}$$

Thus, for A = 1, $X$ = 1.434.

Examples of vertical chlorophyll variation $\nu(x,y,z)$ in the region of interest were drawn from Fulton et al. (1968) and are shown in Fig. 37 . Once more a curve of the form (9.9) with A = 1 provides a good fit.

Using these forms for $\gamma$ and $\nu$, the function $\Omega(x,y)$ as
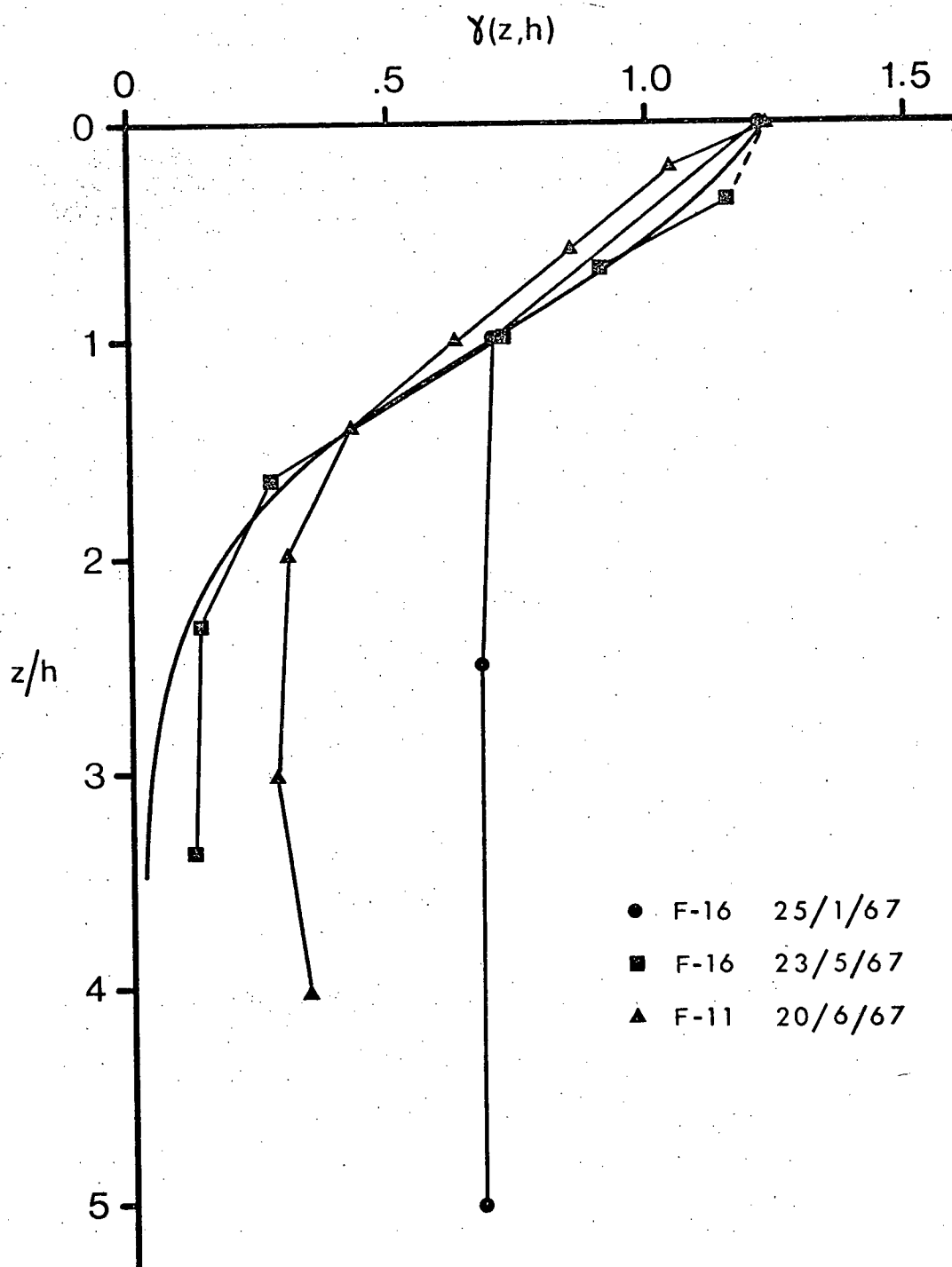
Fig. 35. Vertical profiles of current speed; the curve represents eqn. (9.9) with A = 1, (after Tabata et al., 1970).
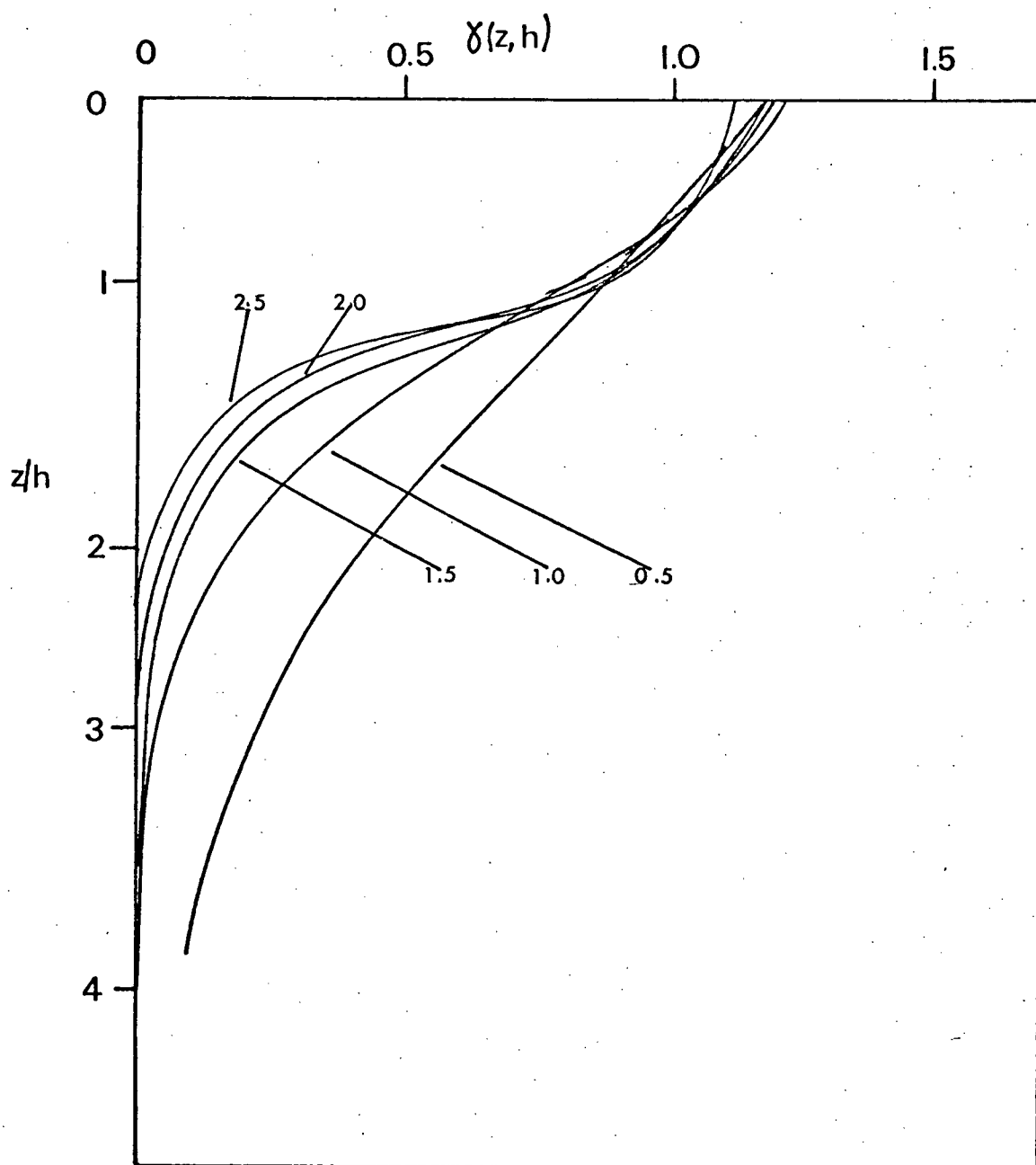
Fig. 36.  Comparison of the effect of different values of A on eqn. (9.9).
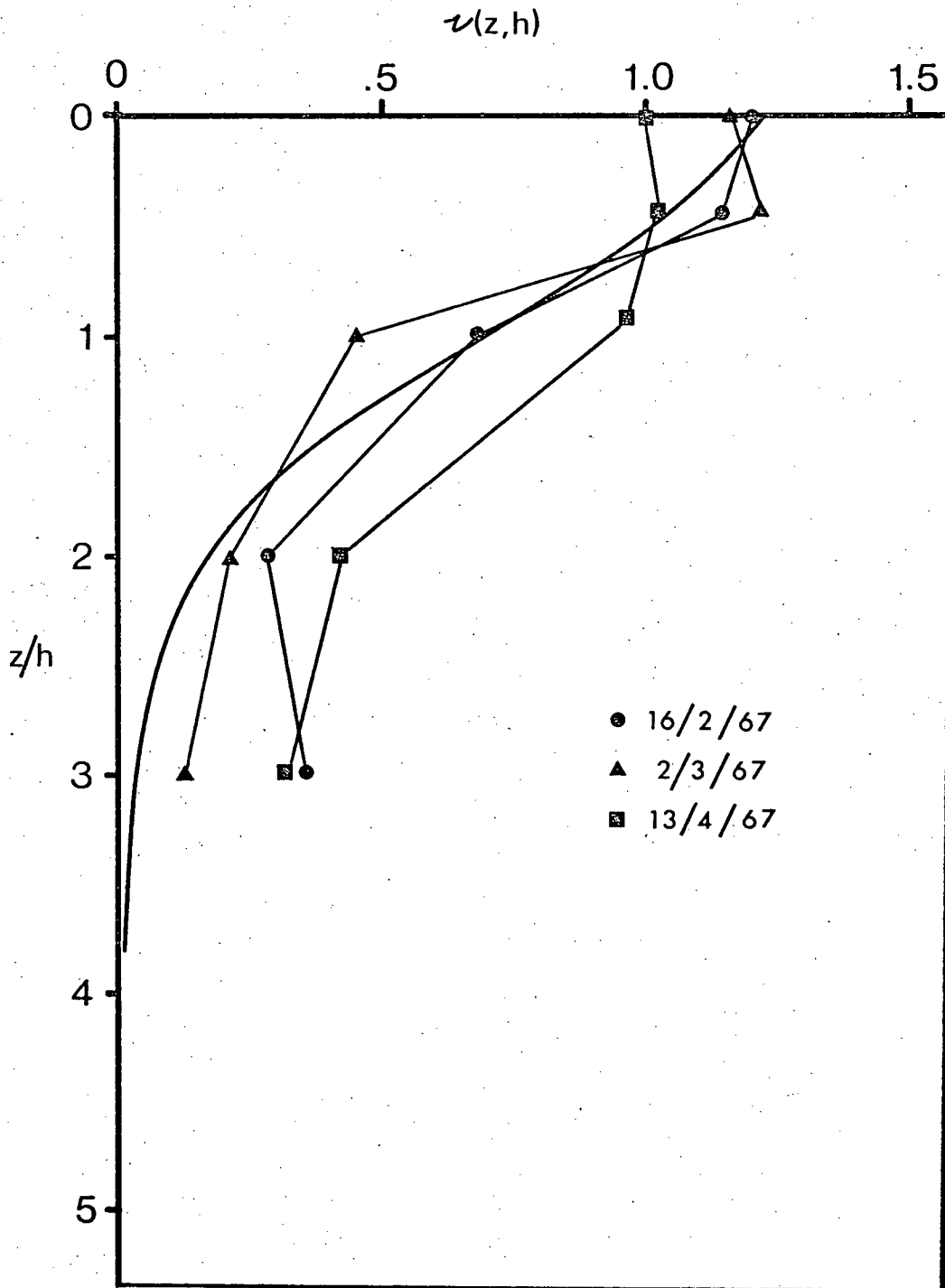
Fig. 37. Vertical profiles of chlorophyll, the curve represents eqn.
(9.9) with A = 1, (after Fulton et al., 1968).

defined in (3.7) becomes

$$\Omega = \frac{1}{K^2} \int_{-h}^{0} \left( 1 + \tanh\left(\frac{z}{h} + 1\right)\right)^2 dz = 1.024\, h \qquad (9.11)$$

and the conservation equation (3.8) takes the form

$$\underline{U} \cdot \nabla M = \frac{0.9761}{h} \int_{-h}^{0} Q\, dz - \frac{M}{h}\left\{ 0.3192\left( w(-h) + \gamma(-h)\underline{U}\cdot\nabla h\right)\right\} \qquad (9.12)$$

iv) Since we now have an analytic expression for $\nu(x,y,z)$, the integral in the grazing term of equation (5.12) can be evaluated. Using (9.9) we obtain

$$\int_{-h}^{0} \gamma\, dz = \frac{h}{A(d_2 K + 2M)}\left\{ A + \ln\cosh(A + A_t)\right.$$

$$\left. - \ln\cosh A_t\right\} \qquad (9.13)$$

where

$$A_t = \operatorname{arctanh}\left( \frac{M}{d_2 K + M}\right) \qquad (9.14)$$

Hence equation (5.12) becomes

$$\int_{-h}^{0} Q\, dz = M\left( \overline{P}h - \frac{GZh}{A(d_2 K + 2M)}\left\{ A + \ln\cosh(A + A_t)\right.\right.$$

$$\left.\left. - \ln\cosh A_t\right\} - w_s(-h)\,\nu(-h)\right) \qquad (9.15)$$

Equations (9.12) and (9.15) may then be used to solve for values of M along pathlines. The concentration of M will increase or decrease depending on wether the integrated source term (the Q term) is large enough to overcome the entrainment dilution term.

CHAPTER 10.    MODEL II: RESULTS

Direct comparison of the streamlines (pathlines) calculated in model II with those of model I is difficult. The problem arises from the fact that calculated velocities are dependent on h(x,y); in model I, h is constant while in model II, h increases away from the river mouth. Fig. 38 and Fig. 39 show the streamlines for two different initial velocities, $U_0$ = 1 m/sec and $U_0$ = 2 m/sec.

On the axis of the plume (y = 0) we can write, using (2.11),(2.3) and (2.4) and recalling that $U_c \leq U$, V(x,0) = 0

$$\frac{\partial V}{\partial y}\bigg|_{y=0} = U\left\{\frac{m}{h}\left(1 - \frac{U_c}{U}\right) + \frac{\partial h}{\partial x}\frac{\gamma(-h)}{h} + \frac{1}{(x + x_0)}\right\} \qquad (10.1)$$

From (9.9) we know that $\gamma(-h) = 1/\chi > 0$. Thus we have divergent flow since the right-hand-side of (10.1) is always $\geq 0$. Also we see that the rate of spreading depends not only on the layer depth, h, but also on the gradient of h. Hence we would expect the rate of spreading to increase when $U_0$ (and thus U) is increased, as is demonstrated by Fig. 38 and Fig. 39. Similarly a larger value of h would decrease the rate of spreading.

The variation of M along a streamline depends upon the sign of the right-hand-side of (9.12). It can be seen that the entrainment dilution term is always a loss term. Since most of the parameters in (9.12) and (9.15) vary along a streamline, it is not easy to determine their net effect on M. As with model I, the field of M was calculated for different values of the various model II parameters. For model II, the parameters held constant are given in Table IV . We will now discuss the influences of the varied parameters on the chlorophyll
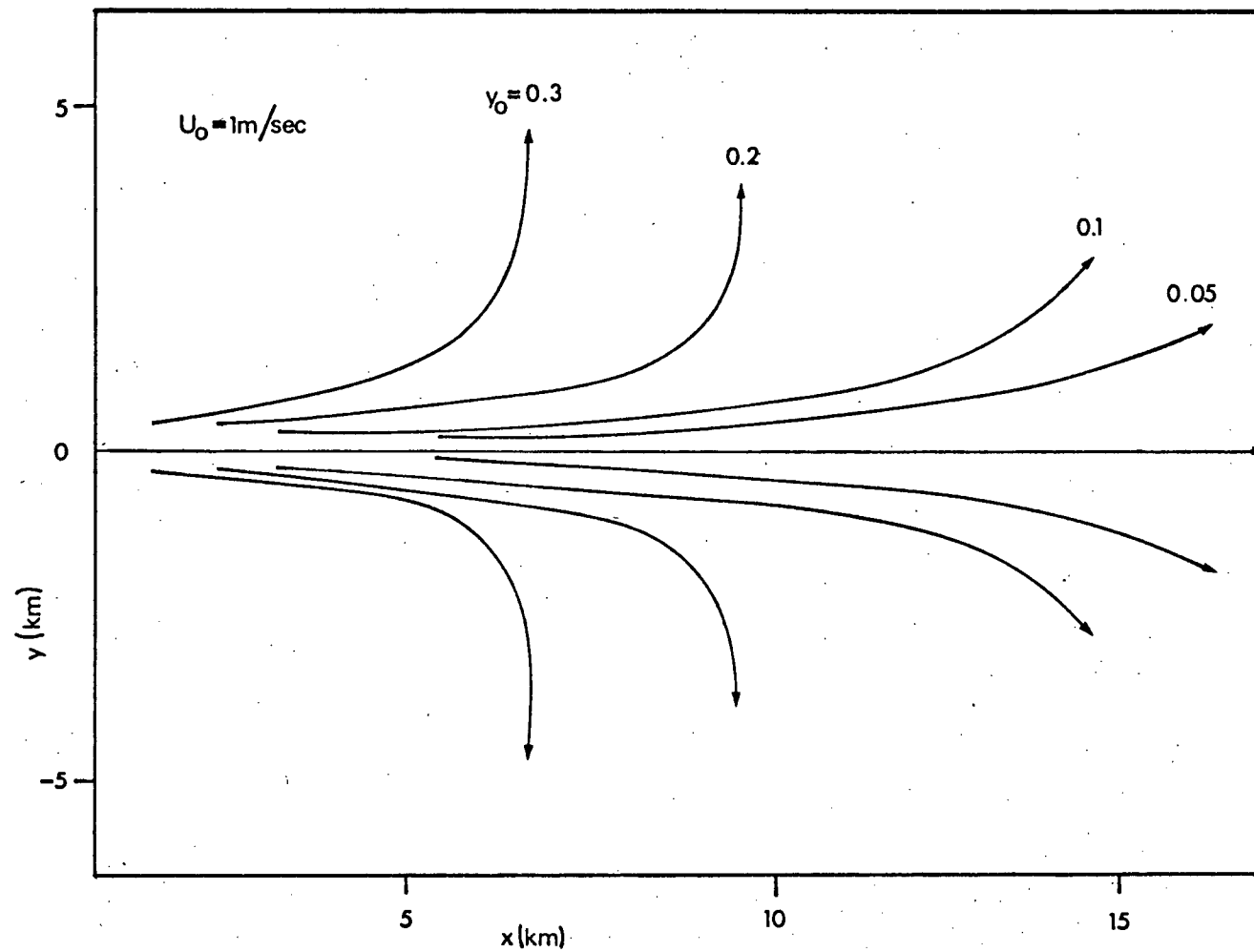
Fig. 38. Streamline pattern of the horizontal velocity; model II with $U_o$ = 1 m/sec.
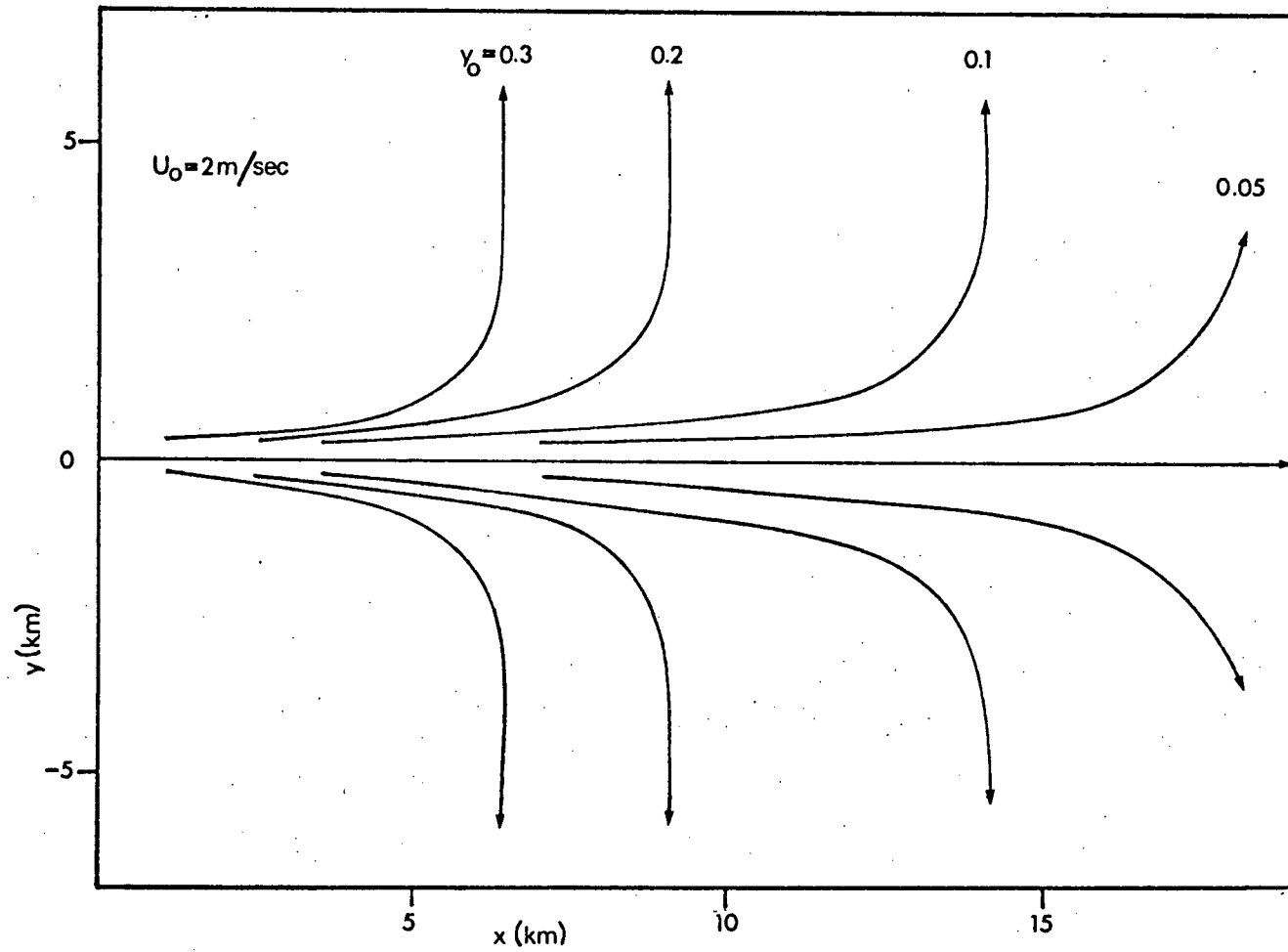
Fig. 39. Streamline pattern of the horizontal velocity; model II with $U_o$ = 2 m/sec.

TABLE IV.    Model II parameters held constant.

| Parameter | Value |
|---|---|
| $d_2$  (mg/m$^3$) | 5.0 |
| B | 3.5 |
| c' | 5.6 |
| $\nu_2$  (m$^2$/sec) | $1.002 \times 10^{-6}$ |
| k    (m$^{-1}$) | $9.35 \times 10^{-5}$ |
| $k_2$ | 96 |
| m | $2.4 \times 10^{-4}$ |
| $c_2$  (m$^{-2}$) | $5.0 \times 10^{-8}$ |
| $r_o$  (m) | $2.5 \times 10^4$ |
| $x_o$  (m) | $5.0 \times 10^3$ |
| b  (min/ly) | 5.56 |
| a' | $1.35 \times 10^{-9}$ |

distribution.

a) Seasonal variation

The variation of M along the axial streamline is illustrated in Fig. 40 for conditions representative of the months of January, March and May respectively. For each curve, the values of parameters which varied are given in Table V. In all three cases a sinking speed of $w_s$ = 1.2 x 10$^{-5}$ m/sec was used.

Refering to Table V , it can be seen that the basic differences in the three cases are: 1) increased river discharge in late spring which increases the velocity, $U_o$ and increases the upper layer depth near the mouth (due to increased stability the layer deepens less rapidly downstream). 2) The increase of the maximum production rate, $P_m$, and the incident solar radiation, $I_o$, towards summer. The resultant increase in productivity is counterbalanced by an increase in the compensation light intensity, $I_c$, and the extinction coeficient, $\mu_o$. 3) The increased zooplankton grazing towards summer.

Of the above effects, the increase of $P_m$ and $I_o$ when coupled with a more gradual increase in the layer depth tends to increase the chlorophyll concentration while the increased values of $U_o$, $I_c$, $\mu_o$ and the layer depth near the mouth tend to increase the chlorophyll sink term. The curves shown in Fig. 40 reflect the balance attained by the source and sink terms in the chlorophyll equation. The results indicate that except for May, all the curves show a steady decrease of chlorophyll away from the river mouth. In May there is an initial decrease with a
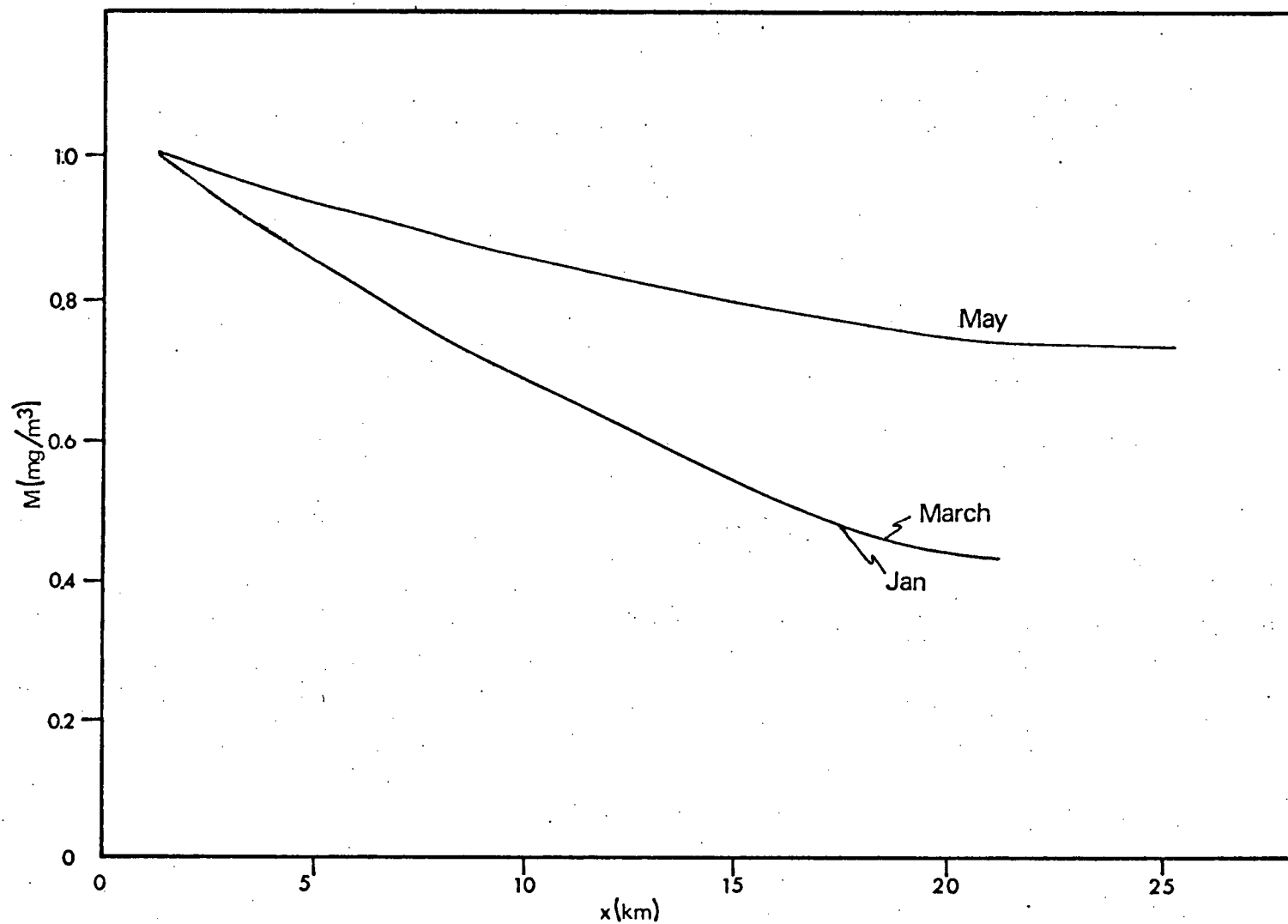
Fig. 40.  Variation of M along y = 0 (model II) showing seasonal variations.

TABLE V.    Seasonal variation of model II parameters.

| Parameter | January | March | May |
|---|---|---|---|
| $h_o$ (m) | 15.0 | 15.0 | 1.0 |
| $f_I$ | 1.13 | 1.13 | 5.00 |
| $U_o$ (m/sec) | 1.0 | 1.0 | 2.0 |
| $P_m$ ($sec^{-1}$) | $1.1 \times 10^{-5}$ | $1.3 \times 10^{-5}$ | $2.2 \times 10^{-5}$ |
| $I_c$ (ly/min) | $0.6 \times 10^{-2}$ | $0.7 \times 10^{-2}$ | $1.0 \times 10^{-2}$ |
| $I_o$ (ly/min) | $3.0 \times 10^{-2}$ | $4.0 \times 10^{-2}$ | $1.0 \times 10^{-1}$ |
| $\mu_o$ ($m^{-1}$) | 0.3 | 0.4 | 0.8 |
| $Z_I$ ($mg/m^3$) | 15 | 150 | 450 |
| $Z_m$ ($mg/m^3$) | 35 | 350 | 1050 |
| $r_I$ (m) | $8.0 \times 10^3$ | $8.0 \times 10^3$ | $1.5 \times 10^4$ |

minimum at about 25 km, then there is a gradual increase. The discussion which follows shows the effect of varying some of the parameters individually.

The reference curve in the discussion below is that obtained by choosing parameter values to maximize the source terms and minimize the sink terms. This produces a curve where M increases with increasing distance from the river mouth, i.e. similar to the comparison curve of model I. The effect of changes in the parameter values is then demonstrated by changing one of the parameters in the reference curve and comparing the resulting curve with the reference curve. The parameter values for the reference curve are those of Table IV and $h_o = 5$ m, $f_I = 2.00$, $U_o = 1$ m/sec, $P_m = 3.1 \times 10^{-5}$ sec$^{-1}$, $\mu_o = 0.3$ m$^{-1}$, $I_o = 1.0 \times 10^{-1}$ ly/min, $I_c = 0.6 \times 10^{-2}$ ly/min, $Z_I = 15$ mg/m$^3$, $Z_m = 35$ mg/m$^3$ and $w_s = 1.2 \times 10^{-5}$ m/sec.

b) Changes in upper layer depth

In Fig. 41 the effect of changes in the depth of the upper layer are compared. With all other factors being kept constant, the chlorophyll distributions for three upper layer depth profiles are compared: (A) $h_o = 5$ m, $f_I = 2.00$ (reference curve) which gives 5m < h < 15m; (B) $h_o = 15$ m, $f_I = 1.13$ which gives 2m < h < 30m; and (C) $h_o = 5$ m, $f_I = 1.40$ which gives 2m < h < 12m.

It is clear from equations (9.12) and (9.15) that variations in the depth of the upper layer are insignificant in the local production and grazing terms. The main effect of variations in h occurs in the hydrodynamic dilution terms
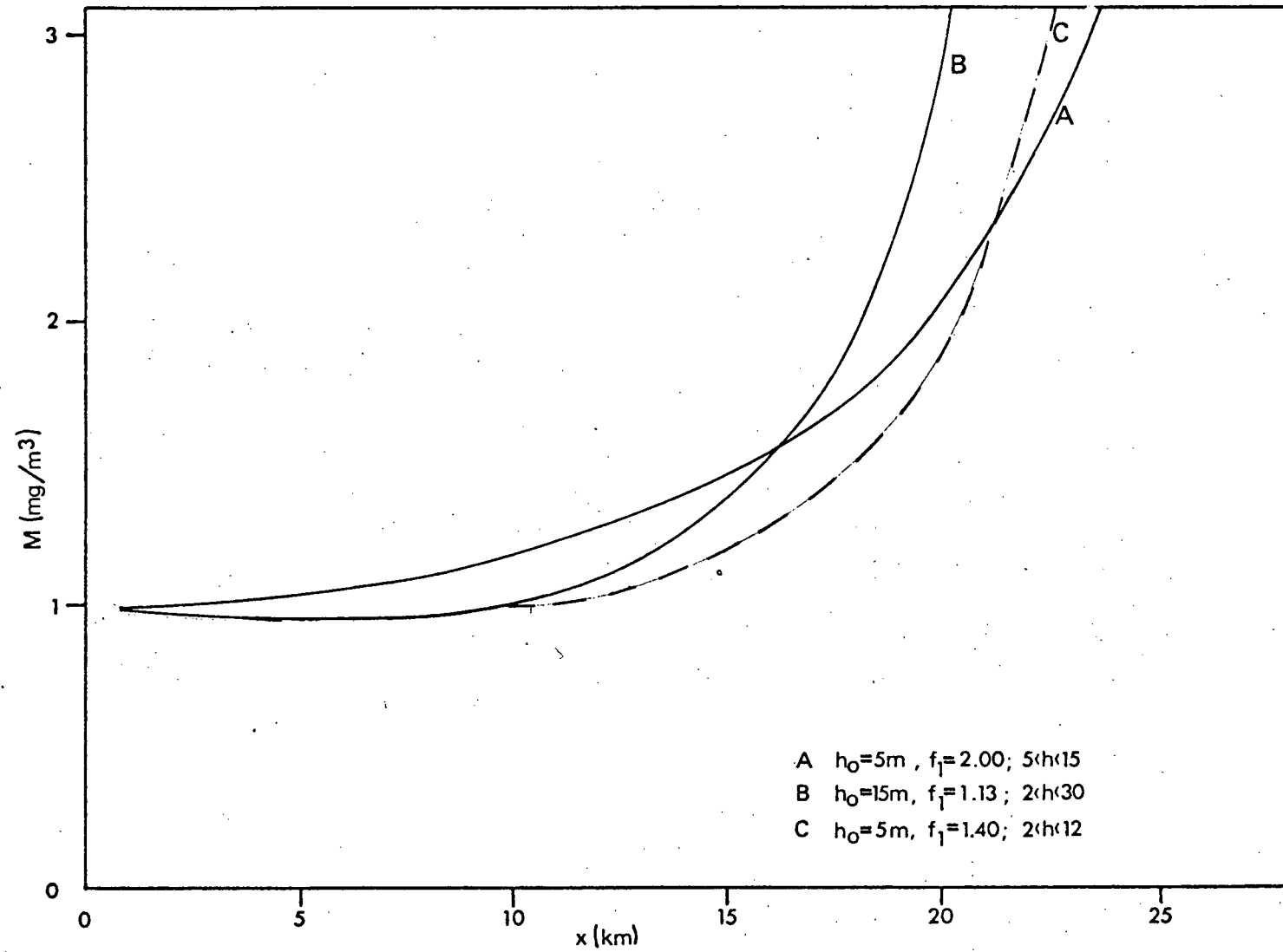
Fig. 41. Variation of M along y = 0 (model II); the effect of changes in the upper layer depth, h.

(proportional to 1/h) in (9.12). Comparing curves A and C for example, it is clear that for $x \leq 15$ km, where $h \approx$ constant, the chlorophyll growth rate of curve A should be more rapid than that of curve C since $1/h_A < 1/h_C$ . On the other hand, once the steep gradient of the upper layer depth is reached ($x \approx 15 - 25$ km), curve C catches up and passes curve A because (with $f_1 = 2.00$ for A, as compared to 1.40 for curve C) the gradient sink-term $\underline{U} \cdot \underline{\triangledown} h$ is larger in A than in C. The relative behavior of curves B and C is similar at small x since the original upper layer depths are equal; curve B, with a smaller dilution by divergence term ($f_1 = 1.13$ for B compared to $f_1 = 1.40$ for curve C), outdistances C in the region of the upper layer depth gradient.

c) Variations in the velocity field

In Fig. 42 the results of changing the strength of the velocity field are illustrated. The curves compared have values of parameters $U_0 = 1$ m/sec and $x_0 = 5 \times 10^3$ m (the reference (upper) curve), $U_0 = 1$ m/sec and $x_0 = 1 \times 10^4$ m (middle curve) and $U_0 = 2$ m/sec and $x_0 = 5 \times 10^3$ m (lower curve). The lower curve illustrates the effect of increasing the downstream velocity at the river mouth; such as happens when the river discharge increases. The situation for a less rapid decrease in U downstream is illustrated by the middle curve.

The less rapid increase of M with distance can be explained by the fact that; 1) the dilution by entrained water from below is increased, 2) with the increased velocity a phytoplankton organism spends less time in transit and for similar local
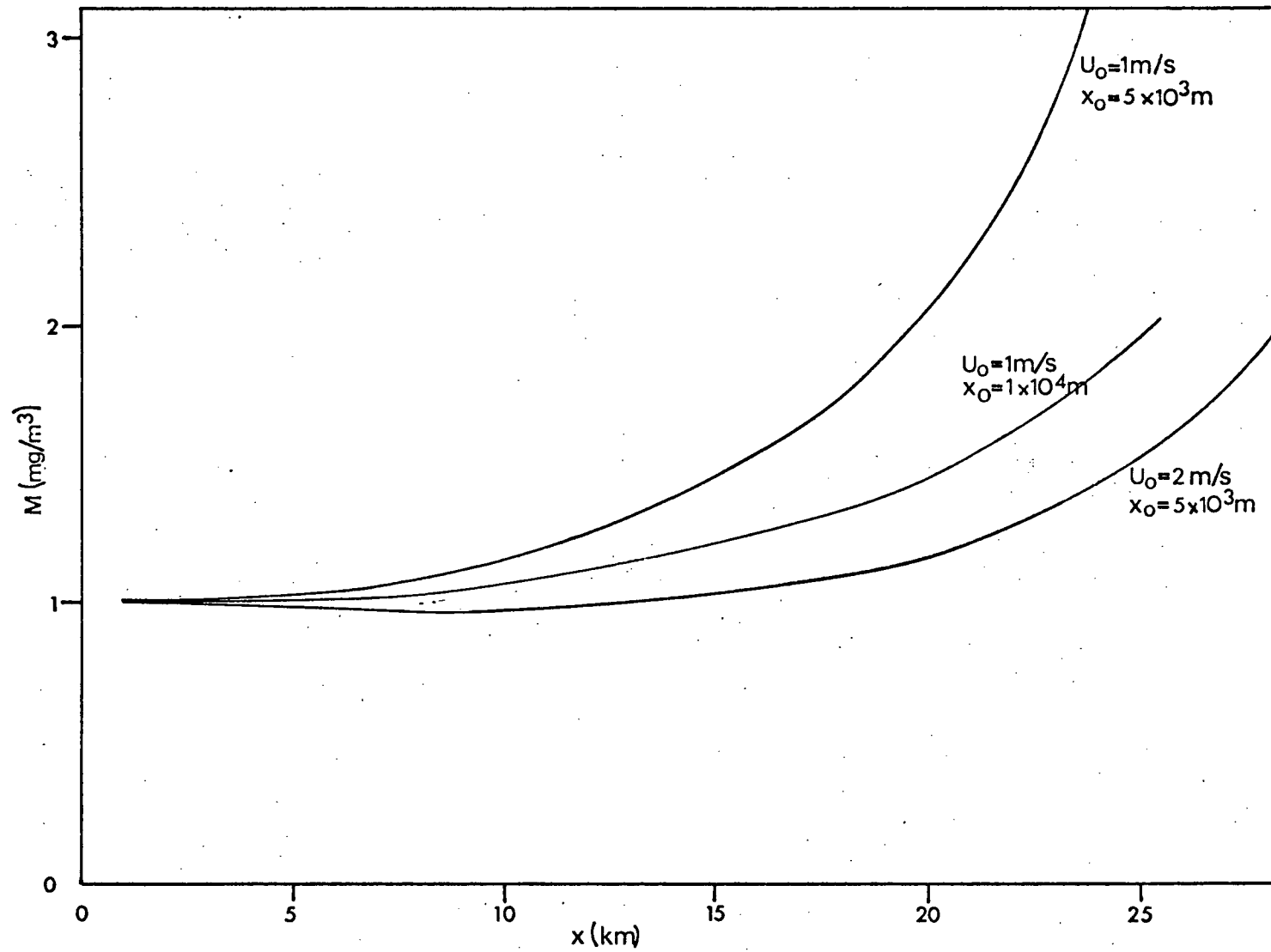
Fig. 42.  Variation of M along y = 0 (model II); the effect of changes in the velocity field.

growth rates, would not attain equally high concentrations at a given distance downstream.

### d) Variations in the production term

The production term has been varied in two ways; by changing the value of the maximum production rate, $P_m$ and by changing the value of the extinction coefficient, $\mu_o$. The resulting curves are illustrated in Fig. 43 . The reference curve (top) has values of $P_m = 3.1 \times 10^{-5}$ sec$^{-1}$, $\mu_o = 0.3$ m$^{-1}$ while the middle curve has $P_m = 3.1 \times 10^{-5}$ sec$^{-1}$, $\mu_o = 0.8$ m$^{-1}$ and the bottom curve has $P_m = 1.1 \times 10^{-5}$ sec$^{-1}$, $\mu_o = 0.3$ m$^{-1}$.

Although both $P_m$ and $\mu_o$ were changed by about the same amount (just less than a factor of 3), the distribution of M appeared less sensitive to changes in $\mu_o$ than to changes in $P_m$. Increasing $\mu_o$ decreased M as did decreasing $P_m$, as one would expect.

### e) Variations in the grazing term

Fig. 44 illustrates the effect of increasing the grazing rate by increasing the zooplankton biomass by a factor of 30. The top curve is the reference curve ($Z_1 = 15$ mg/m$^3$; $Z_m = 35$ mg/m$^3$) while the bottom curve ($Z_1 = 450$ mg/m$^3$; $Z_m = 1050$ mg/m$^3$) has the increased grazing term. Although there is a large increase in the grazer population, the chlorophyll concentration is not decreased very much.

When the initial concentration of M, $M_o = M(1,y)$ (ie. at x = 1 km) is increased to 3 mg/m$^3$ from 1 mg/m$^3$ then the curve of $M/M_o$ lies between those for the above two cases. Thus it
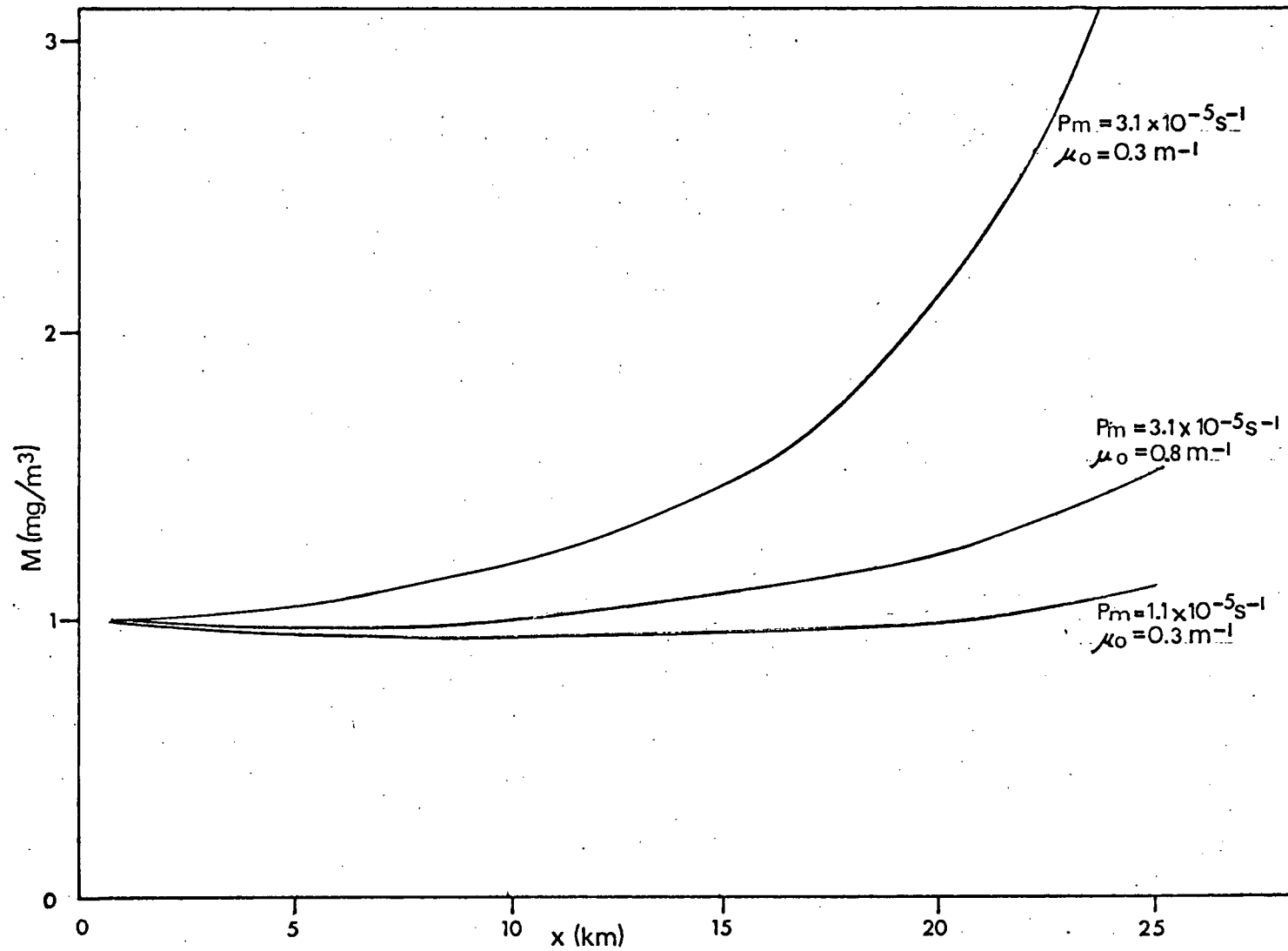
Fig. 43. Variations of M along y = 0 (model II); the effect of changes in the production rate by variations in $P_m$ and $\mu_o$.
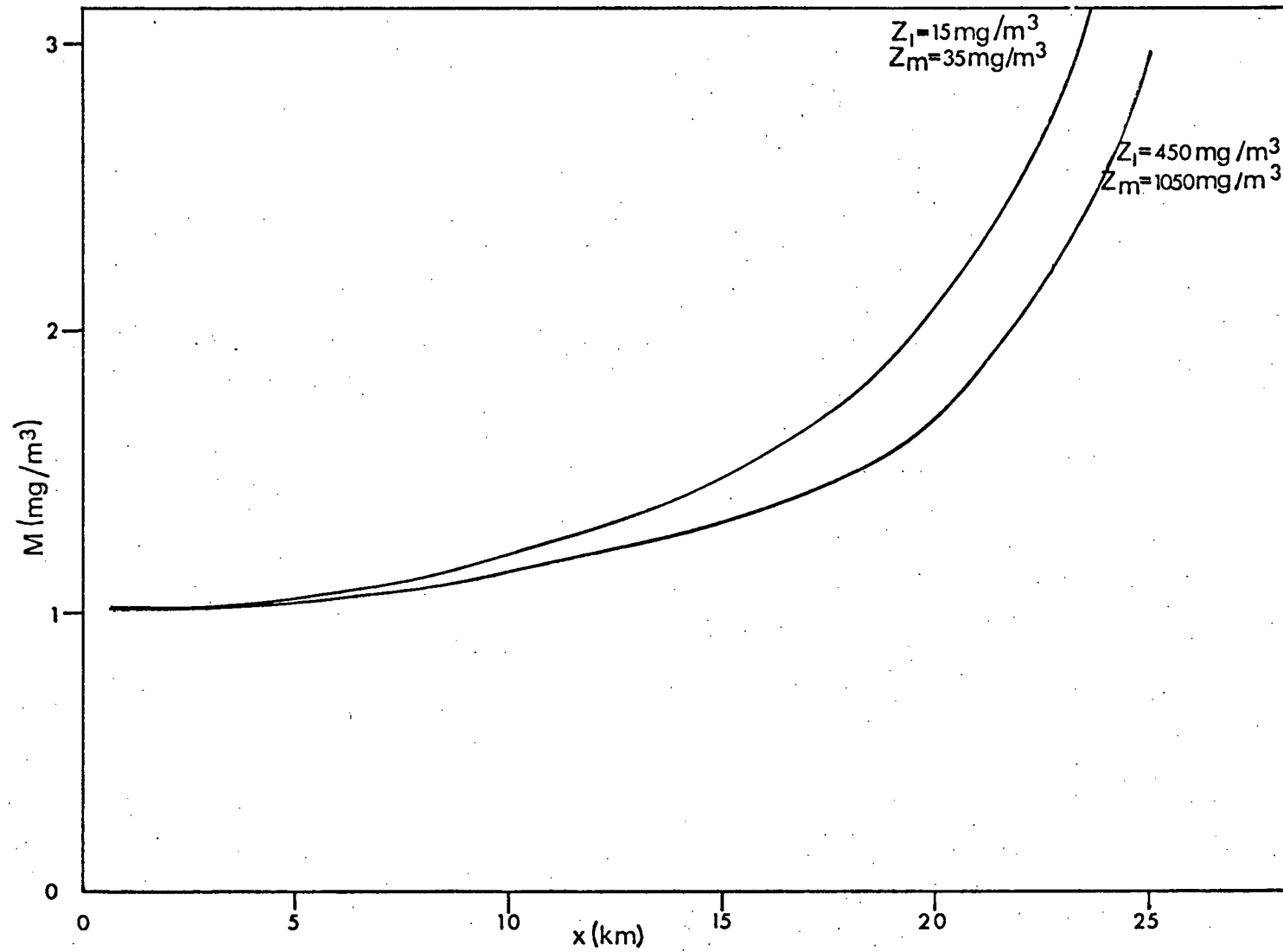
Fig. 44. Variation of M along y = 0 (model II); the effect of changes in the grazing term by increasing $Z_l$ and $Z_m$.

appears that the grazing term is not one of the more important terms.

f) Variations in the sinking rate

The phytoplankton sinking rate was increased from $w_s = 1$ m/day of the reference curve to $w_s = 5$ m/day. These curves are shown in Fig. 45 with the top curve being the reference curve. The increased sinking rate results in a much reduced chlorophyll concentration.

g) Lateral distribution of chlorophyll

To illustrate the lateral distribution of chlorophyll we have chosen the case illustrated in Fig. 46 ($U_o = 1$ m/sec, $x_o = 10$ km). The parameters are the same as the middle curve of Fig. 42 which shows the distribution of M along $y = 0$ (the axis of the velocity field).

In contrast to model I (Figures 31 and 32) two completely distinct distributions are not found for model II. The most common pattern for model II (Fig. 46) resembles Fig. 31 of model I. Provided M shows either a monotonic increase or decrease, the lines of constant M are convex towards positive x, ie. the locii of points $(x,y)$ of M = constant are located such that as x increases the magnitude of y decreases. The few cases that differ from Fig. 46 are those where there is first a decrease and then an increase in M with distance from the river mouth. Near the river mouth (where M is decreasing) the contours of constant M are closed, while in the region where M is increasing the contours of M = constant resemble those of Fig. 46. If one
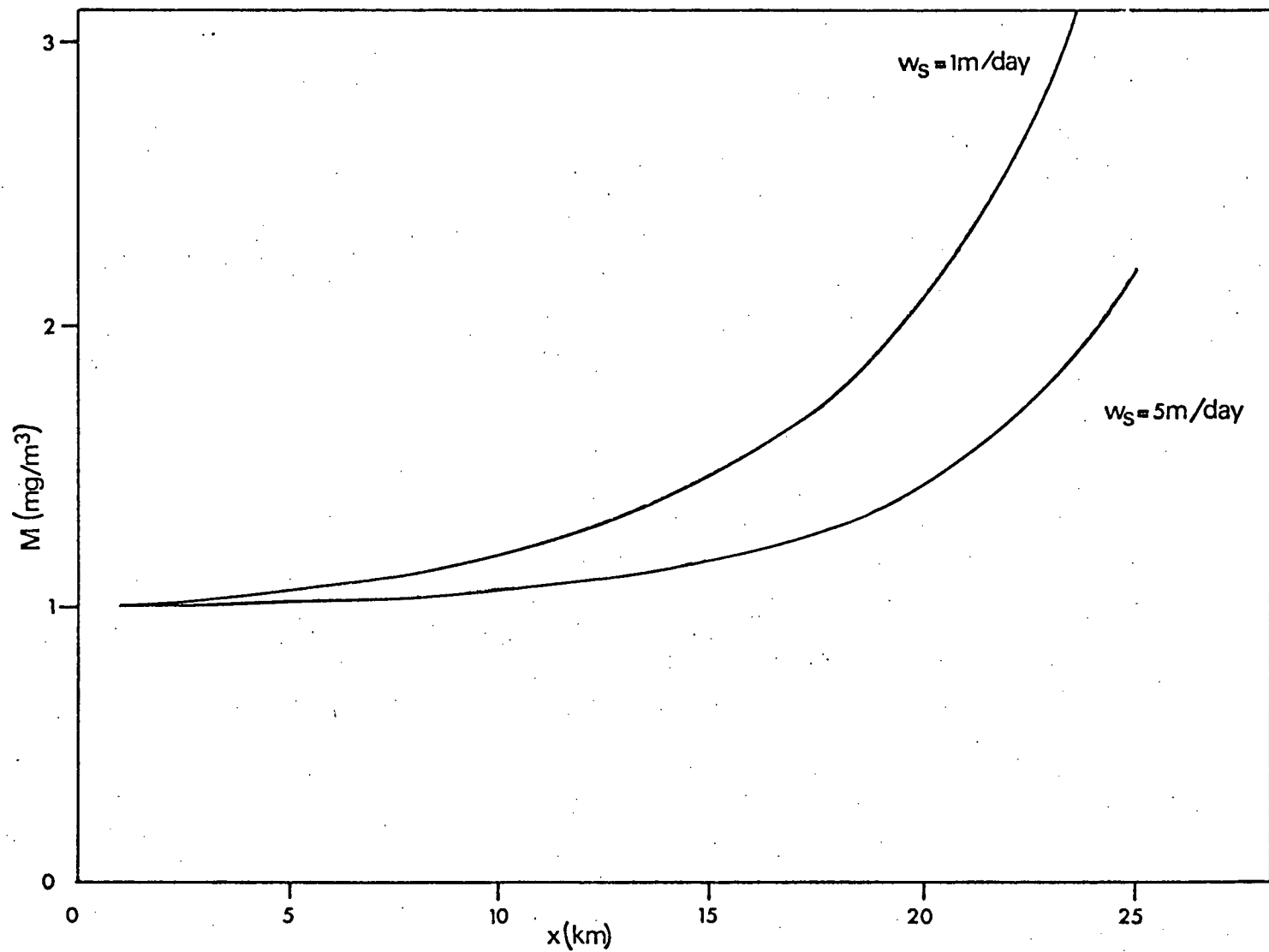
Fig. 45. Variation of M along y = 0 (model II); the effect of increasing the sinking rate.
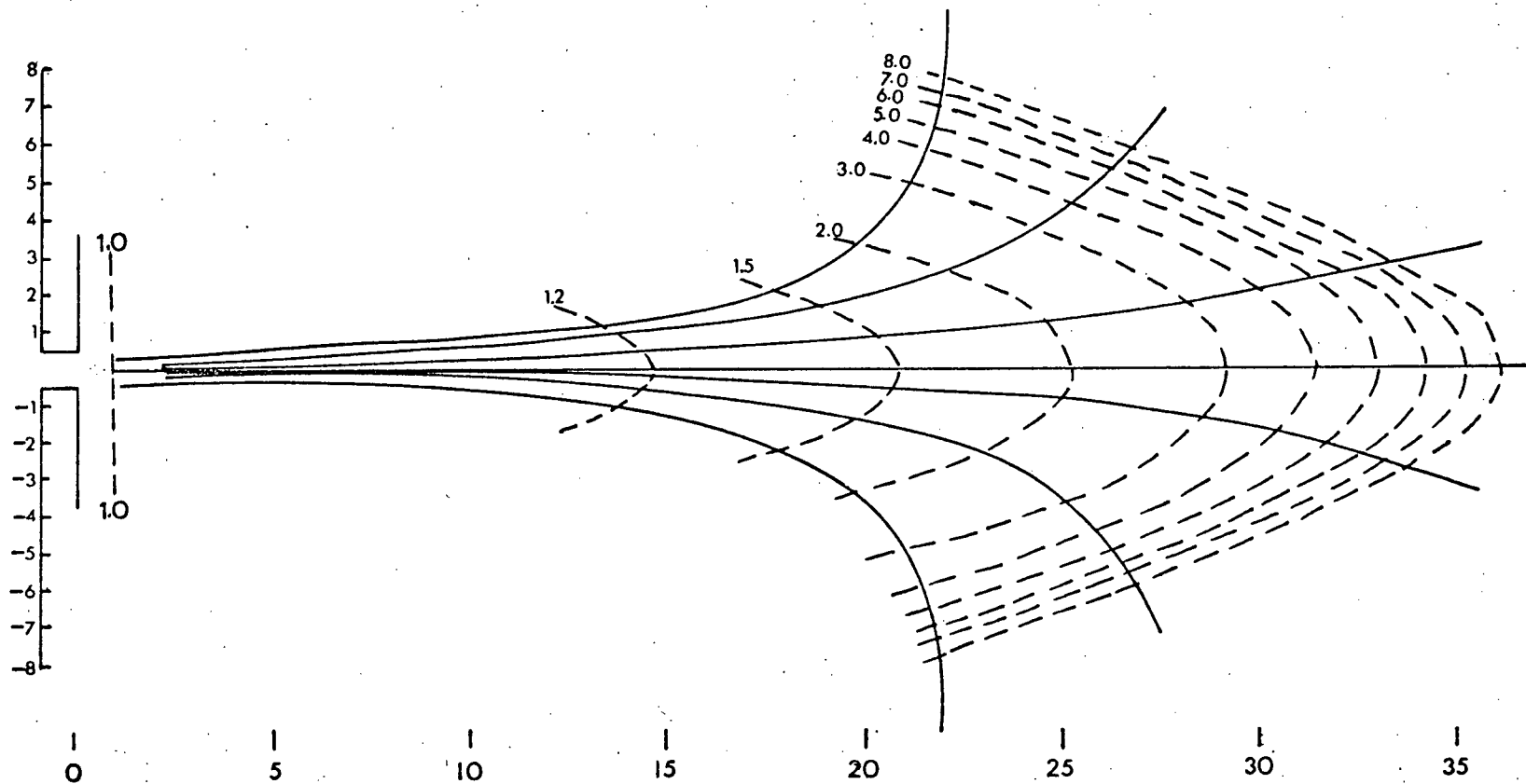
Fig. 46.  Horizontal distribution of M for model II; solid lines are streamlines, dashed lines are contours of M = constant, $U_o$ = 1 m/sec, $x_o$ = 10 km.

looks just at the region where M is decreasing, then the M contours look similar to those of Fig. 32 of model I.

Discussion

Model II, which has been discussed above, has produced essentially the same results as model I, even though greater realism was introduced into model II. Probably the single most important difference between the two models is the variation of the upper layer thickness with x and y in model II, since it affects both the velocity field and the production term. Using the same parameter values in both models led to lower values of M in the second model when looking at seasonal differences. Again it became apparent that the available light, the magnitude of $P_m$ and the advection by the velocity field were the most important parameters while zooplankton grazing had relatively little influence on M. In none of the model runs was it possible to produce a downstream maximum such as we set out to study (Fig. 5).

The reduced values of M in the second model (as compared to model I) can be explained in part by the increase in the layer depth which decreases the average light intensity, thus reducing the size of the production term. Another factor is the formulation used for the depth integrated production term. It will be recalled that one of the assumptions used in the model is that the phytoplankton population is vertically mixed over time periods that are short relative to the growing time, so that light of varying intensities is experienced at different depths. Thus we used a depth-averaged light intensity in

equation (5.3). To check the effect of this assumption we compared $\bar{P} \int \nu \, dz/h$ to $\int P\nu \, dz/h$ for various values of extinction coefficient, $\mu$, and various values of layer thickness, h. Some of the resulting curves are shown in Fig. 47 . It can be seen that only when the layer thickness or the extinction coefficient become sufficiently large, so that the average light intensity decreases enough, does the assumption lead to an under-estimate of the production term. The curves diverge noticeably for $I(z)/I_o < 0.027$. Thus the lower values of M in model II can be attributed, at least partly, to the layer depth variation and the assumption that the plankton experience a depth-averaged light intensity.
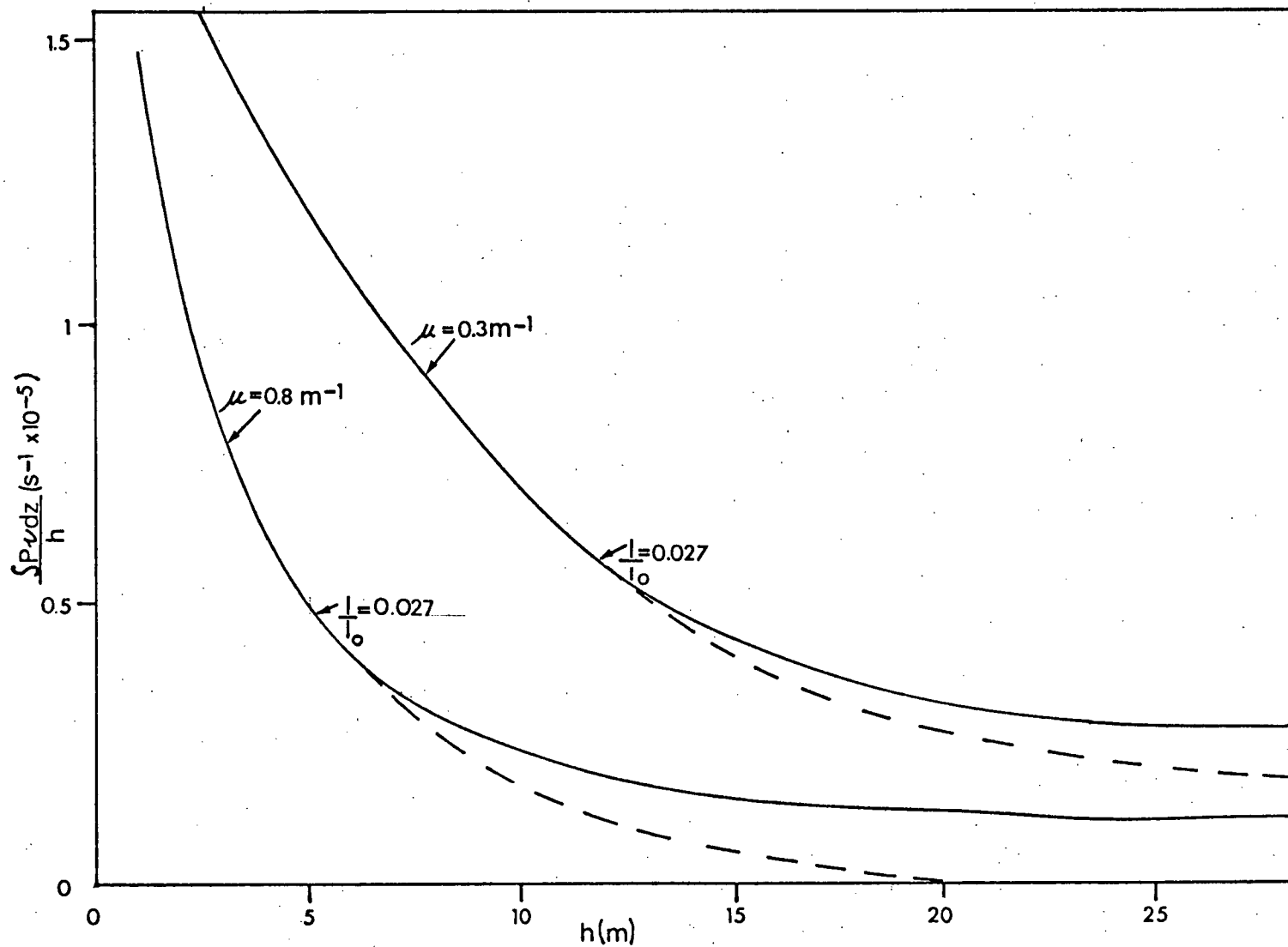
Fig. 47. Comparison of $\overline{P} \int \nu \, dz/h$ and $\int P\nu \, dz/h$ as a function of layer depth, dashed line represents the results for $\overline{P}$.

# CHAPTER 11.   CONCLUSIONS

The  two models discussed above have given an indication of the relative importance of the various parameters that determine the chlorophyll distribution.  The two most important  terms  in the  chlorophyll  conservation  equation  appear  to  be  the production term and the advection term, with  the  sinking  term being  of  somewhat  lesser  importance and the grazing term the least important.

The production term is  affected  by  the  insolation,  the turbidity  of  the  water,  the depth of the upper layer and the maximum  production  rate  (through  water  temperature).   The increase  in  the  incident radiation, the decrease in the upper layer thickness (through  increased  stability  due  to  greater fresh  water  input)  and the increase in the maximum production rate all tend to increase production as winter changes to spring and summer.  On the other hand the increased turbidity tends  to decrease the available light in the water column, decreasing the production term.

The  advection  term  also  varies  with  the season; river discharge increasing  from  winter  to  summer.   The  increased discharge  tends  to  increase the velocity components, (u,v,w), giving rise to a greater flushing rate (shorter residence  time) and  increased  mixing  and entrainment. However, the increased mixing is inhibited somewhat by the  greater  stability  of  the water column as runoff increases.

It  appears that the natural stability of the phytoplankton population in the Strait of Georgia may  be  attributed  to  the fact that although insolation, the upper layer thickness and the

production rate serve to increase the chlorophyll concentration as winter changes to summer, the increased turbidity and advection work in the opposite direction, limiting the size of the blooms. Only when an imbalance occurs is there a large increase in the population. One mechanism for this imbalance (or perhaps a result of it) may be patchiness.

The results of these studies point to further work that could be done to improve the realism of the model. It is felt that the single most important step is to develop a better model of the velocity field for river estuaries such as the Fraser River. It has been shown that advection is very important in determining the chlorophyll distribution, hence to attempt further modelling without a better velocity field model would not prove very useful. Recent measurements of flow in the Fraser River plume have shown how the river discharge is pulsed by tidal modulation. Also the downstream velocity does not appear to decay as $1/x$ (as the analogy with jets suggests) but rather more slowly (S. Pond, pers. com.). Further work on this problem is presently underway at this Institute.

A second deficiency of the present models is the fact that time dependent changes are not included in the formulation. This is not very important for long time scales (eg. seasonal variations) since the time required for the phytoplankton population to achieve equilibrium is much shorter than that required for the long period variations to be felt. However, when such things as the diurnal variation of the insolation, the diurnal vertical migration of zooplankton and the tidally induced variations in the velocity field are considered in

conjunction with the non-linearity of some of the terms in the chlorophyll conservation equation, the limitations of the present models can be appreciated, particularly since the grazing is about 180° (i.e. 1/2 day) out of phase with the photosynthetic production.

Spatial inhomogeneity must also be considered. We have shown in Chapter 10 that, in general, averaging the effect of the vertical structure of the chlorophyll distribution and the available light did not introduce large errors. However, the combined effect of the vertical chlorophyll distribution and the vertical migration of the zooplankton population must be investigated in conjunction with a time-dependent formulation.

Last but not least is the problem of choosing values for the biological parameters. Most of the biological parameters can take on a large range of values. Part of that is due to natural variations between species, geographical areas and in time. Another is that laboratory measurements may give different results than field studies. The problem is not a simple one to resolve. However, it indicates that realistic models must have input from field studies in the particular area of interest in order to choose the correct parameter values. In our study the problems of shelf-shading and nutrient limitation were not considered; they would become more important at the higher chlorophyll concentrations.

In summary, although it was not possible to produce the downstream maximum in the distribution of chlorophyll that we set out to explain, it was shown that the light available in the water column, the value of $P_m$ and the velocity field are

important in determining the chlorophyll distribution. The effect of changes in these parameters must be considered when evaluating the results of natural or man-made changes to the system, such as damming the Fraser River, constructing a nuclear power plant or discharging possible pollutants.

REFERENCES

Abraham, G., 1960. Jet diffusion in liquid of greater density. J. Hyd. Div., Proc. ASCE 86, HY6, 1-13.

Antia, N.J., C.D. McAllister, T.R. Parsons, K. Stephens and J.D.H. Strickland 1963. Further measurements of primary production using a large-volume plastic sphere. Limnol. Oceanogr. 8, 166-183.

Caperon, J., 1967. Population growth in micro-organisms limited by food supply. Ecology 48(5), 715-722.

Fulton, J.D., O.D. Kennedy, K. Stephens and J. Skelding, MS 1968. Data record; physical, chemical and biological data, Strait of Georgia, 1967. Fish. Res. Bd. Canada, Man. Rep. No. 968.

Gargett, A.E., 1976. Generation of internal waves in the Strait of Georgia, British Columbia. Deep-Sea Research 23(1), 17-32.

Giovando, L.F. and S. Tabata, MS 1970. Measurements of surface flow in the Strait of Georgia by means of free-floating current followers. Fish. Res. Bd. Canada, Tech. Rep. No. 163, 69 pp.

Hodgins, D.O., 1974. Salinity intrusion in the Fraser River, British Columbia. Ph.D. dissertation, Univ. of British Columbia.

Ivlev, V.S., 1961. Experimental ecology of the feeding of fishes. Translated by D. Scott. Yale Univ. Press, New Haven. 302 pp.

Keulegan, G.H., 1966. The mechanism of an arrested saline wedge. pp. 546-574 in Estuary and Coastline Hydrodynamics, A.T. Ippen, ed. McGraw-Hill, N.Y. 744 pp.

Parsons, T.R., MS 1965. A general description of some factors governing primary production in the Strait of Georgia, Hecate Strait and Queen Charlotte Sound and the Pacific Ocean. Fish. Res. Bd. Canada, Man. Rep. No. 193.

Parsons, T.R. and B.R. de Lange Boom, 1972. The control of ecosystem processes in the sea. pp. 29-58 in The Biology of the Oceanic Pacific, C.B. Miller, ed. Oregon State Univ. Press, Corvallis. 155 pp.

Parsons, T.R., R.J. LeBrasseur and W.E. Barraclough, 1970. Levels of production in the pelagic environment of the Strait of Georgia, British Columbia: a review. J. Fish. Res. Bd. Canada 27, 1251-1264.

Parsons, T.R., R.J. LeBrasseur, J.D. Fulton and O.D. Kennedy, 1969. Production studies in the Strait of Georgia. Part II. Secondary production under the Fraser River plume, February to May, 1967.

J. exp. mar. Biol. Ecol. 3, 39-50.

Parsons, T.R., K. Stephens and R.J. LeBrasseur, 1969. Production studies in the Strait of Georgia. Part I. Primary production under the Fraser River plume, February to May, 1967. J. exp. mar. Biol. Ecol. 3, 27-38.

Parsons, T.R. and M. Takahashi, 1973. Biological Oceanographic Processes. Pergamon, Oxford. 186 pp.

Platt, T., 1972. Local phytoplankton abundance and turbulence. Deep-Sea Res. 19, 183-188.

Riley, G.A., H. Stommel and O.A. Bumpus, 1949. Quantitative ecology of the western North Atlantic. Bull. Bingham Oceanogr. Coll. 12, 1-169.

Smayda, T.J., 1970. The suspension and sinking of phytoplankton in the sea. Oceanogr. Mar. Biol. Ann. Rev. 8, 353-414.

Steele, J.H., 1962. Environmental control of photosynthesis in the sea. Limnol. Oceanogr. 7, 137-150.

Stefan, H. and F.R. Schiebe, 1970. Heated discharge from flume into tank. J. Sanit. Eng. Div., Proc. ASCE 96, SA6, 1415-1433.

Stephens, K., J.D. Fulton and O.D. Kennedy, MS 1969. Summary of biological oceanographic observations in the Strait of Georgia, 1965-1968. Fish. Res. Bd. Canada, Tech. Rep. No. 110.

Strickland, J.D.H., 1958. Solar radiation penetrating the ocean. A review of requirements, data and methods of measurements, with particular reference to photosynthetic productivity. J. Fish. Res. Bd. Canada 15, 453-493.

Tabata, S., MS 1972. The movement of Fraser River-influenced surface water in the Strait of Georgia as deduced from a series of aerial photographs. Marine Sciences Branch, Pac. Mar. Sc. Rep. No. 72-6, 69 pp.

Tabata, S., L.F. Giovando, J.A. Stickland and J. Wong, MS 1970. Current velocity measurements in the Strait of Georgia - 1967. Fish. Res. Bd. Canada, Tech. Rep. No. 169, 245 pp.

Takahashi, M., K. Fujii and T.R. Parsons, 1973. Simulation study of phytoplankton photosynthesis and growth in the Fraser River estuary. Mar. Biol. 19, 102-116.

Thomas, D.J., 1975. The distribution of zinc and copper in Georgia Strait, British Columbia: Effects of the Fraser River and sediment-exchange reactions. M.Sc. dissertation, Univ. of British Columbia.

Tully, J.P. and A.J. Dodimead, 1957.  Properties of the water in the
    Strait of Georgia, British Columbia and influencing factors.  J.
    Fish. Res. Bd. Canada 14, 241-319.

Waldichuck, M., 1957.  Physical oceanography of the Strait of Georgia,
    British Columbia.  J. Fish. Res. Bd. Canada 14, 321-486.

Wiegel, R.L., 1970.  Ocean dynamics.  pp. 123-228 in Hydronautics, H.
    E. Sheets and V.T. Boatwright Jr., ed.  Academic Press, N.Y.
    454 pp.

## APPENDIX: TEMPERATURE AND SALINITY DATA

Abbreviations used:

    CRN  --  cruise number, G for Gulf

    HR    --  time observation started (GMT)

    STN  --  station number

    DY    --  date, (day/month/year)

Note: The first 5 stations of cruise 2 (profiles to 20 m) correspond to the single number stations in Fig. 14. The stations preceded by a 2 in Fig. 14 correspond to the 14 cruise 2 stations with profiles to 50 m.

| CRN: G- 1 | HR: 1814 | |
|:---:|:---:|:---:|
| STN: 01 | DY: 02/11/71 | |
| Depth (m) | Temp. (°C) | Sal. (‰) |
| 0 | 8.7 | 20.4 |
| 1 | 9.2 | 25.6 |
| 2 | 9.3 | 27.0 |
| 3 | 9.0 | 26.4 |
| 5 | 9.2 | 26.6 |
| 7 | 9.3 | 28.4 |
| 10 | 9.2 | 28.7 |
| 15 | 9.4 | 29.1 |
| 20 | 9.2 | 29.4 |
| 30 | 9.4 | 30.1 |
| 50 | 9.4 | 30.2 |

| CRN: G- 1 | HR: 1856 | |
|:---:|:---:|:---:|
| STN: 02 | DY: 02/11/71 | |
| Depth (m) | Temp. (°C) | Sal. (‰) |
| 0 | 8.8 | 24.3 |
| 1 | 8.9 | 25.5 |
| 2 | 8.8 | 26.0 |
| 5 | 9.0 | 26.3 |
| 10 | 10.0 | 28.5 |
| 15 | 9.8 | 28.8 |
| 20 | 9.7 | 28.6 |
| 30 | 9.7 | 30.1 |
| 50 | 9.7 | 30.3 |
| 75 | 9.7 | 30.8 |

| CRN: G- 1 | HR: 1922 | |
|---|---|---|
| STN: 03 | DY: 02/11/71 | |
| Depth (m) | Temp. (°C) | Sal. (‰) |
| 0 | 8.8 | 24.6 |
| 1 | 8.9 | 27.0 |
| 2 | 8.8 | 26.9 |
| 5 | 9.0 | 27.5 |
| 7 | 9.2 | 27.9 |
| 10 | 9.5 | 28.7 |
| 15 | 9.5 | 29.0 |
| 20 | 9.6 | 29.0 |
| 30 | 9.6 | 29.5 |
| 50 | 9.8 | 30.5 |
| 75 | 9.7 | 30.9 |

| CRN: G- 1 | HR: 1948 | |
|---|---|---|
| STN: 04 | DY: 02/11/71 | |
| Depth (m) | Temp. (°C) | Sal. (‰) |
| 0 | 8.7 | 24.3 |
| 1 | 8.6 | 24.2 |
| 2 | 8.8 | 25.7 |
| 5 | 9.3 | 27.3 |
| 7 | 9.2 | 27.3 |
| 10 | 9.3 | 27.5 |
| 15 | 9.5 | 27.9 |
| 20 | 9.6 | 28.4 |
| 30 | 9.6 | 29.3 |
| 50 | 9.5 | 30.2 |
| 75 | 9.8 | 30.9 |

| CRN: G- 1 | | HR: 2014 |
| STN: 05 | DY: | 02/11/71 |
| Depth (m) | Temp. (°C) | Sal. (‰) |
| --- | --- | --- |
| 0 | 8.7 | 24.2 |
| 1 | 8.6 | 24.4 |
| 2 | 8.5 | 24.7 |
| 5 | 9.0 | 27.4 |
| 7 | 9.1 | 27.6 |
| 10 | 9.2 | 28.4 |
| 15 | 9.4 | 29.3 |
| 20 | 9.4 | 29.5 |
| 30 | 9.4 | 29.8 |
| 50 | 9.1 | 30.2 |

| CRN: G- 1 | | HR: 2047 |
| STN: 06 | DY: | 02/11/71 |
| Depth (m) | Temp. (°C) | Sal. (‰) |
| --- | --- | --- |
| 0 | 9.0 | 25.7 |
| 1 | 8.8 | 25.8 |
| 2 | 8.8 | 26.0 |
| 5 | 8.9 | 26.1 |
| 7 | 9.2 | 27.5 |
| 10 | 9.2 | 27.9 |
| 15 | 9.8 | 28.9 |
| 20 | 9.6 | 29.4 |
| 30 | 9.6 | 29.6 |
| 50 | 9.4 | 30.3 |
| 75 | 9.7 | 30.7 |

| CRN: G- 1    HR: 2116 | | |
|:---:|:---:|:---:|
| STN: 07    DY: 02/11/71 | | |
| Depth (m) | Temp. (°C) | Sal. (‰) |
| 0 | 9.0 | 27.0 |
| 1 | 9.0 | 27.6 |
| 2 | 8.9 | 27.3 |
| 5 | 8.9 | 27.6 |
| 7 | 8.8 | 28.0 |
| 10 | 9.0 | 28.2 |
| 15 | 9.2 | 28.5 |
| 20 | 9.7 | 28.8 |
| 30 | 9.4 | 29.9 |
| 50 | 9.2 | 30.2 |
| 75 | 9.8 | 30.8 |

| CRN: G- 1    HR: 2141 | | |
|:---:|:---:|:---:|
| STN: 08    DY: 02/11/71 | | |
| Depth (m) | Temp. (°C) | Sal. (‰) |
| 0 | 8.9 | 27.3 |
| 1 | 8.8 | 27.4 |
| 2 | 8.8 | 27.6 |
| 5 | 8.8 | 27.7 |
| 7 | 8.8 | 27.7 |
| 10 | 8.9 | 27.7 |
| 15 | 9.2 | 28.5 |
| 20 | 9.2 | 28.6 |
| 30 | 9.6 | 29.4 |
| 50 | 9.4 | 30.3 |
| 75 | 9.8 | 30.8 |

| CRN: G- 1 HR: 2212 | | | CRN: G- 1 HR: 2236 | | |
| STN: 09 DY: 02/11/71 | | | STN: 10 DY: 02/11/71 | | |
| Depth (m) | Temp. (°C) | Sal. (‰) | Depth (m) | Temp. (°C) | Sal. (‰) |
|---|---|---|---|---|---|
| 0 | 9.0 | 28.1 | 0 | 9.0 | 28.1 |
| 1 | 9.0 | 28.1 | 1 | 8.9 | 28.2 |
| 2 | 9.0 | 28.2 | 2 | 8.8 | 28.3 |
| 5 | 9.0 | 28.2 | 5 | 8.8 | 28.4 |
| 7 | 8.9 | 28.2 | 7 | 8.8 | 28.4 |
| 10 | 9.1 | 28.4 | 10 | 8.8 | 28.6 |
| 15 | 9.2 | 28.6 | 15 | 9.0 | 28.9 |
| 20 | 9.1 | 28.9 | 20 | 9.0 | 28.9 |
| 30 | 9.4 | 29.4 | 30 | 9.3 | 29.5 |
| 50 | 9.3 | 30.4 | 50 | 9.3 | 30.5 |
| 75 | 9.6 | 31.0 | 75 | 9.5 | 31.0 |

| CRN: G- 1 HR: 0041 | | |
| STN: 1 DY: 03/11/71 | | |
| Depth (m) | Temp. (°C) | Sal. (‰) |
|---|---|---|
| 0 | 8.1 | 23.3 |
| 1 | 8.0 | 23.2 |
| 2 | 8.0 | 23.5 |
| 5 | 8.4 | 25.7 |
| 7 | 8.7 | 28.4 |
| 10 | 8.8 | 28.6 |

| CRN: G- 2 | | HR: 2120 |
|---|---|---|
| STN: 01 | | DY: 09/02/72 |
| Depth (m) | Temp. ($^0$C) | Sal. (‰) |
| 0 | 5.0 | 27.2 |
| 1 | 5.0 | 27.3 |
| 2 | 5.2 | 28.9 |
| 3 | 5.5 | 29.9 |
| 5 | 5.6 | 30.5 |
| 7 | 5.6 | 30.5 |
| 10 | 5.8 | 30.8 |
| 15 | 6.0 | 30.9 |
| 20 | 6.2 | 30.9 |

| CRN: G- 2 | | HR: 2220 |
|---|---|---|
| STN: 02 | | DY: 09/02/72 |
| Depth (m) | Temp. ($^0$C) | Sal. (‰) |
| 0 | 5.4 | 30.1 |
| 1 | 5.4 | 30.1 |
| 2 | 5.5 | 30.2 |
| 3 | 5.5 | 30.3 |
| 5 | 5.5 | 30.3 |
| 7 | 5.5 | 30.3 |
| 10 | 5.6 | 30.4 |
| 15 | 5.8 | 30.6 |
| 20 | 6.0 | 30.9 |

| CRN: G- 2 | | HR: 2322 |
|---|---|---|
| STN: 03 | | DY: 09/02/72 |
| Depth (m) | Temp. ($^0$C) | Sal. (‰) |
| 0 | 4.8 | 23.4 |
| 1 | 4.9 | 27.6 |
| 2 | 4.9 | 28.0 |
| 3 | 5.0 | 29.7 |
| 5 | 5.1 | 30.2 |
| 7 | 5.3 | 30.2 |
| 10 | 5.4 | 30.3 |
| 15 | 5.6 | 30.4 |
| 20 | 5.6 | 30.5 |

| CRN: G- 2 | | HR: 0025 |
|---|---|---|
| STN: 04 | | DY: 10/02/72 |
| Depth (m) | Temp. ($^0$C) | Sal. (‰) |
| 0 | 4.6 | 18.6 |
| 1 | 4.7 | 21.6 |
| 2 | 5.2 | 27.6 |
| 3 | 5.5 | 29.3 |
| 5 | 5.7 | 30.5 |
| 7 | 5.7 | 30.6 |
| 10 | 5.9 | 30.6 |
| 15 | 5.9 | 30.6 |
| 20 | 5.9 | 30.8 |

| CRN: G- 2 | | HR: 0220 |
| STN: 05 | | DY: 10/02/72 |
| Depth (m) | Temp. (°C) | Sal. (‰) |
| --- | --- | --- |
| 0 | 3.1 | 12.9 |
| 1 | 4.0 | 22.0 |
| 2 | 4.1 | 22.6 |
| 3 | 4.3 | 25.9 |
| 5 | 5.1 | 30.2 |
| 7 | 5.8 | 30.5 |
| 10 | 5.6 | 30.5 |
| 14 | 5.7 | 30.6 |
| 19 | 6.1 | 31.0 |

| CRN: G- 2 | | HR: 1205 |
| STN: 01 | | DY: 10/02/72 |
| Depth (m) | Temp. (°C) | Sal. (‰) |
| --- | --- | --- |
| 0 | 4.3 | 24.0 |
| 1 | 5.1 | 27.4 |
| 2 | 5.4 | 30.3 |
| 3 | 5.6 | 30.6 |
| 5 | 5.8 | 30.7 |
| 7 | 6.3 | 31.0 |
| 10 | 6.4 | 31.0 |
| 15 | 5.9 | 31.4 |
| 20 | 5.7 | 31.4 |
| 29 | 5.7 | 31.4 |
| 38 | 5.7 | 31.4 |
| 48 | 5.5 | 31.4 |

| CRN: G- 2 HR: 1250 | | |
| STN: 02 DY: 10/02/72 | | |
| Depth (m) | Temp. ($^{o}$C) | Sal. (‰) |
| --- | --- | --- |
| 0 | 3.9 | 19.8 |
| 1 | 3.9 | 20.1 |
| 2 | 4.5 | 24.1 |
| 3 | 4.6 | 25.5 |
| 5 | 5.2 | 29.7 |
| 7 | 5.4 | 30.1 |
| 10 | 5.9 | 31.1 |
| 15 | 6.1 | 31.2 |
| 20 | 6.2 | 31.2 |
| 30 | 6.4 | 31.3 |
| 40 | 6.4 | 31.3 |
| 50 | 5.8 | 31.3 |

| CRN: G- 2 HR: 1333 | | |
| STN: 03 DY: 10/02/72 | | |
| Depth (m) | Temp. ($^{o}$C) | Sal. (‰) |
| --- | --- | --- |
| 0 | 3.3 | 15.8 |
| 1 | 4.0 | 20.6 |
| 2 | 4.2 | 23.3 |
| 3 | 5.0 | 28.5 |
| 5 | 5.2 | 30.1 |
| 7 | 5.3 | 30.5 |
| 10 | 5.6 | 31.0 |
| 15 | 5.8 | 31.2 |
| 20 | 5.8 | 31.3 |
| 30 | 6.1 | 31.3 |
| 40 | 6.1 | 31.4 |
| 50 | 6.1 | 31.4 |

| CRN: G- 2    HR: 1409 | | | CRN: G- 2    HR: 1440 | | |
| STN: 04    DY: 10/02/72 | | | STN: 05    DY: 10/02/72 | | |
|---|---|---|---|---|---|
| Depth (m) | Temp. ($^{o}$C) | Sal. (‰) | Depth (m) | Temp. ($^{o}$C) | Sal. (‰) |
| 0 | 4.2 | 21.6 | 0 | 4.8 | 25.8 |
| 1 | 4.2 | 21.9 | 1 | 5.0 | 28.1 |
| 2 | 4.2 | 23.4 | 2 | 5.0 | 28.1 |
| 3 | 5.2 | 29.5 | 3 | 5.3 | 30.3 |
| 5 | 5.3 | 30.1 | 5 | 5.3 | 30.3 |
| 7 | 5.5 | 30.3 | 7 | 5.5 | 30.5 |
| 10 | 5.7 | 30.6 | 10 | 5.6 | 30.5 |
| 15 | 5.9 | 30.7 | 15 | 5.8 | 30.7 |
| 20 | 5.9 | 30.7 | 20 | 5.9 | 30.7 |
| 30 | 6.1 | 30.7 | 30 | 6.1 | 30.9 |
| 40 | 6.3 | 31.0 | 40 | 6.3 | 31.0 |
| 50 | 6.7 | 31.2 | 50 | 6.6 | 31.2 |

| CRN: G- 2 HR: 1511 | | | CRN: G- 2 HR: 1553 | | |
| STN: 06 DY: 10/02/72 | | | STN: 07 DY: 10/02/72 | | |
|---|---|---|---|---|---|
| Depth (m) | Temp. (°C) | Sal. (‰) | Depth (m) | Temp. (°C) | Sal. (‰) |
| 0 | 5.1 | 29.2 | 0 | 5.2 | 29.6 |
| 1 | 5.3 | 29.2 | 1 | 5.2 | 29.7 |
| 2 | 5.0 | 29.0 | 2 | 5.2 | 29.7 |
| 3 | 5.1 | 29.0 | 3 | 5.2 | 29.9 |
| 5 | 5.3 | 29.9 | 5 | 5.2 | 29.9 |
| 7 | 5.4 | 30.3 | 7 | 5.2 | 30.1 |
| 10 | 5.4 | 30.4 | 10 | 5.3 | 30.3 |
| 15 | 5.5 | 30.5 | 15 | 5.5 | 30.5 |
| 20 | 5.8 | 30.9 | 20 | 5.6 | 30.6 |
| 30 | 6.3 | 31.0 | 30 | 5.7 | 30.6 |
| 40 | 6.7 | 31.3 | 40 | 6.0 | 30.9 |
| 50 | 6.9 | 31.3 | 50 | 6.0 | 31.0 |

| CRN: G- 2 | | HR: 1622 |
| --- | --- | --- |
| STN: 08 | DY: | 10/02/72 |
| Depth (m) | Temp. (°C) | Sal. (‰) |
| 0 | 4.8 | 27.2 |
| 1 | 5.0 | 29.5 |
| 2 | 5.0 | 29.1 |
| 3 | 5.1 | 29.5 |
| 5 | 5.1 | 29.9 |
| 7 | 5.2 | 30.2 |
| 10 | 5.4 | 30.3 |
| 15 | 5.5 | 30.4 |
| 19 | 5.6 | 30.5 |
| 29 | 5.9 | 30.9 |
| 39 | 6.3 | 31.0 |
| 48 | 6.8 | 31.3 |

| CRN: G- 2 | | HR: 1648 |
| --- | --- | --- |
| STN: 09 | DY: | 10/02/72 |
| Depth (m) | Temp. (°C) | Sal. (‰) |
| 0 | 4.7 | 28.9 |
| 1 | 5.0 | 29.2 |
| 2 | 5.0 | 29.1 |
| 3 | 5.1 | 29.3 |
| 5 | 5.2 | 30.1 |
| 7 | 5.2 | 30.1 |
| 10 | 5.2 | 30.1 |
| 15 | 5.2 | 30.2 |
| 20 | 5.4 | 30.5 |
| 30 | 6.1 | 30.9 |
| 40 | 6.5 | 31.2 |
| 50 | 6.7 | 31.3 |

| CRN: G- 2 | | HR: 1720 |
|---|---|---|
| STN: 10 | DY: | 10/02/72 |
| Depth (m) | Temp. (°C) | Sal. (‰) |
| 0 | 3.3 | 17.8 |
| 1 | 4.8 | 26.7 |
| 2 | 5.1 | 28.7 |
| 3 | 5.1 | 28.8 |
| 5 | 5.2 | 29.5 |
| 7 | 5.3 | 29.9 |
| 10 | 5.5 | 30.2 |
| 15 | 5.6 | 30.5 |
| 20 | 5.8 | 31.0 |
| 30 | 6.0 | 31.4 |
| 40 | 6.0 | 31.4 |
| 50 | 6.0 | 31.4 |

| CRN: G- 2 | | HR: 1747 |
|---|---|---|
| STN: 11 | DY: | 10/02/72 |
| Depth (m) | Temp. (°C) | Sal. (‰) |
| 0 | 4.2 | 23.5 |
| 1 | 4.8 | 26.8 |
| 2 | 4.8 | 27.3 |
| 3 | 5.0 | 28.1 |
| 5 | 5.5 | 30.0 |
| 7 | 5.5 | 30.2 |
| 10 | 5.5 | 30.5 |
| 15 | 5.5 | 30.7 |
| 20 | 6.1 | 31.3 |
| 30 | 6.6 | 31.4 |
| 40 | 6.5 | 31.6 |
| 50 | 6.2 | 31.6 |

| CRN: G- 2 | HR: 1816 | |
| --- | --- | --- |
| STN: 12 | DY: 10/02/72 | |
| Depth (m) | Temp. (°C) | Sal. (‰) |
| 0 | 3.5 | 15.6 |
| 1 | 5.0 | 27.4 |
| 2 | 5.5 | 30.2 |
| 3 | 5.4 | 30.3 |
| 5 | 5.8 | 31.0 |
| 7 | 6.1 | 31.0 |
| 10 | 6.2 | 31.4 |
| 15 | 6.2 | 31.5 |
| 20 | 6.3 | 31.5 |
| 30 | 5.9 | 31.5 |
| 40 | 5.7 | 31.6 |
| 50 | 5.7 | 31.5 |

| CRN: G- 2 | HR: 1846 | |
| --- | --- | --- |
| STN: 13 | DY: 10/02/72 | |
| Depth (m) | Temp. (°C) | Sal. (‰) |
| 0 | 4.5 | 25.5 |
| 1 | 4.7 | 25.2 |
| 2 | 5.1 | 30.1 |
| 3 | 5.2 | 30.0 |
| 5 | 5.4 | 30.2 |
| 7 | 5.4 | 30.2 |
| 10 | 5.4 | 30.2 |
| 15 | 5.8 | 30.6 |
| 20 | 6.0 | 30.7 |
| 30 | 6.0 | 30.9 |
| 40 | 6.0 | 31.1 |
| 50 | 6.3 | 31.1 |

| CRN: G- 2 | HR: 1921 | |
|---|---|---|
| STN: 14 | DY: 10/02/72 | |
| Depth (m) | Temp. (°C) | Sal. (‰) |
| 0 | 4.7 | 26.6 |
| 1 | 5.2 | 27.6 |
| 2 | 5.4 | 30.0 |
| 3 | 5.5 | 30.1 |
| 5 | 5.5 | 30.2 |
| 7 | 5.5 | 30.2 |
| 10 | 5.5 | 30.2 |
| 15 | 5.5 | 30.2 |
| 20 | 5.5 | 30.4 |
| 30 | 5.9 | 30.6 |
| 40 | 6.4 | 30.9 |
| 50 | 6.8 | 31.1 |

| CRN: G- 3 | HR: 1910 | |
|:---:|:---:|:---:|
| STN: 01 | DY: 20/03/72 | |
| Depth (m) | Temp. (°C) | Sal. (‰) |
| 0 | 7.2 | 23.0 |
| 1 | 7.0 | 23.0 |
| 2 | 6.8 | 23.6 |
| 3 | 6.8 | 24.1 |
| 5 | 6.7 | 26.8 |
| 7 | 6.7 | 28.1 |
| 10 | 6.6 | 28.6 |
| 15 | 6.4 | 29.9 |
| 20 | 6.3 | 30.4 |

| CRN: G- 3 | HR: 1958 | |
|:---:|:---:|:---:|
| STN: 02 | DY: 20/03/72 | |
| Depth (m) | Temp. (°C) | Sal. (‰) |
| 0 | 6.7 | 25.6 |
| 1 | 6.7 | 25.8 |
| 2 | 6.6 | 26.1 |
| 3 | 6.5 | 27.0 |
| 5 | 6.5 | 27.4 |
| 7 | 6.5 | 27.4 |
| 10 | 6.4 | 27.9 |
| 15 | 6.2 | 30.0 |
| 20 | 6.5 | 30.2 |

| CRN: G- 3 | HR: 2025 | |
|:---:|:---:|:---:|
| STN: 03 | DY: 20/03/72 | |
| Depth (m) | Temp. (°C) | Sal. (‰) |
| 0 | 6.9 | 24.8 |
| 1 | 6.8 | 25.0 |
| 2 | 6.7 | 27.4 |
| 3 | 6.6 | 27.8 |
| 5 | 6.5 | 27.7 |
| 7 | 6.4 | 28.6 |
| 10 | 6.3 | 28.8 |
| 15 | 6.4 | 29.9 |
| 20 | 6.5 | 30.3 |

| CRN: G- 3 | HR: 2055 | |
|:---:|:---:|:---:|
| STN: 04 | DY: 20/03/72 | |
| Depth (m) | Temp. (°C) | Sal. (‰) |
| 0 | 7.5 | 18.5 |
| 1 | 7.0 | 22.1 |
| 2 | 7.1 | 22.7 |
| 3 | 6.8 | 23.4 |
| 5 | 6.6 | 26.0 |
| 7 | 6.8 | 28.4 |
| 10 | 6.7 | 29.1 |
| 15 | 6.3 | 29.9 |
| 20 | 6.3 | 30.4 |

| CRN: G- 3 | HR: 2115 | |
|---|---|---|
| STN: 05 | DY: 20/03/72 | |
| Depth (m) | Temp. (°C) | Sal. (‰) |
| 0 | 7.1 | 15.7 |
| 1 | 6.7 | 20.8 |
| 2 | 6.5 | 21.6 |
| 3 | 6.6 | 22.1 |
| 5 | 6.6 | 26.8 |
| 7 | 6.8 | 28.8 |
| 10 | 6.6 | 29.9 |
| 15 | 6.4 | 30.4 |
| 20 | 6.5 | 30.5 |

| CRN: G- 3 | HR: 2149 | |
|---|---|---|
| STN: 06 | DY: 20/03/72 | |
| Depth (m) | Temp. (°C) | Sal. (‰) |
| 0 | 6.9 | 17.8 |
| 1 | 6.9 | 19.9 |
| 2 | 7.1 | 20.0 |
| 3 | 7.1 | 21.4 |
| 5 | 6.7 | 26.3 |
| 7 | 6.7 | 29.7 |
| 10 | 6.8 | 29.7 |
| 15 | 6.7 | 30.5 |
| 20 | 6.7 | 30.9 |

| CRN: G- 3 | HR: 2215 | |
|---|---|---|
| STN: 07 | DY: 20/03/72 | |
| Depth (m) | Temp. (°C) | Sal. (‰) |
| 0 | 7.0 | 16.4 |
| 1 | 7.2 | 18.6 |
| 2 | 7.1 | 20.0 |
| 3 | 7.1 | 20.3 |
| 5 | 6.6 | 29.0 |
| 7 | 6.6 | 29.2 |
| 10 | 6.6 | 30.0 |
| 15 | 6.8 | 30.3 |
| 20 | 6.7 | 30.4 |

| CRN: G- 3 | HR: 2247 | |
|---|---|---|
| STN: 08 | DY: 20/03/72 | |
| Depth (m) | Temp. (°C) | Sal. (‰) |
| 0 | 5.5 | 6.8 |
| 1 | 5.4 | 6.9 |
| 2 | 5.6 | 8.5 |
| 3 | 5.7 | 14.6 |
| 4 | 6.1 | 23.7 |
| 6 | 6.5 | 27.5 |
| 8 | 6.6 | 30.7 |
| 12 | 6.5 | 30.9 |
| 15 | 6.4 | 30.7 |

| CRN: G- 4 | | HR: 1840 |
|---|---|---|
| STN: 01 | | DY: 17/04/72 |
| Depth (m) | Temp. (°C) | Sal. (‰) |
| 0 | 6.9 | 27.3 |
| 1 | 6.9 | 27.6 |
| 2 | 6.9 | 27.8 |
| 3 | 6.9 | 27.5 |
| 5 | 6.8 | 27.6 |
| 7 | 6.8 | 27.8 |
| 10 | 6.8 | 28.2 |
| 15 | 6.7 | 29.1 |
| 20 | 6.6 | 29.6 |

| CRN: G- 4 | | HR: 1915 |
|---|---|---|
| STN: 02 | | DY: 17/04/72 |
| Depth (m) | Temp. (°C) | Sal. (‰) |
| 0 | 6.9 | 27.7 |
| 1 | 6.9 | 27.6 |
| 2 | 6.9 | 27.6 |
| 3 | 6.9 | 27.6 |
| 5 | 6.9 | 27.7 |
| 7 | 6.9 | 27.8 |
| 10 | 6.9 | 28.2 |
| 15 | 6.6 | 29.5 |
| 20 | 6.6 | 30.0 |

| CRN: G- 4 | | HR: 2000 |
|---|---|---|
| STN: 03 | | DY: 17/04/72 |
| Depth (m) | Temp. (°C) | Sal. (‰) |
| 0 | 6.9 | 27.8 |
| 1 | 6.8 | 28.2 |
| 2 | 6.8 | 28.1 |
| 3 | 7.0 | 28.1 |
| 5 | 7.0 | 28.1 |
| 7 | 7.0 | 28.1 |
| 10 | 7.0 | 28.2 |
| 15 | 6.7 | 29.3 |
| 20 | 6.7 | 29.7 |

| CRN: G- 4 | | HR: 2025 |
|---|---|---|
| STN: 04 | | DY: 17/04/72 |
| Depth (m) | Temp. (°C) | Sal. (‰) |
| 0 | 7.1 | 28.2 |
| 1 | 7.0 | 28.3 |
| 2 | 6.9 | 28.2 |
| 3 | 6.9 | 28.1 |
| 5 | 6.7 | 28.1 |
| 7 | 6.9 | 28.1 |
| 10 | 6.8 | 28.3 |
| 15 | 7.0 | 28.5 |
| 20 | 6.6 | 30.3 |

| CRN: G- 4 | | HR: 2059 |
|---|---|---|
| STN: 05 | DY: | 17/04/72 |
| Depth (m) | Temp. (°C) | Sal. (‰) |
| 0 | 7.3 | 27.1 |
| 1 | 7.2 | 27.1 |
| 2 | 7.2 | 27.0 |
| 3 | 7.2 | 27.1 |
| 5 | 6.9 | 27.4 |
| 7 | 6.8 | 27.9 |
| 10 | 6.8 | 27.9 |
| 15 | 6.7 | 28.1 |
| 20 | 6.7 | 29.3 |

| CRN: G- 4 | | HR: 2124 |
|---|---|---|
| STN: 06 | DY: | 17/04/72 |
| Depth (m) | Temp. (°C) | Sal. (‰) |
| 0 | 7.5 | 26.9 |
| 1 | 7.4 | 27.0 |
| 2 | 7.3 | 27.3 |
| 3 | 7.0 | 27.6 |
| 5 | 6.9 | 27.8 |
| 7 | 6.9 | 27.8 |
| 10 | 6.8 | 28.3 |
| 15 | 6.6 | 30.0 |
| 20 | 6.7 | 30.4 |

| CRN: G- 4 | | HR: 2150 |
|---|---|---|
| STN: 07 | DY: | 17/04/72 |
| Depth (m) | Temp. (°C) | Sal. (‰) |
| 0 | 7.6 | 25.0 |
| 1 | 7.5 | 25.8 |
| 2 | 7.5 | 25.2 |
| 3 | 7.5 | 25.5 |
| 5 | 7.2 | 26.0 |
| 7 | 6.9 | 27.1 |
| 10 | 6.7 | 29.3 |
| 15 | 6.6 | 30.0 |
| 20 | 6.6 | 30.1 |

| CRN: G- 4 | | HR: 2241 |
|---|---|---|
| STN: 08 | DY: | 17/04/72 |
| Depth (m) | Temp. (°C) | Sal. (‰) |
| 0 | 5.8 | 2.0 |
| 1 | 5.8 | 6.7 |
| 2 | 6.3 | 17.3 |
| 3 | 6.5 | 21.3 |
| 5 | 6.7 | 23.9 |
| 7 | 6.8 | 28.9 |
| 10 | 6.7 | 29.3 |
| 15 | 6.7 | 29.7 |
| 20 | 6.7 | 30.1 |

| CRN: G- 5 | | HR: 1815 |
| STN: 01 | | DY: 11/05/72 |

| Depth (m) | Temp. (°C) | Sal. (‰) |
|---|---|---|
| 0 | 9.5 | 10.6 |
| 1 | 9.6 | 13.8 |
| 2 | 10.5 | 24.7 |
| 3 | 10.6 | 26.0 |
| 5 | 10.3 | 27.0 |
| 7 | 8.8 | 27.8 |
| 10 | 7.7 | 28.9 |
| 15 | 7.5 | 29.5 |
| 20 | 7.4 | 29.6 |

| CRN: G- 5 | | HR: 1847 |
| STN: 02 | | DY: 11/05/72 |

| Depth (m) | Temp. (°C) | Sal. (‰) |
|---|---|---|
| 0 | 9.6 | 11.1 |
| 1 | 10.1 | 18.6 |
| 2 | 10.1 | 18.7 |
| 3 | 10.3 | 22.3 |
| 5 | 10.0 | 27.5 |
| 4 | 9.5 | 27.8 |
| 10 | 8.5 | 28.4 |
| 15 | 7.5 | 29.3 |
| 20 | 7.2 | 29.9 |

| CRN: G- 5 | | HR: 1925 |
| STN: 03 | | DY: 11/05/72 |

| Depth (m) | Temp. (°C) | Sal. (‰) |
|---|---|---|
| 0 | 10.7 | 7.5 |
| 1 | 10.8 | 10.4 |
| 2 | 10.6 | 18.2 |
| 3 | 10.4 | 22.1 |
| 5 | 10.1 | 27.0 |
| 7 | 9.9 | 27.1 |
| 10 | 8.8 | 27.7 |
| 15 | 7.9 | 28.7 |
| 20 | 7.3 | 29.3 |

| CRN: G- 5 | | HR: 2000 |
| STN: 04 | | DY: 11/05/72 |

| Depth (m) | Temp. (°C) | Sal. (‰) |
|---|---|---|
| 0 | 10.7 | 7.0 |
| 1 | 10.6 | 12.3 |
| 2 | 10.8 | 16.4 |
| 3 | 10.5 | 21.9 |
| 5 | 10.3 | 26.9 |
| 7 | 10.2 | 27.3 |
| 10 | 9.0 | 27.8 |
| 15 | 7.5 | 29.1 |
| 20 | 7.1 | 29.9 |

| CRN: G- 5 |  | HR: 2020 |
|:---:|:---:|:---:|
| STN: 05 |  | DY: 11/05/72 |

| Depth (m) | Temp. (°C) | Sal. (‰) |
|:---:|:---:|:---:|
| 0 | 11.1 | 14.4 |
| 1 | 11.1 | 15.2 |
| 2 | 11.1 | 15.9 |
| 3 | 11.0 | 17.1 |
| 5 | 10.5 | 26.8 |
| 7 | 9.7 | 27.3 |
| 10 | 8.2 | 28.2 |
| 15 | 7.7 | 28.9 |
| 20 | 7.1 | 29.7 |

| CRN: G- 5 |  | HR: 2042 |
|:---:|:---:|:---:|
| STN: 06 |  | DY: 11/05/72 |

| Depth (m) | Temp. (°C) | Sal. (‰) |
|:---:|:---:|:---:|
| 0 | 11.0 | 12.9 |
| 1 | 11.0 | 13.0 |
| 2 | 11.1 | 12.7 |
| 3 | 11.3 | 15.0 |
| 5 | 10.9 | 24.8 |
| 7 | 10.4 | 27.2 |
| 10 | 9.7 | 27.5 |
| 15 | 7.6 | 29.2 |
| 20 | 7.2 | 29.7 |

| CRN: G- 5 |  | HR: 2100 |
|:---:|:---:|:---:|
| STN: 07 |  | DY: 11/05/72 |

| Depth (m) | Temp. (°C) | Sal. (‰) |
|:---:|:---:|:---:|
| 0 | 10.4 | 13.7 |
| 1 | 10.7 | 16.5 |
| 2 | 10.7 | 19.4 |
| 3 | 10.7 | 21.5 |
| 5 | 9.8 | 26.7 |
| 7 | 8.7 | 28.1 |
| 10 | 7.4 | 28.7 |
| 15 | 7.0 | 29.7 |
| 20 | 6.8 | 30.2 |

| CRN: G- 5 |  | HR: 2130 |
|:---:|:---:|:---:|
| STN: 08 |  | DY: 11/05/72 |

| Depth (m) | Temp. (°C) | Sal. (‰) |
|:---:|:---:|:---:|
| 0 | 8.2 | 0.0 |
| 1 | 7.8 | 0.0 |
| 2 | 9.4 | 15.8 |
| 3 | 10.1 | 21.2 |
| 5 | 7.5 | 29.6 |
| 7 | 7.3 | 29.7 |
| 10 | 7.3 | 29.8 |
| 15 | 7.2 | 29.8 |
| 16 | 7.2 | 29.9 |